REPUBLIC OF TURKEY
MARMARA UNIVERSITY
INSTITUTE OF HEALTH SCIENCES

THREE-DIMENSIONAL EVALUATION OF SKELETOFACIAL ASYMMETRY IN SKELETAL CLASS III PATIENTS TREATED WITH DOUBLE-JAW ORTHOGNATHIC SURGERY

STAVROULA SARAFOPOULOU

MASTER THESIS

DEPARTMENT OF ORTHODONTICS

SUPERVISOR

Asst. Prof. Dr. Kadir BEYCAN

ISTANBUL, 2018

TEZ ONAYI

Kurum	: Marmara Üniversitesi Sağlık Bilimleri Enstitüsü
Programın seviyesi	: Yüksek Lisans
Anabilim Dalı	: Ortodonti Anabilim Dalı
Tez Sahibi	: Stavroula SARAFOPOULOU
Tez Başlığı	: Three-dimensional evaluation of skeletofacial asymmetry in skeletal Class III patients treated with double-jaw orthognathic surgery
Sınav Yeri	: Marmara Üniversitesi Diş Hekimliği Fak. Ortodonti A.D.
Sınav Tarihi	: 16.08.2018

Tez tarafımızdan okunmuş, kapsam ve kalite yönünden Yüksek Lisans Tezi olarak kabul edilmiştir.

Danışman (Unvan, Adı, Soyadı)	**Kurumu**	**İmza**
Dr. Öğr. Üyesi Kadir BEYCAN	Marmara Üniversitesi	
Sınav Jüri Üyeleri (Unvan, Adı, Soyadı)		
Prof. Dr. Ahu ACAR	Marmara Üniversitesi	
Dr. Öğr. Üyesi Berza YILMAZ ŞEN	Bezmialem Üniversitesi	

Yukarıdaki jüri kararı Enstitü Yönetim Kurulu'nun 05/09/2018 tarih ve 13. sayılı kararı ile onaylanmıştır.

Prof. Dr. Göksel ŞENER
Sağlık Bilimleri Enstitüsü Müdürü

-Sınav evrakları 3 iş günü içinde ıslak imzalı tek kopya halinde Enstitüye teslim edilmelidir.
-Bu form bilgisayar ortamında doldurulacaktır.

Beyan Formu:

Bu tezin kendi çalışman olduğunu, planlamasından yazımına kadar hiçbir aşamasında etik dışı davranışımın olmadığını, tezdeki bütün bilgileri akademik ve etik kurallar içinde elde ettiğimi, tez çalışmasıyla elde edilmeyen bütün bilgi ve yorumlara kaynak gösterdiğimi ve bu kaynakları kaynaklar listesine aldığımı, tez çalışması ve yazımı sırasında patent ve telif haklarını ihlal edici bir davranışımın olmadığını beyan ederim.

01.08.2018

Stavroula SARAFOPOULOU

AFFIRMANCE:

I affirm that this thesis study belongs to me. There is no immoral attitude in all stages from the planning stage of thesis to the writing stage. I gained all the information in the terms of academic and ethical rules. I stated sources for the information gained not with this study. I showed the source in the list of sources, and again there is no copyright infringement in study and writing stage.

01.08.2018

Stavroula SARAFOPOULOU

ACKOWNLEDGEMENTS

First and foremost, I would like to express my sincere gratitude to my supervisor Asst. Prof. Dr. Kadir Beycan, , whose insights, knowledge and experience led to the completion of this research project. With his valuable help I was able to surpass many technical difficulties that I faced, since he was always willing to offer his help and scientific guidance.

Besides my advisor, I would particularly like to thank Prof. Dr. Ahu Acar. Despite being the Head of the Department, she never fails to help anyone working there. Her in-depth experience and knowledge assisted me a lot throughout the duration of my Master's program. She has been an ideal professor who at times leaves you speechless as the amount of hardwork and dedication she brings to our department cannot be described in words.

I would also like to express my deepest gratitude to all my professors Prof. Dr. Sibel Biren, Prof. Dr. Fulya Özdemir, Assc. Prof. Dr. Çağla Şar, Assis.Prof Dr. Nuray Yılmaz and Asst. Prof. Dr. Yasemin Bahar Acar for their immeasureable efforts throughtout my masters and for generously sharing their experience and science, I am honored to have been taught by you. My sincere thanks also goes to my former professors Prof. Dr. Nejat Erverdi, Prof. Dr. Nazan Küçükkeles, Prof. Dr. Banu Çakırer Bakkalbaşı for everything they provided during my first and second year.

I would like to thank all my friends and colleagues in the department, we shared unfogettable moments and you became my family away from home, you will always be remembered and cherished.

Above all, I would like to express my love and gratitude to my family and my life partner for providing me with unfailing support and continuous encouragement throughout the years.

CONTENTS

ABBREVIATIONS

1. mm: millimetre
2. °: Degrees
3. et al.: and others
4. fig: Figure
5. 2D: two-dimensional
6. 3D: three-dimensional
7. CBCT**:** Cone-Beam Computed Tomography
8. SNA: Sella Nasion A point angle (at Nasion)
9. SNB: Sella Nasion B point angle (at Nasion)
10. ANB: A point Nasion B point angle (at Nasion)
11. SN: Sella-Nasion distance
12. GoGn: Gonion-Gnathion distance
13. BSSO: Bilateral sagittal split osteotomy set-back of the mandible
14. CT: Computed Tomography
15. PNS: Posterior Nasal Spine
16. SP: Symphysis and parasymphysis
17. MP: Mandibular body
18. MA: Mandibular angle
19. IVRO: Intraoral vertical ramus osteotomy
20. DICOM: Digital Imaging Communications in Medicine

21. MIMICS: Materialize Interactive Medical Image Control Systems
22. FOV: Field of View or Imaging area
23. HU: Hounsfield Units
24. STL: Stereolithography
25. MSP: Mid-sagittal Plane
26. HP: Horizontal Plane
27. CP: Coronal Plane
28. R: Right
29. L: Left
30. Dev: Deviated
31. Opp: Opposite
32. OP1: Occlusal Preoperative Plane
33. OP2: Occlusal Postoperative Plane
34. MP1: Mandibular Preoperative Plane
35. MP2: Mandibular Postoperative Plane
36. RP L1: Left Ramal Preoperative Plane
37. RP R1: Right Ramal Preoperative Plane
38. RP L2: Left Ramal Postoperative Plane
39. RP R2: Right Ramal Postoperative Plane
40. CP L1: Left Coronoid Preoperative Plane
41. CP R1: Right Coronoid Preoperative Plane

42. CP L2: Left Coronoid Postoperative Plane

43. CP R2: Right Coronoid Postoperative Plane

44. G1: Gonial Preoperative Plane

45. G2: Gonial Postoperative Plane

46. Or: Orbitale

47. Po: Porion

48. Me: Menton

49. A: A point

50. B: B point

51. Gt: Genial tubercle

52. Go: Gonion

53. J: Jugale

54. Pog: Pogonion

55. Cor: Coronoid

56. Co top: Condyle top

57. Co med: Condyle medial

58. Co lat: Condyle lateral

59. Pn: Pronasale

60. Sn: Subnasale

61. C: Columella

62. Al: Alare

63. Ab: Alar base

64. NoS: Nostril Superior

65. NoI: Nostril Inferior

66. NoL: Nostril lateral

67. Pog’: Soft tissue Pogonion

68. Go: Soft tissue Gonion

69. Ls: Labrale Superius

70. Ch: Cheilion

71. En: Endocanthion

72. Ex: Exocanthion

73. SD: Standard Deviation

74. SPSS: Statistical Package for Social Sciences

75. ICC: Intraclass Correlation Coefficient

76. AC:Alar base cinch sutures

77. BMI: Body mass index

78. TMJ: Temporomandibular joint

79. ELSA: The reference point located equidistant to the points located in the centre of each foramen spinosum

80. MDFM. The mid-dorsal point of the foramen magnum

81. SLEAM: The supero-lateral border of the external auditory meatus

FIGURE LIST

TABLE LIST

1. SUMMARY

THREE-DIMENSIONAL EVALUATION OF SKELETOFACIAL ASYMMETRY IN SKELETAL CLASS III PATIENTS TREATED WITH DOUBLE-JAW ORTHOGNATHIC SURGERY

Stavroula SARAFOPOULOU
Asst. Prof. Dr. Kadir BEYCAN

AIM: The purpose of this study is to investigate pre- and postsurgically the skeletofacial asymmetry of skeletal Class III, orthognathically treated patients, using Cone-Beam Computed Tomography (CBCT).

MATERIALS AND METHODS: The sample of this retrospective study consists of CBCT records of 20 skeletal Class III patients (5 males, 15 females, mean age 22,35±5,16 years), who underwent combined orthodontic and surgical treatment at the Department of Orthodontics, Faculty of Dentistry, Marmara University. The CBCTs of all patients, taken before and after 4-6 months postoperatively, are analyzed by Mimics 19.0 software. In order to assess the asymmetry, a morphometric midsagittal plane is conducted and landmark displacement of 50 skeletal, dental and soft tissue landmarks is calculated in all three planes of space. Moreover, the skeletofacial asymmetry is assessed by linear and angular measurements of the skeletal, dental and soft tissue structures and possible factors contributing to the appearance of facial asymmetry are quantified. Finally, the asymmetry of the nose and the postoperative changes in the nose area are evaluated.

RESULTS AND CONCLUSION: Preoperatively, Coronoid, Genial tubercle, Gonion and soft tissue Gonion presented significant asymmetry. Residual asymmetry was found, postsurgically, in Coronoid, Condyle, Gonion, Mandibular body length and soft tissue Gonial area. Condyle and Coronoid asymmetry, asymmetry in Gonial area, Ramus length and Lateral ramal inclination discrepancy were correlated with Menton deviation. Alar base, Interalar and Internostril width tend to increase after the orthognathic surgery. Nasiolabial angle has a tendency to decrease after maxillary impaction, whereas it increases in maxillary advancement. 3d diagnosis achieved with computer-aided surgical simulation and evaluation of individual nasal characteristics are indicated since they deliver better and more predictable outcomes in the treatment of Class III asymmetric cases.

KEYWORDS: Asymmetry, Orthognathic surgery, Class III, Morphometrics

2. ÖZET

ÇİFT ÇENE CERRAHİSİYLE TEDAVİ EDİLMİŞ İSKELETSEL SINIF III HASTALARDAKİ YÜZ ASİMETRİSİNİN 3 BOYUTLU DEĞERLENDİRİLMESİ

Stavroula SARAFOPOULOU
Yrd. DoçDr. Kadir BEYCAN

AMAÇ: Bu çalışmanın amaçı ortognatik cerrahi ile tedavi edilmiş iskeletsel sınıf III hastalarda cerrahi öncesi ve sonrasındaki iskeletsel asimetrinin CBCT kullanılarak incelenmesidir.

GEREÇ VE YÖNTEM: Bu çalışmada Marmara Üniversitesi Diş Hekimliği Fakültesi Ortodonti anabilim dalında ortodonti ve ortognatik cerrahi ile tedavi edilen 20 adet iskeletsel sınıf III hastanın (5 erkek, 15 kadın, ortalama yaş 22,35±5,16) CBCT kayıtları kullanılmıştır. Tüm hastaların CBCT kayıtları cerrahiden önce ve cerrahiden 4-6 ay sonra alınmış ve Mimics 19.0 yazılımıyla analiz edilmiştir. Asimetriyi değerlendirmek için morfometrik midsagital düzlem rehber alınmıştır. 50 iskeletsel, yumuşak doku ve dişşel landmarkın yeri uzayın 3 yönünde hesaplanarak belirlenmiştir. Ayrıca iskeletsel, dişsel ve yumuşak dokulardaki iskeletofasiyal asimetri; doğrusal ve açısal ölçümlerle değerlendirilmiştir ve yüzde asimetri oluşumuna yardımcı olan olası faktörlerin niceliği belirlenmiştir. Son olarak burun asimetrisi ve cerrahi sonrası burun çevresindeki değişim değerlendirilmiştir.

BULGULAR VE SONUÇ: Cerrahi öncesi, Koronoid, Genial Tüberkül, Gonion, yumuşak doku Gonion belirgin asimetri gösterdi. Cerrahi sonrası, Koronoid, Kondil, Gonion, Mandibular korpus uzunluğu ve Gonial bölgedeki yumuşak dokuda rezidüel asimetri bulundu. Kondil ve Koronoid asimetrisi, Gonial bölgedeki asimetri, Ramus uzunluğu, Lateral ramal eğimdeki farklılık; Menton bölgesindeki deviasyonla ilişkilidir. Alar taban, Interalar ve Internostril genişlik ortognatik cerrahi sonrası artma eğilimindedir. Nasiolabial açı; maxillar ilerletme cerrahisi sonucu artma eğilimindeyken, maxiller gömülme cerrahisi sonrası azalma eğilimindedir. Bilgisayar destekli cerrahi simulasyon ile 3 boyutlu teşhiş yapılmıştır ve sınıf III asimetri vakalarında daha iyi ve doğru tahmin edilebilen sonuçlar verdiğinden kişiye özgü burun karakteristiğinin değerlendirmesi yapılmıştır.

ANAHTAR KELİMELER: Asimetri, Ortognatik Cerahi, Sınıf III, Morfometrik

3. INTRODUCTION AND AIMS

The main treatment modality for severe Class III skeletal deformity in adults is the orthognathic surgical approach. Even after early growth modification treatment, by using reverse pull headgear, there is a potential risk of relapse in patients with unfavourable growth pattern. In literature, it has been reported that there is a 25-33% relapse possibility after adolescence. Patients who have a return of their skeletal problem are candidates for orthognathic surgery after the end of growth (Hagg et al, 2003; Baccetti et al, 2004; Wells et al, 2006). Thus, it can be deduced that even after the most attentive preventive and interceptive orthodontic care, the need for treatment of Cl III skeletal disharmony in adults cannot be eliminated to zero.

Correction of severe dentoskeletal malocclusions has a triple objective to achieve: functional efficiency, structural balance and aesthetics. Physical health of individuals with severe malocclusions may be altered or compromised in several ways such as temporomandibular joint and masticatory dysfunction, resistance of the upper airway, speech disorders and compromised oral hygiene (Legan, 1992; Reyneke, 2010). However, when the orthognathic surgical approach is concerned, it appears that its objectives have changed in priority. In current society, facial appearance has an impact on person' s interrelationships, and it affects social and psychological development (Soncul and Bamber, 2004; Liu et al, 2009; Kim et al, 2013a). Therefore, one of the most strong motives and concerns of patients with maxillofacial deformities seeking treatment is the cosmetic improvement. Although functional efficiency and structural balance still remain important for the final treatment outcome, facial harmony has prevailed as a modern treatment goal (Ackerman et al, 1999; Proffit 2000).

Facial asymmetry is a very frequent feature in Class III malocclusions with mandibular prognathism (Haraguchi et al, 2002). The pattern of facioskeletal asymmetry is compound because of the spatial interplay of bone, dentition,and soft tissues (Kusayama et al, 2003; Ishizaki et al, 2010; Cheong and Lo, 2011) and it may

be due to the asymmetric anatomy of structures per se and the displacement of the maxillomandibular complex or just the mandible (Baek et al, 2007; Baek et al, 2012).

In lieu of the spatial complexity of the dentition, the bony and soft tissue structures of the face, the correction of severe facial asymmetry is a great challenge and a crucial prerequisite in a successful orthognathic reconstructive surgery (Motta et al, 2010; Lin et al, 2016). Surgical treatment planning depends on the diagnosis of the etiologic structures of facial asymmetry. Asymmetry in maxillary height, ramus length, ramus inclination from a frontal and a lateral view, mandibular body length and height may cause chin deviation and apparent facial asymmetry (Hwang et al, 2006). Soft tissues response to surgical correction of skeletal asymmetry also plays a role to the final outcome (Jung et al 2009). Residual asymmetry of the facial contour is a common consequence, creating the need for a second corrective surgery (Edler et al, 2004; Reyneke, 2010). Favorable treatment outcomes in orthognathic surgical treatment can be achieved if the criteria of a comprehensive diagnosis, accurate treatment planning, and a sound surgical technique are closely adhered to (Reyneke, 2010).

Traditionally, a posteroanterior cephalogram, a frontal facial photography and submentovertex view were used to diagnose the presence and degree of facial asymmetry. However, two-dimensional radiographs of complex three-dimensional structures like the facial skeleton have characteristic impediments due to the projection methods. Magnification and distortion of the image, results in interpretation error and may lead to misdiagnosis (Bergersen, 1980; Ahlqvist et al, 1983). Since precise and quantitative evaluation is a key component in the diagnosis of facial asymmetry, a three-dimensional examination utlizing two-dimensional radiographs apparently cannot be legitimately validated.

CBCT technique is nowadays widely used in the diagnosis, treatment planning, surgical guidance, evaluation of the results and follow-up controls of the maxillofacial-deformity treatment. Apparently, one of its most important characteristics, when used for evaluation of the surgical outcome, is that it incorporates both the hard and soft facial tissues into the same image. This allows the investigation of the possible relation between their alterations (Kwong et al, 2008).

In light of these facts, the objective of this study is to investigate pre- and postsurgically the asymmetry of dentofacial and soft tissue structures in skeletal Class III patients, who underwent double-jaw surgery. Furthermore, contributions from dentoskeletal structures and soft tissues leading to facial asymmetry are examined and the outcome of the bimaxillary surgery is evaluated as regard the facial harmony and the symmetry of the underlying structures. Since nose appearance plays a significant role in the overall aesthetic balance and symmetry of the face, nose asymmetry and changes after the surgery were also assessed.

4. LITERATURE REVIEW

1. Class III malocclusion

1. Definition of Class III malocclusion

In Angle´s classification of malocclusion (1899) Class III malocclusion is described as abnormal relationship of the jaws, with all the lower teeth occluding mesially to normal the width of one bicuspid or even more in severe cases. Angle (1899) also observed that in Class III cases the mandibular angles appeared to be more obtuse than in the normal subjects. Moreover he stated that in some cases there was an overdevelopment in "certain localities of the body". In other cases, where the jaw seemed normal in form, he suggested that the protrusion was caused by the temporomandibular articulation being farther anterior than normal.

It is now well established that Class III malocclusion is not only attributed to dental irregularities but is almost always related to an underlying skeletal discrepancy. Skeletal maxillary retrusion, mandibular protrusion, or some combination of both may coexist. Moreover, an excessive or deficient vertical facial dimension frequently appears and affects the diagnostic and therapeutic decisions (Posnick, 2013).

2. Prevalence of Class III malocclusion

The prevalence of the Class III malocclusion varies greatly among and within different population groups (Hardy et al, 2012). It shows a relatively low incidence in Caucasian populations, whereas its incidence has been found to be much higher in Asians. It has been reported to be 1-5% for Caucasians, (Emrich et al, 1965; Haynes, 1970; Foster and Day, 1974; Burgersdijk et al, 1991; Salonen et al, 1992; Tod, 1997;

Ciuffolo et al., 2005), 9-22.4% for Asians (Chan, 1974; Tang, 1994; Soh et al., 2005), and 9% for Latins (Silva and Kang, 2001). Moreover, the third National Examination Survey (NHANES III) presented incidence of Class III malocclusion as 0.8% in white, 2% in black, and 1.6% in Mexican-American populations (Brunelle et al., 1996; Proffit et al, 1998).

The prevalence of Class III malocclusion in Turkey has been reported in the studies of Sayin and Turkkahraman, 2004, Gelgor et al, 2007, Uslu et al, 2009 with different results of 12%, 18.44%, 10.3%, respectively.

Except the ethnic background, the incidence of Class III malocclusion differs in females and males and it has been described about three times higher in males than females (El-Mangoury et al, 1990, Baccetti et al, 2005).

Moreover, data from NHANES-III in 1990s show that Class III problems increase with age. This can be explained by the expected late growth spurt in the mandible as compared with the maxilla. (Proffit et al, 1998).

3. Components of Class III malocclusion

The Class III skeletal problem can present in many forms including mandibular protrusion, maxillary retrusion, or a combination of both.

Mandibular prognathism was found to be the etiology in 20%-46% of the Class III cases, while in 19.5%-37% of the malocclusions maxillary retrognathism was found to be the reason. However, in 7.5%-60% of the cases, a combination of both maxillary deficiency and mandibular excess were detected (Sanborn, 1955; Dietrich, 1970; Jacobson et al, 1974; Ellis and McNamara, 1984; Guyer et al, 1986; Williams and Andersen, 1986).

True mandibular prognathism can be identified in the profile of the patients by examining their neck form in conjunction with their throat length. Prognathic

patients possess prominent chin with decreased mentolabial fold and thin lower lip (Sinclair and Proffit, 1991).

Common characteristics of maxillary deficiency patients are an increased neck-chin angle and submental area with sunken in facial appearance and thin upper lip. They frequently have narrow alar base, more horizontally oriented Columella and obtuse Nasiolabial angle (Sinclair and Proffit, 1991).

In addition, a significant vertical component exists in Class III malocclusions. A relationship between the vertical growth of the maxilla and the anteroposterior position of the mandible has been described in the literature. If maxilla does not grow vertically, there is an indirect effect on mandible, which then rotates upward and forward, causing an appearance of mandibular prognathism that may be attributable to the rotation of the mandible than its size (Proffit et al, 2007).

From the frontal view, Class III patients present sunken-appearing cheeks and flat and relatively short upper lip with reduced vermillion exposure. Middle one third of the face appears flat and long and alar base is narrow with paranasal flattening (Posnick, 2013). Complete maxillary deficiency is also expressed with infraorbital, malar and paranasal deficiencies. An area of sclera is sometimes visible beneath the pupils as a result of infraorbital deficiency. Maxillary incisor display at rest is usually decreased in these patients (Sinclair and Proffit, 1991). Narrow maxillary arch width is manifested as excessive negative space in the buccal corridors. Also from frontal view, mandible is apparently prominent with a reduced labiomental fold (Posnick, 2013).

As regard the dental characteristics, Class III molar and canine malocclusion with anterior open bite and negative overjet are frequently observed. Mandibular incisors are usually upright or lingually inclined, with minimal attached gingiva over the labial aspects of them. Interdental spacing with flared mandibular incisors may also be seen, especially in the presence of an anterior open bite with lip incompetence (Posnick, 2013). Because of the constriction of the maxilla in all three planes of space, maxillary deficient patients may have severe maxillary crowding with flared incisors and missing or underdeveloped maxillary lateral incisors. They

often have a strong crossbite tendency because of the narrowness of their maxilla, and this may create buccal tipping of the maxillary molars in order to compensate (Bagheri et al, 2012).

4.1.3 Etiopathogenesis of Class III malocclusion

A developing Class III malocclusion can exhibit mandibular skeletal protrusion, maxillary skeletal retrusion (midfacial deficiency), or some combination of the two. The development of a Class III jaw disharmony is believed to be multifactorial and complex. Etiopathogenesis of mandibular prognathism and maxillary deficiency are addressed separately, as they may be independent characteristics of Class III subjects.

1. Etiopathogenesis of mandibular prognathism

Throughout history, a well-recognized genetic component of mandibular prognathism and Class III malocclusion has been described. Numerous studies have shown a significantly higher incidence of this phenotype in the relatives of affected probands (Inaki, 1938; Stiles and Luke, 1953; Kraus et al, 1959; Schulze and Wiese, 1965). Extensive studies of Class III incidence in progenies of Japanese families showed an incidence of 18%, 31% or 40% in cases that the mother, the father or both parents were affected, respectively (Inaki, 1938; Suzuki, 1961). In a study of severe Class III children, it was found that one-third had a parent with the same skeletal pattern and one-sixth had a Class III sibling (Litton et al, 1970). Concordance for mandibular prognathism among twin pairs raised from published reports was 81.0–83.3% for monozygotic twin pairs and 10.0–13.3% for dizygotic (Lundström, 1948; Schulze, 1965). However, the inheritance pattern of mandibular prognathism is not clear; findings have been reported suggesting autosomal-dominant inheritance (Keeler, 1935; Kraus 1959), autosomal-recessive inheritance (Downs, 1928; Inaki, 1938), dominant inheritance with incomplete penetrance (Stiles and Luke, 1953;

Wolff et al, 1993; El-Gheriani et al, 2003), or a polygenic model of transmission (Litton et al, 1970).

Although mandibular prognathism presents a strong family tendency, the rate of developing mandibular prognathism in patients with a positive family history (49.3%) is not higher than those with a negative one (50.7%) (Susami, 1968). Therefore, the incidence of mandibular prognathism may rely on candidate genes being expressed, with gene-environment interactions establishing the severity of mandibular prognathism. The relative involvement of genetic and environmental components in the etiopathogenesis of mandibular prognathism is not clear.

Local environmental factors have also been implicated in affecting the development of both the maxilla and mandible and ultimately creating a Class III jaw disharmony. Various environmental factors have been found to conduce to the development of mandibular prognathism, such as endocrine disturbance (acromegaly, gigantism, pituitary adenomas), habitual posture (habit of protruding the mandible), nasoairway obstruction (enlarged tonsils), congenital anatomic defects (cleft lip-cleft palate) and trauma (instrumental deliveries) (Downs, 1928; Gold, 1949; Pascoe et al, 1960; Monteleone et al, 1963; Schoenwetter, 1974; Diewert, 1983; McNamara, 1984; McNamara, 1987; Chang et al, 2002; Chang et al, 2005a; Chang et al, 2005b).

For example, if the mandible is constantly positioned forward, the condylar process may exhibit some growth in order to keep the articulation with the glenoid fossa. Harvold's experiments on monkeys demonstrated that forward posturing of the mandible to assist mouth breathing created a tendency to mandibular prognathism (Harvold, 1979). It may be concluded from this study that a growing child with a large tongue or reduced pharyngeal dimensions, and who keeps his mandible forward to breathe, could experience excessive mandibular growth.

Etiopathogenesis of mandibular prognathism may also be syndromic. Through modern literature, Crouzons and Apert syndrome have been blamed for the mandibular prognathic phenotype (Horsey, 2007).

2. Etiopathogenesis of maxillary deficiency

Maxillary deficiency has a familial predisposition, for instance, if the father presents with sunken cheekbones and bulging eyes, the child is most likely to inherit the same traits (Kreiborg, 1981).

However, the presence of the class III problem, and especially maxillary deficiency, in medical syndromes such as Pffeifer, Treacher Collins-Franceschetti, Crouzon ,and achondroplastic dwarfism obviates the genetic etiology (Horsey, 2007).

Maxillary deficiency is also a feature in fetal alcohol syndrome. Common facial trait includes narrow, small eyes with large epicanthal folds, flat midface and smooth groove in upper lip (Carlo, 2007). One of the complications may be cleft formation in newborns. Cleft lip and palate usually affects growth of the maxilla in all planes and may cause midfacial hypoplasia. However, iatrogenic effect is more commonly linked to maxillary deficiency of cleft patients. Cleft repair imposes restriction in skeletal and soft tissue growth as a result from the periosteal stripping during the surgery and scar tissue formation.

3. Pseudo-Class III malocclusion

Finally, pseudo-Class III malocclusion in the mixed dentition that is not corrected may be the cause of a skeletal Class III problem as the patient grows. Pseudo-class III malocclusion is defined as a functional anterior crossbite due to a forward mandibular displacement into a position in which posterior teeth can occlude comfortably (Kumar et al, 2011). Premature contacts, early loss of primary molars, minor transverse maxillary discrepancy, proclined lower and ectopic retroclined upper incisors may lead to mandibular displacement (Rabie and Gu, 2000; Kanno et al, 2007; Kumar et al, 2011). If not treated in due course, pseudo-Class III malocclusion may affect the normal development of the jaws and give raise to a true

skeletal Class III problem, as a result of restricted maxillary growth and mandibular overgrowth (Major and Glover, 1992; Proffit et al, 2007).

4. Diagnosis of Class III malocclusion

When examining a Class III adult patient it must be found out whether anteroposterior discrepancy is a result of the maxilla, the mandible, or both jaws. Moreover, the existence of the vertical component and the vertical development of the jaws should be evaluated. Clinical examination from a frontal and a profile view may reveal some usual manifestations of the Class III modality. The lateral cephalometric analysis provides many of the necessary skeletal and dental measurements, such as the anteroposterior and vertical relationships of the maxilla and mandible to cranial base and the inclinations of the anterior teeth, and hence facilitates a more precise diagnosis. (Ngan et al, 1997).

Clinical preliminary analysis may also be of help in the diagnosis of skeletal Class III disharmony. Upon frontal evaluation, detection of inferior sclera show in subjects with natural head position and straight gaze or a deep paranasal triangle may be signs of maxillary deficiency (Meneghini, 2005). Via the profile view maxillary retrognathism may be expressed through: i) increased total anterior facial height, ii) flatness of malar, infraorbital, cheek and paranasal region iii) clockwise rotation of the upper lip outline, iv) chin overprojection and iv) normally shaped labiomental fold (Arnett and Bergman, 1993).

As far as the clinical diagnosis of pure mandibular prognathism is concerned, in the profile view the following features are observed 1) a concave profile, 2) slightly over-projected chin , 3) normally shaped labiomental fold, 4) well defined and clockwise rotated mandibular border outline , 5) pleasing total chin-throat-neck outline length, as well as cervicomental angle (Meneghini, 2005).

Nevertheless, attention should be given in cases were anterior vertical deficiency causes an anticlockwise rotation of normal shaped-sized mandible and a pseudo mandibular protrusion phenotype. Vertical maxillary deficiency, also known as hypo divergent skeletal pattern, low angle case, short face or skeletal deep bite is characterized in the frontal view by short vertical axis of the face, with a large reduction of the lower facial third height and a relative increase of facial widths. The

profile view confirms and adds some important diagnostic elements such as: 1) reduction of the lower anterior face height, 2) long appearance of the nose, 3) counterclockwise rotated and excessively concave of the upper lip outline, 4) extremely deep and unnatural labiomental fold, 5) counterclockwise rotated in a nearly horizontal position mandibular border outline. This affects the chin projection, which seems to be increased, 6) extremely short throat length (Meneghini, 2005).

The most consistent findings seem to be the dental characteristics which include Angle's Class IlI molar relationship, retroclined mandibular incisors, proclined maxillary incisors, and an edge-to-edge incisor relationship or anterior crossbite (Ngan et al, 1997). Transverse maxillary deficiency and posterior crossbite are frequent findings in Class III patients.

Although clinical evaluation may be valuable, the clinician should refer to radiographic measurements and examination for a quantitative and precise diagnosis of the skeletal discrepancy. Mostly these measurements are performed in lateral cephalograms.

Steiner analysis suggested the SNA, SNB, ANB angular measurements to assess the skeletal sagittal growth discrepancy. ANB angle provides information on anteroposterior relationship of the maxilla and mandible to the anterior cranial base (Abdullah et al, 2006). In a case of concave profile, the ANB value is usually below 2°, with decreased SNA and increased SNB values indicating maxillary rethognathism and mandibualar prognathism, respectively (Steiner, 1959). Nevertheless, geometric studies have shown that variance in the length of the cranial base and/or rotation of the jaws may distort the validity of this measurements. When the Nasion is posteriorly positioned the ANB is increased and the opposite occurs when Nasion is more forward. Moreover, in high-angle cases with clockwise rotation of mandible, ANB value is increased which is representative of the true skeletal pattern (Bishara et al, 1983).

McNamara (1984) presented Nasion perpendicular line as a reference line to assess the anteroposterior position of the maxilla and its relationship to the cranial base. If A point is found less than 1 mm or posterior to the reference line, it is an

indication of maxillary deficiency. The nasion perpendicular is generally a reliable line of orientation for determining maxillary position. One exception may be Class III patients with short anterior cranial base, where because of the posterior position of nasion an erroneous nasion perpendicular is constructed, giving the wrong appearance of a protruded maxilla. Another problem may arise when excessive tipping of the upper incisors exists and may affect the position of A point. For all these reasons, Mc Namara pointed out that clinicial should not rely just on radiographic evaluation and that clinical examination should take precedence.

Another useful value introduced by Rickets in 1961 is the Maxillary depth. It enables clinician to evaluate the maxilla in relation to the true position of the head. If maxillary depth is less than 90°, it is usually a sign of maxillary deficiency. Although it is analogous to SNA, it is not affected by variations in the position of the sella. According to Rickett's analysis (1981), maxillary height represents the vertical relation of the maxilla to the cranium and values lower than 50 degrees show vertical maxillary deficiency.

Ricketts (1981) introduced the fraction of the linear measurement, in mm, of anterior cranial base (SN) to the Go-GN distance in an effort to correlate anterior cranial base and mandibular length. This fraction should be in the form of $\frac{x}{x+7}$. When the denominator increases it expresses the presence of a big mandible. In the same spirit Roth introduced the fraction of the linear measurement of anterior cranial base to the Go-Me distance. This fraction should be in the form of $\frac{x}{x}$. If the distance Go-Me constructed is bigger than SN then it is indicative of mandibular prognathism. The method of Roth has the advantage that excludes symphysis from the calculation.

The differential diagnosis of a pseudo-Class III malocclusion and the detection of a functional shift play a detrimental role in the therapeutic decisions. Clinically, it should be evaluated if there is a discrepancy of jaws relationship between centric relation and centric occlusion. These patients tend to have a Class I skeletal relationship, normal profile and a Class I molar relation in centric relation, but a Class III skeletal and dental pattern in centric occlusion. On cephalometric analysis, pseudo-Class III malocclusion shows Class I or mild Class III skeletal

relationship, a normal SNA if diagnosed early, whereas SNB is normal or slightly increased. Maxillary incisors are usually retroclined and lower incisors are proclined (Graber et al, 1997).

Jacobson et al (1974) conducted a cephalometric study to recognize the various types of skeletal Class III patterns. In comparison to individuals with normal skeletal patterns, it was found out that Class III individuals have a more obtuse Gonial angle, a shorter anterior cranial base, a longer posterior cranial base, more retroclined lower incisors and more proclined upper incisors (Jacobson et al, 1974; Guyer et al, 1986). Moreover, the Class III population often has a more acute cranial base angle (N-S-Ba), resulting in a more anteriorly positioned glenoid fossa that positions the mandible more forward (Horsey, 2007).

Three-dimensional imaging provides images of craniofacial structures free from perspective distortion, magnification errors or superimposition related with two-dimensional images (Farronato et al, 2000). Nowadays, CBCT-synthesized cephalograms have been introduced and they can communicate the three-dimensional characteristics of the facial skeleton precisely. CBCT-synthesized cephalograms have been used to perform cephalometric analyses, which assist the assessment of dentoskeletal relationship and facial asymmetry and the three-dimensional treatment planning (Farronato et al, 2000; Elisabetta et al, 2013; Rodriguez-Cardenas et al, 2014).

2. Facial asymmetry

1. Significance of facial asymmetry

Asymmetry is defined as a lack of equality or equivalence between parts or aspects of a unit (Oxford dictionary, 2010). There is mild asymmetry of the human body in all individuals. As regard the face, symmetry and balance can be expressed as equivalence in dimensions, form and arrangement of the facial features on the two opposite sides of the midsagittal plane (Peck and Peck, 1970). Perfectly bilateral face

symmetry is mainly a theoretical concept and seldom exists in living organisms (Farkas and Cheung, 1981; Peck et al, 1991).

The pattern of facioskeletal asymmetry is complex because of the spatial interplay of bone, dentition and soft tissues, including the muscles, the skin, and the fat (Hayashi et al, 2004; Baek et al, 2007; Ishizaki et al, 2010; Cheong and Lo, 2011). Asymmetry of facial skeleton may involve the anatomy of skeletal structures per se and the postural deviation of the maxillomandibular complex or just the mandible (Baek et al, 2007; Baek et al, 2012).

Skeletal asymmetry may be partially or completely masked by the soft tissues, the dental compensation or change of the head posture (Burstone, 1998; Haraguchi et al, 2002). Despite the potential camouflage by the soft tissues investigators suggested that asymmetry is also a common finding in the facial soft tissues (Haraguchi et al, 2002). Consequently, both the skeleton and the soft tissues of the craniofacial region should be examined thoroughly for adequate diagnosis of asymmetry (Nur et al, 2016). Peck et al (1991) and Masuoka et al (2005) discovered clear deviations between the extent of skeletal asymmetries identified through cephalometric measurements and the subjective appraisals of the faces. This result shows how variations in the soft tissue thickness in transverse and sagittal directions may alter the clinical imprecion of skeletal asymmetry (Dahan, 1968; Masuoka et al,2005)

The degree of asymmetry ranges from almost imperceptible to a gross abnormality. The threshold of acceptable asymmetry is subjective, and slight facial asymmetry can be found even in aesthetically attractive faces. According to Farkas and Cheung (1981), up to 3 mm of deviation is indistinguishable in a normal face, while Peck et al (1991) report that up to 4 mm asymmetry between right and left orbits can be indiscernible. Occlusal cant within the range of 1^{o} to 3^{o} has been observed in healthy patients and such cants are not detectable (Ferrario et al, 1993; Padwa et al, 1997).

However, it has been shown that highly-asymmetrical faces are found unattractive. In the study of Haraguchi et al (2002) 2D facial photographs of a

Japanese sample of 220 skeletal Class III patients were assessed by orthodontic judges and it was found out that the specialists were sensitive to jaw deviation of approximately 4 mm. When asymmetry is easily detectable, it can have major implications for the patient, regarding psychology, function and aesthetics. Severe or pathologic asymmetry of the craniofacial complex affecting skeletal, soft and dental tissues is that exceeds the acceptable norms, requires precise diagnosis and combined orthodontic and surgical treatment.

2. Asymmetry in the Class III population

Facial asymmetry is a relatively frequent manifestation. The incidence of clinically noticeable asymmetry has been described as 23% in the orthodontic population (Willems et al, 2001) and 21-38.6% in individuals with dentofacial deformities (Samman et al, 1992; Severt and Proffit, 1997; Chew, 2006). Facial asymmetry is a common feature in Class III malocclusions with mandibular prognathism, with a frequency of 40-80%, possibly because of excessive mandibular growth in the case of mandibular prognathism (Severt and Proffit, 1997; Willems et al, 2001; Haraguchi et al, 2002; Yoon et al, 2004; Chew, 2006). Facial asymmetry may also involve maxillary occlusal cant, nasal tip deviation, zygomatic arch discrepancy, and orbital dystopia (Severt and Proffit, 1997). Therefore, thorough evaluation of facial asymmetry is crucial in skeletal Class III patients.

The lower third of the face deviates more commonly and at greater distances than the middle and upper thirds. In a retrospective study of Severt and Proffit (1997), who examined 1460 patients with dentofacial deformity of the university clinic of North Carolina with respect to facial asymmetry, it was demonstrated that 34% of the subjects had a clinically detectable asymmetry. Moreover, 40% of skeletal Class III patients presented a degree of asymmetry and it was concluded that individuals with a class II skeletal pattern were less likely to display facial asymmetry. In this study facial asymmetry affected the lower face in 74%, the midface in 36%, and the upper face in only 5% of the examined subjects. The reason

for the increased prevalence of lower facial asymmetry may be the fact that the mandible is a mobile bone that grows over a longer period than the maxilla (Haraguchi et al, 2002; Kwon et al, 2006).

Haraguchi et al (2002) found that in a sample of 220 Japanese skeletal Class III adults 80% displayed a skeletal asymmetry and 56% of them had an asymmetry at the soft tissue level. This is a much higher rate than that detailed by Severt and Proffit (1997), however, the methods used to evaluate the asymmetry were not standardized

Most studies of minor nonpathologic asymmetry have demonstrated that the right hemiface is frequently wider than the opposite left (Shah and Yoshi, 1978; Burke, 1979; Koff et al, 1981; Farkas et al, 1981; Koff et al; 1985; Ferrario et al, 1993). However, some reports have showed no significant difference between the size of the right and left halves of the face (Peck et al, 1991; Ferrario et al, 1995) or have found the left hemiface to be wider (Vig and Chewitt, 1975; Chebib and Chamma, 1981).

3. Etiology of facial asymmetry

The etiology of facial asymmetry is found to be related to genetics as well as to environmental influences during the fetal, infant, or adolescent periods (Lundström, 1961; Pirttiniemi, 1994; Haraguchi et al, 2002).

It has been documented that, excluding mandibular prognathism, about 50% of the variation of facial skeletal features may be affected by inheritance, whereas the remaining 50% may be related to environmental influences (Proffit, 2000). This means that severe dentofacial deformities cannot be explained purely by inheritance (Mulick, 1965).

Facial asymmetry can be classified into three main categories regarding the etiology, (1) congenital, arising prenatally; (2) developmental, originating during growth with undefined etiology; and (3) acquired, resulting from disease or injury (Hegtvedt, 1993; Cohen, 1995; Reyneke et al, 1997).

Prenatal restriction of growth is not usual, but when it happens it affects both facial form and the function and the effects are severe. Intrauterine pressure on the fetus head or pressure in the birth canal during parturition may result in molding of the skull and facial bones, creating apparent skeletofacial asymmetry. Such constriction of growth may occur in the case that a limb presses against the face in utero, which may cause a depression in the midface region. Fortunately, in such cases after the birth growth continues normally and the facial deformity tends to stabilize or even improve (Darras et al, 2015). Similar constriction can affect the mandible and this is classically observed in individuals with Pierre Robin syndrome. The bending of the head tightly against the chest disturbs the forward growth of the mandible. However, these individuals tend to improve with growth and they may reach normal mandibular length (Darras et al, 2015; Zellner et al, 2017).

Congenital disorders that present with facial asymmetry include neurofibromatosis, torticollis, positional plagiocephaly, craniosynostosis (Hegtvedt, 1993; Cohen, 1995; Reyneke et al, 1997). Several craniofacial syndromes exhibit some degree of facial asymmetry. Usually these individuals have characteristic facial appearance and require complex treatment with multidisciplinary approach. Such syndromes include; Crouzon syndrome, Hemifacial microsomia, Orofacial syndrome, Aperts's Syndrome and cleft lip and palate (Proffit, 2000).

The developmental form of facial asymmetry is non-syndromic and idiopathic in nature, and it does not unfrequently affect metabolically normal individuals.. The asymmetry is not apparent at birth or in infancy, but appears gradually and often becomes obvious in the teenage years (Shah and Yoshi, 1978; Cheong and Lo, 2011). Increased vertical growth on one side of the mandible causes compensatory changes in the maxilla and its dentition that is clinically exhibited as a maxillary occlusal cant. The degree to which this compensatory growth occurs depends on the rate of growth of the mandible (Obwegeser and Makek, 1986).

Usually it is self-limiting with varying degrees of deformity experienced. Excessive growth may stop spontaneously or require intervention. There is no previous history of facial trauma or any disease causing the asymmetry (Shah and Yoshi, 1978; Cheong and Lo, 2011). The literature reports that continuous facial pressure during sleep only on one side, habitual mastication on one side or deleterious oral habits as some possible causes of the deformity. The aforementioned factors might be responsible for increasing skeletal development on the opposite side. However, the hypotheses are controversial and cannot be scientifically validated, due to the lack of well-controlled extensive studies (Lundström, 1961; Rossi et al, 2003; Haraguchi et al, 2008).

Facial asymmetry in childhood can be usually secondary to fracture of the condyle because of trauma. A trauma history was found in 14% of the patients with asymmetry that were examined in the University of North Carolina (Severt and Proffit, 1997). If growth interruption occurs on the affected side while normal development continues on the unaffected side, a chin asymmetry towards the side of the fractured condyle may be caused. The intra-articular bleeding and resulting haematoma formation that follows traumatic episodes may cause an ankylosis in the temporomandibular region and, consequently, a loss of function (Severt and Proffit, 1997; Chia et al, 2008). The earlier the fracture occurs the prognosis is better and following condylar fracture 75% of children exhibit normal growth. Infrequently, the asymmetry can be the result of a destructive process that involves the tempromandibular joint (Proffit, 2000).

Facial asymmetry may appear under some other conditions, including fibrous dysplasia, osteochondroma, childhood radiotherapy, facial tumors, cysts, infections and other pathology (Chia et al, 2008; Cheong and Lo, 2011). Moreover, there is a number of conditions that may lead to condyle resorption. These comprise poststeroid therapy, juvenile rheumatoid arthritis, and orthognathic surgery (Hwang et al, 2004; Chia et al, 2008). Rheumatoid arthritis in a child can affect the temporomandibular joint bilaterally or unilaterally, altering the mandibular structure and function. Rheumatoid arthritis affects bone and cartilage and can cause destruction of the joint and disc. In the case of unilateral condylar resorption,

mandibular asymmetry will occur. The fact that it usually affects multiple joints within the body contributes to the diagnosis (Chia et al, 2008).

Functional lateral displacement of the mandible, as for example in the presence of buccal crossbite, may also be responsible for asymmetric development of the mandible. Some authors suggest that in presence of crossbite, mandibular development is restricted on that side and may result in shortening of the ramal height and development of a mandibular asymmetry (Schmid et al, 1991; van Keulen et al, 2004).

Disturbances of muscular activity have also the potential to influence the jaws growth and may be a cause of facial asymmetry. This can be explained because the activity of the muscles affects the bone formation at the point of muscles attachment. Moreover, muscles are a part of the soft-tissue matrix that is responsible for the displacement of the skeletal unit and consequent bone deposition (Gorlin et al, 1990; Proffit et al, 2000). Muscular dysfunction is most likely to result from damage to the motor nerve. Consequently, muscle atrophy or dysfunction results in underdevelopment of the relative part of the face, with a deficiency of both hard and soft tissues (Washburn, 1946; Gardner et al, 1980; Byrd, 1984; Proffit et al, 2000).

4. Evaluation of facial asymmetry

The diagnostic methods used for the evaluation of facial asymmetry in the literature can be classified according to the utilization of ionizing radiation or not (x-ray and non-x-ray methods).

1. Non-x-ray methods

Facial indirect anthropometric techniques can be divided in contact methods (electromagnetic and electromechanical digitizers, ultrasound probes) and optical/non contact methods (photography, laser scanners, optoelectronic

instruments, stereophotogrammetry, Moiré topography) (De Menezes and Sforza 2010).

1. Photography

Facial and intraoral photographs have been used to assess and monitor facial asymmetry. For that purpose, facial photographs of patients with asymmetry can be taken in frontal view, in profile view and three-quarter profile view from both right and left sides. Inferior and superior views of mandible may also be useful records. A frontal photograph of the patient taken in occlusion while biting on a tongue spatula will document a transverse occlusal cant. The intraoral photographs will give a record of the occlusion and they should be taken both in centric occlusion and in centric relation in case that the patient exhibit a functional displacement of the mandible (Edler et al, 2001; Edler et al, 2002; Chia et al, 2008; Hwang et al, 2009; Lee et al, 2010).

The key requirement in dental photography is the sufficient standardization of the photographic setup, especially as regard the patient position. With this approach reproducibility of the records is high and the measurements can relate well to clinical opinion (Edler et al, 2001; Edler et al, 2002). Edler et al (2004) carried out computerized measurements, obtained by digitizing mandibular outlines from standardized facial photographs and they found out that the parameters of the mandibular size and shape are useful in the analysis of mandibular asymmetry.

Photography is a simple, inexpensive and noninvasive method of capturing and recording soft tissue facial asymmetry and it has been adopted by the medical community in order to enhance the patient record. However, several factors may cause disparity when contrasting two apparently similar photographic images: distance between subject and camera, camera angulation, roll-pitch-yaw orientation of the head, and photographic protocol inconsistencies (Lane and Harrell, 2008). Taking the above into account, photography is not a valid means of accurate

diagnosis of the asymmetric structures, thus it cannot be used in the treatment planning.

2. Stereophotogrammetry

Stereophotogrammetry is a sophisticated software technique based on the fundamental principle of taking multiple photographic images of the same object from different angles to acquire a three-dimensional image. It has been implemented in orthodontics to monitor growth, assess the outcome of the treatment and evaluate asymmetry (Hajeer et al, 2004; Chia et al, 2008; Lane and Harrell, 2008). To decrease inaccuracy from head movements as well as changes in expression of the face, pictures from two sides of the face are taken simultaneously with reduced duration of exposure (Hajeer et al, 2004).

Hajeer et al. (Hajeer et al. 2004) examined the preoperative and postoperative facial soft tissue asymmetry of 44 patients separated in three groups: Class III treated by maxillary advancement, Class III treated by bimaxillary surgery, Class II treated by maxillary impaction and mandibular advancement. 3D facial images were taken with a stereophotogrammetry-based imaging system (C3D® system) and were analyzed by a custom-written software (the Facial Analysis Tool®-FAT). This study showed that orthognathic surgery improved facial symmetry, especially in skeletal Class III patients treated by double-jaw operation. The patients treated by single-jaw surgery did not exhibit significant improvement of asymmetry. Finally, in Class II patients facial symmetry deteriorated after orthognathic surgery, particularly at the nose tip and chin prominence. The authors concluded that during maxillary impaction and mandibular advancement the surgeon should take precautions to prevent asymmetry of the tip of the nose or the prominence of the chin.

Hornado et al (2006) studied 32 patients that underwent maxillary movement with upward rotation, maxillary movement with downward rotation, or maxillary movement without rotation. The 3d photographs were taken with the 3dMDface System (3dMD, Atlanta, Ga) and preoperative and postoperative measurements were

performed for interalar width, internostril width, nasal tip projection, columellar length and nasolabial angle. According to the results of this study, there is a statistically significant increase in postoperative interalar width and internostril width after maxillary movement, but no predictable correlation could be demonstrated between the amount of change and maxillary movement. However, nasal tip projection, columellar length did not present a statistically significant change, with the data showing both decreases and increases. Interestingly, impaction of maxilla did have a statistically significant increase in the nasolabial angle. The authors demonstrated that the 3D digital imaging technique can be a sensitive diagnostic implement in analyzing the head and neck region.

Ubaya et al (2012) evaluated the 3D naso-maxillary complex soft tissue morphology following Le Fort I maxillary advancement and compared the findings with a local reference group with harmonious facial appearance. Stereophotogrammetric images of the subjects were captured using the Di3D system (Di3D, Dimensional Imaging, Hillington Park, Glasgow, UK). An increase in the nasal base width was found in the orthognathic group compared with the reference group, as well a decrease in the nasiolabial angle in the female orthognathic subgroup. According to the authors, 3D soft tissue analysis based on stereophotogrammetry provides a realistic measurement of facial appearance and provides an invaluable diagnostic tool.

Choi et al (2014) examined the postoperative soft tissue changes in a sample of 25 Asian Class III patients who had been treated by double-jaw rotational surgery with mandibular setback and posterior impaction of maxilla. For that purpose, 3D photographs of each face were captured with a 3D stereophotogrammetric camera setup and the software program modular system version 2.0 (Canfield, Vectra, USA). The authors reached the conclusion that the 3D camera was efficient in frontal soft tissue analysis, and allowed quantitative measurements of the changes in frontal soft tissue landmarks and facial proportions. They concluded that the stereophotogrammetric analysis was superior to the conventional 2D cephalometric analysis in the assessment of postoperative soft tissue changes.

3. Surface laser scanning

Surface laser scanning is widely used to obtain a 3D image of the facial soft tissues and enables the evaluation of the postoperative result. The fundamental principle of this method is that a laser light source illuminates the face, and digital cameras capture the reflected light; the depth information is acquired by triangulation geometry (McCance et al. 1992; Moss et al, 1994; Day and Robert, 2006).

3D laser scanning has proved to be a simple, non-contact, noninvasive method that does not expose the patient to any ionizing radiation. It uses a nonhazardous laser, reproduces the color and texture of soft tissues well, and reconstructs 3D images on the related software (McCance et al, 1992; Baik et al, 2010). Kau et al (2006) examined the reliability of three-dimensional soft tissue analysis with the use of a laser scanning system, and found soft tissue appearance capture to be clinically reproducible within a week. 90% of the facial morphology was accurate to within 0.7-0.8 mm. Further advantages are its ability to perform auto-calibration and to achieve automatic image distortion correction (Hajeer et al, 2004; Day and Robert, 2006; Ramieri et al, 2006). It is a very useful tool in auditing surgical outcome and it can be used presurgically as a visualization technique to be used to communicate the expected changes to both clinicians and patients (Miller et al, 2007).

Soncul and Bamber (2004) examined the effects of Class III bimaxillary orthognathic surgery on facial soft tissues with the use of optical surface scans. 3D pre- and postoperative optical surface images were superimposed on 5 markers, including the right and left Endocanthion, the right and left Exanthion and the soft tissue Nasion. The soft tissue changes following orthognathic surgery are not easy to predict, changes may range from 30% on the nasal tip to 80% on Subnasale and from 50% on subcomissural region corresponding to lateral parts of the mandibular body to 100% on the Pogonion.

Verdenik and Ihan Hren (2014) examined postoperative changes of soft tissue tissues in regions of the face that are not directly affected by surgical movements of the underlying jaw bones. The sample consisted of 83 Class III adults classified into

3 groups according to the type of surgery they underwent: bilateral sagittal split osteotomy set-back of the mandible (BSSO), Le Fort I advancement of the maxilla, or a combination of both. 3D scans were carried out before surgery and at 6 months after surgery using an Artec 3D scanner, which uses the flying triangulation method to capture a 3D surface (Ettl, Arold, Yang and Hausler 2012) and the STL formats were analyzed using the computer program RapidForm 2006 (INUS Technology Inc.). The pre and post-surgical surface models were registered on the forehead and both orbits. As expected, soft tissue changes were greater in the regions where the underlying skeletal units had been repositioned, but regardless of the operation performed, soft tissue changes did occur over the whole face. Changes in the lower lip and chin region in the Le Fort I group and in the nose, cheek, and upper lip regions in the BSSO group confirmed the concept of the facial soft tissue mask acting as one unit.

4. Electromagnetic digitizer

Electromagnetic digitizers define the three-dimensional coordinates of facial landmarks that are previously marked on the actual skin surface of the patient, which directly correspond to anatomical and anthropometric structures (De Menezes and Sforza, 2010). The facial landmarks are digitized one by one using a stylus connected to the digitizer (Ozsoy et al, 2009). Electromagnetic digitizer is superior to the two-dimensional methods (Soncul and Bamber 2004) but also to the optical methods (laser scanners, three-dimensional range-cameras, and stereophotogrammetry). It defines the spatial position of landmarks and it eliminates any discrepancy between the actual anthropometric points and their digital equivalents, that may occur in the non-contact optical methods (White et al. 2004). The data obtained with electromagnetic digitizer has been proved to be equivalent to the conventional anthropometric measurements (Sforza et al, 2004).

One important disadvantage of the electromagnetic digitizers is that the acquisition of only single, selected landmarks from the entire facial surface impedes the generation of life-like facial models. Moreover, data acquisition time is a

drawback; the digitization of the landmarks lasts approximately 1 minute. Movements of facial muscles, as well as global head movements, during digitization may produce errors (Sforza et al. 2007; De Menezes and Sforza, 2010).

Ferrario et al (2001) assessed the effects of sex and age on 3-dimensional (3D) soft-tissue facial asymmetry of normal subjects with a 3D computerized electromagnetic digitizer (3Draw; Polhemus Inc, Colchester, VT). The sample consisted of 314 normal subject and 23 soft tissue landmarks were digitized for each. A slight soft-tissue facial asymmetry was found in normal subjects, but no gender- or age-related correlation was observed. Tragion, Gonion, and Zygion were the most asymmetric points, whereas the least asymmetric was Endocanthion.

Sforza et al (2007) studied 9 patients with severe skeletal Class III malocclusion and moderate-to-severe mandibular asymmetry that underwent mandibular setback by sagittal split osteotomy and LeFort I maxillary advancement. The three-dimensional coordinates of 50 facial landmarks were defined with a three-dimensional computerized electromagnetic digitizer (3 Draw, Polhemus Inc, Colchester, VT). The measurements were compared not only within the same patient (2.5 months preoperatively and 9 months postoperatively), but also with reference standards derived from healthy people of similar characteristics in terms of sex, age, and ethnicity. Patients presented higher degree of asymmetry than normal subjects preoperatively, particularly in the gonion area. Postoperatively, total and lateral asymmetry was considerably improved.

5. Optoelectronic digitizer

The optoelectronic system uses an automatic image analyzer (ELITE, BTS, Milan, Italy) that provides the 3-D metric coordinates of selected landmarks introduced into a work volume of calibrated dimensions. The landmarks are recognized by means of wireless, stroboscopically illuminated retroreflective markers and two high-resolution infrared-sensitive video cameras with electronic shutters. The two cameras capture the subject under different points of view, and the software provides a single stereophotogrammetric image of the landmarks (Ferrario et al, 1999).

Ferrario et al (1994) used an optoelectronic device (ELITE system: BTS, Milan, Italy) to evaluate the asymmetry in 80 normal adults with no craniofacial or dental disorders. A certain degree of soft-tissue facial asymmetry was found in the normal adults, and it was evident especially in the middle and lower thirds of the face. The right side of face was larger than the left side.

Ferrario et al (1999) performed a quantitative analysis of soft tissue facial morphology changes in a sample of 5 skeletal Class III asymmetric patients that were treated by mandibular setback and maxillary advancement. The 3-dimensional coordinates of 22 facial soft tissue points were defined on each subject through an optoelectronic device (3-Dimensional Facial Morphometry; 3DFM). Results showed that the overall facial soft tissue asymmetry was deteriorated postoperatively, but asymmetry in the lower third of face was improved.

2. X-ray methods

Craniofacial asymmetry has been traditionally diagnosed through panoramic, submentovertex and posteroanterior radiographs. However, conventional radiographic techniques have inherent limitations due to projection techniques, since complex 3-dimensional structures are projected onto a flat 2-D surface. Distortion and magnification errors may lead to misdiagnosis. Given the importance of precision in the diagnosis and treatment planning of craniofacial deformities, computed tomography (CT) was introduced and enabled accurate detection and quantitative measurement of asymmetry. Finally, cone-beam CT (CBCT) was developed for 3-dimensional (3D) imaging of the maxillofacial area and has become popular in dentistry, orthodontics, and maxillofacial surgery.

1. Panoramic radiography

Orthopantomograms provide an opportunity to assess the osseous structures and the dentition in the mandible and the maxilla with relative ease. Although panoramic radiographs facilitate the evaluation of the architecture of the condyle and of any discrepancies within the body or ramus of the mandible, they are subject to

magnification, distortion and superimposition problems (Bagheri et al, 2012). It has been shown that vertical measurements, though more precise than horizontal or angular measurements, they are still not reliable representations of the anatomical structures they correspond to (Van Elslande et al, 2008). Because of these limitations they cannot be used for accurate measurements and diagnosis of mandibular asymmetry. The orthopantomogram is one of the routine radiographic projections in the initial assessment of orthodontic patients and, although its diagnostic capacity to detect mandibular asymmetry is low, it can assist as a general overview image, indicating other special investigation.

2. Submentovertex radiographs

The submentovertex radiograph was incorporated in the assessment of facial asymmetry, because it identifies the position and the orientation of the condyles and it offers the advantage that the median sagittal reference plane can be defined on cranial structures (Ritucci and Burstone, 1981). Since cranial base is separated from the facial bones and has been shown to possess a high degree of symmetry, it can be used as reference to determine the midsagittal plane (Pearson and Woo, 1935; Kwon et al, 2006). The bowing and warping of the mandible caused by the asymmetric growth can be visualized for both diagnostic and treatment considerations (Bagheri et al, 2012). Several methods for analyzing the submentovertex view have been described (Fosberg et al, 1984; Lew and Tay, 1993) but the patient posture during x-ray exposure can affect the reliability of the method (Lew and Tay, 1993). As a two-dimensional image it has inherent sources of error including magnification, superimposition of the anatomical structures and difficulty to detect deformities in the midface region, and distortion (Fosberg et al, 1984; Kim et al, 2015).

3. Posteroanterior cephalogram

The posteroanterior cephalogram allows the comparison of left and right facial halves and has been used in the evaluation of facial asymmetry. Unequal

enlargement and distortion are minimized since the left and right structures are located at the same distance from the film and x-ray source. Discrepancies between the midlines of the skeletal structures and the dentition can also be evaluated. Finally, functional deviation can be also examined through the comparison of posteroanterior views at the centric occlusion and open mouth positions (Grummons and Kappeyne van de Coppello, 1987; Chia et al, 2008; Cheong et al, 2011).

In most cases, posteroanterior cephalogram can be a useful tool to diagnose the presence and degree of facial asymmetry, but it does not provide precise information to assess the causes of the asymmetry and assist the treatment planning (Hwang et al, 2006). Posteroanterior cephalograms may be misleading, because vertical head rotation may cause projection errors and width measurements have not been found reliable for the diagnosis of asymmetry (Pirttiniemi et al, 1996; Koh et al, 2003; Tai et al, 2014). Moreover, in a posteroanterior cephalogram it is impossible to identify anatomical structures on the posterior part of the face, because these are overlaid or obscured by the more anterior anatomical structures. Since head positioning for cephalometry is based on the external auditory meatus, asymmetric external auditory meati may modify the symmetry of other anatomical structures.

In a study carried out in 2011 (de Moraes et al, 2011), craniofacial asymmetry was assessed and two-dimensional posteroanterior cephalometric measurements and three-dimensional CBCT measurements were compared with physical measurements on 10 dry human skulls. Radiopaque markers were placed on the skulls and physical measurements were made with a digital caliper. Apparently symmetrical normal skulls had some discrepancies between the right and left sides. When the methods were compared, there was poor correspondence between the digital 2D and the physical measurements and almost perfect correspondence between the CBCT and the physical measurements. CBCT offers more precise assessment of craniofacial asymmetry in comparison with digital 2D images.

Kim et al (2013b) compared two-dimensional measurements obtained by lateral and posteroanterior cephalometrics with three-dimensional CBCT measurements in two groups of patients with either only mandibular asymmetry or mandibular and midfacial asymmetry. This study showed significant inter-

dimensional differences in gonial angle, ramus length, lateral ramus inclination, occlusal cant, mandibular body height and maxillary height in all types of asymmetry. According to Kim et al (2013b) two-dimensional analysis of asymmetry is not accurate and CBCT analysis should be performed in asymmetric cases.

4. The Computed Tomography (CT)

CT scans incorporate radiographic techniques with computerized volumetric reconstruction and are able to generate computerized 3D images. They have high diagnostic value because of their clarity and accuracy and there is no overlapping of images or distortion of images. The images produced are of three-dimensional form; hence, they can be viewed from various points and angles.

One important advantage of CT scans is the display and visualization of soft and hard tissue information in the same image. This enables the registration of pre- and postoperative images according to predefined hard tissue points of interest and establishes both the hard and soft tissue landmarks in the same Cartesian coordinate system (Swennen et al. 2005). Furthermore, with CT scans, the operator is able to edit the properties of the image, including such characteristics as opacity and gray scale, in order to enhance visibility or detail as needed. CT offers the option of volume rendering. In volume rendering, the volume of a structure is windowed and leveled to optimize for the tissues of interest and an opacity level assigned to various displayed tissues. This enables the simultaneous visualization of layered tissues. The scans may also be viewed in cross sections, or individual structures may be segmented and isolated for optimal viewing (Quintero, Trosien, Hatcher and Kapila 1999; Swennen et al. 2005). Moreover, standardized head positioning is not as critical with CT scans as it is with the conventional radiographs because the head reorientation is possible using the appropriate software (Swennen et al. 2005).

On the other hand, CT has significant disadvantages, such as the high cost, the high radiation exposure to patients, artifacts created by foreign objects like

restoration and prosthetics and inadequate soft tissue contrast (Karatas and Toy, 2014). Due to these disadvantages, CT is rarely indicated for orthodontic reasons.

Maeda et al (2006) suggested a classification system for facial asymmetry based on 3-dimensional-computed tomography images. Preoperative CT images were taken and investigated for 49 patients with maxillofacial deformities. Asymmetry indices were calculated for some skeletal landmarks in the maxilla, mandibular body and the mandibular ramus region. According to the topography of asymmetry the following classification system was created: Subjects in Group I (44.9%) present no asymmetry, while Groups II or III were created for subjects without or with maxillary asymmetry, respectively, and they were subcategorized. In Group IIA (8.2%), asymmetry was shown solely in the mandibular body, and in Group IIB (18.4%), additional asymmetry was shown in the mandibular ramus. Group IIIA (6.1%) showed asymmetry only in the maxillary region, and Group IIIB (22.4%) showed asymmetry in all 3 regions. Of course, attention should be paid to the increased radiation exposure to patients on these examinations. The dose reduction should be performed with preservation of sufficient image quality and may be accomplished through the use of the CBCT.

Baek et al (2007) examined the skeletodental factors contributing to chin point deviation of facial asymmetry in a CT study of 40 Korean female skeletal Class III patients. According to the results of this study, greater growth and mesial inclination of the ramus and more maxillary vertical excess in the nondeviated side were the reasons of facial asymmetry in the skeletal class III patients.

Jung et al (2009) investigated postsurgical changes caused by mandibular setback surgery in the hard and soft tissues of skeletal Class III malocclusion patients with or without facial asymmetry. 17 Class III patients diagnosed with mandibular prognathism and treated with bilateral sagittal split ramus osteotomy only were divided into two group according to the Menton deviation from the facial midline (symmetry group:n=8; Menton deviation less than 4mm, asymmetry group: n 9; Menton deviation more than 4 mm). CT scans were taken 1 month before and 6 months after the orthognathic surgery. The measurements of hard tissue changes showed that a degree of skeletal asymmetry remained after surgical correction in the

asymmetry group. As regard the soft tissues in the symmetry group, there were significant changes on the chin, lower lip and gonial angle area on both sides. However, in asymmetry group, significant changes occurred not only on the chin and lower lip but also on the upper lip and mouth corner in the deviated side and the gonial angle in the nondeviated side.

You et al (2010) used 3D-CT images to examine the asymmetry of morphology and dimensions in condylar, coronoid, angular, body, and chin units of the mandibles in Class III patients. According to the degree of Menton deviation, patients were separated in the symmetry group (n=20) and the asymmetry group (n=30). Linear measurements, as well as the ramal and body volumes were calculated in the hemi-mandibles. On the nondeviated side of the asymmetric group, condylar and body unit lengths and ramal volume were significantly greater, and coronoid unit length was significantly shorter compared with the deviated side. Angular and chin unit lengths and body volume were not significantly divergent between the two sides. According to these results, both condylar and body units seemed to contribute to mandibular asymmetry, with a more essential role of the condylar unit.

Yáñez-Vico et al (2011) evaluated the skeletal symmetry of 21 patients using CT scans. Except the symmetry of specific skeletal landmarks, they examined the following values that have been find to cause asymmetry: ramal height, mandibular body length, mandibular angle, maxillary height, frontal and lateral ramal inclination. The Gonion appeared as the most asymmetric landmark in all subjects, and the Anterior Nasal Spine demonstrated the least discrepancy. This finding was in agreement with the results of a previous CT study of Katsumata et al (2005). The lateral inclination of the mandibular ramus emerged as the value with the greatest deviation, followed by the frontal ramal inclination. Deviations in lateral and frontal inclinations of the mandibular ramus impose obvious facial asymmetry and have an impact on the surgical treatment plan for correction of the craniofacial asymmetry.

5. The Cone Beam Computed Tomography (CBCT)

The Cone Beam Computed Tomography (CBCT) technique was introduced in the 1990s (Kau et al. 2005). Innately, CBCT data is illustrated as undistorted inter-relational images in the orthogonal planes; though, there are several modalities, such as maximum intensity projection, surface or volumetric rendering which enable 3D visualization of the craniofacial complex and soft tissue boundaries like facial outline (Evans et al, 2013).

CBCT scans combine the imaging advantages of CT scans with a significantly decreased lower radiation exposure and shorter scan acquisition time. This is attributed to the fact that CBCT scanners use a cone-beam geometry and, consequently, a sole scanning rotation of the X-ray source and detector around the subject (Mah et al, 2003; Kau et al. 2005; Swennen et al. 2005; El and Palomo 2010; Kau and Richmond 2010). Moreover, the cost of CBCT is low compared to CT and image processing is easier since it is restricted in the head and face region. CBCT technique is an in-office imaging, thus it is available for the routine dentofacial diagnosis (Swennen and Schutyser 2006; Karatas and Toy 2014).

In the last few years there has been a dramatic increase in the use of CBCT in orthodontics, assisting the diagnosis and the treatment planning evaluation of the outcome and follow-up control of maxillofacial-deformity treatment. The most important advantage that CBCT scans can generate numerous linear or curved planar projections currently used in orthodontic diagnosis, cephalometric analysis, and treatment planning. Furthermore, 3D images can be reconstructed from the data obtained by a single CBCT scan (Evans et al, 2013).

CBCT technology has found particular applications in orthodontics and it is the diagnostic method of choice for examination of dental structural or positional anomalies, temporomandibular joint pathology, dentofacial deformities and craniofacial anomalies and the assessment of airway morphology (Grauer et al., 2010). CBCT is nowadays incorporated in all stages of orthognathic surgical treatment. It assists the diagnosis of the skeletofacial deformity, detecting any asymmetry of the affected structures and it enables 3D virtual surgical planning and surgical guidance. With the available software tools osteotomies, virtual repositioning simulation of the jaws, distraction osteogenesis and other procedures

can be effectively performed. CBCT has also been employed in the evaluation of the surgical outcome and, apparently, one of the main advantages is that it displays both the hard and soft tissues into the same image. This allows the investigation of the possible relation between their alterations (Swennen and Schutyser, 2006; Chan et al., 2007).

However, there are few disadvantages in CBCT imaging. One major disadvantage is the limited contrast resolution, particularly because of relatively high scatter radiation during scanning, and inherent flat panel detector related artifacts. Although CBCT provides clinical sufficiency for examination of hard tissues, it is not sufficient for soft tissue evaluation (Ludlow and Ivanovic, 2008; White and Pharoah, 2009). However, Fourie et al (2011a) showed that the CBCT soft tissue measurements are of high reproducibility and accuracy. In another study (Fourie et al, 2011b), linear soft tissue measurements obtained manually on cadaver heads were compared to 3D measurements from three different methods (CBCT, laser surface scanning and Di3D stereo- photogrammetry). All the 3D scanning systems appeared to be very reliable when compared to the physical measurement.

Though radiation dose of CBCT scans is significantly lower compared to CT scans, risks have also been noted and CBCT examinations cannot be carried out on a routine basis for every patient, but it should be utilized only for selected cases where the benefit outweighs the cost. The effective radiation dose of CBCT can be influenced by the factors of patient size, field of view (FOV), region of interest, and resolution. The operator should perform a careful selection of these parameters to improve the efficiency of the diagnostic information and decrease the patient's exposure (Horner, 2009; Abibi et al, 2012).

Although streaking and motion artifacts or image artifacts created by metal brackets and restorations are largely reduced with current CBCT units, they are not totally eliminated (Scarfe, Farman and Sukovic 2006; Swennen and Schutyser 2006; Abibi et al, 2012; Karatas and Toy 2014).

The published investigations

Lee et al (2011) studied the correlation between soft and hard tissues changes in class III orthognathic patients using CBCT . 18 Class III surgical patients were separated into 2 groups according to the severity of their Menton deviation. The CBCTs were taken before and 6 months after surgery. The results revealed significant correlations between soft and hard tissue changes on the horizontal and sagittal axes in both groups, but their proportions were different between the two groups. The effect of hard tissue to soft tissue changes was greater in the presence of asymmetry.

Lee et al (2012) conducted a CBCT study to investigate the differences in mandibular morphology and dimensions between the two sides of the face in two groups: 38 subjects with normal occlusion and 28 skeletal Class III patients with facial asymmetry. Significant differences were found between the deviated and contralateral sides of the asymmetry group in condylar and ramus heights, posterior part of the mandibular body, and mediolateral ramal and anteroposterior condylar inclinations in comparison to those of the normal subjects. The deviated side of the asymmetry group had a significantly larger mediolateral ramal inclination than the nondeviated side.

Hwang et al (2012) used CBCT analysis to identify the asymmetry of soft tissue landmarks in normal occlusion subjects. 27 soft tissue landmarks, 9 midline and 9 pairs of bilateral landmarks, were localized in 3D coordination system. The midline landmark asymmetry ranged from 0.6 to 1.5mm and was generally lower compared to bilateral landmark asymmetry, which varied from 1,5 to 4,6mm. The discrepancies between the right and left side showed a tendency to increase according to the lower and lateral positioning of the landmarks in the face.

Lee et al (2013) studied the relation between the asymmetric mandibular prognathism and a fundamental difference in soft tissue thickness and the effect of the asymmetric mandibular setback surgery on the contour and thickness of the soft tissues. The sample of this study was consisted of skeletal class III patients with significant mandibular chin deviation greater than 6 mm at the Pogonion, who had

undergone CBCT before and 6 months after surgery. Preoperatively, the deviation side had a more prominent hard and soft tissue contour, but a thinner soft tissue thickness, which masked the hard tissue asymmetry. Postoperatively, there was a great improvement in the hard and soft tissue contour and the symmetry of soft tissue thickness. Most of the soft tissue thickness changes correlated negatively with the hard tissue changes and favorable response of the soft tissues was observed postsurgically.

Kim et al (2013a) analyzed CBCT images of prognathic patients who had undergone either bimaxillary surgery or only mandibular setback surgery to assess soft tissue changes of the middle and lower third of the face and identify any differences between the single or double-jaw surgery groups. The findings showed significant differences in the middle third of the face between the single- and double-jaw surgery groups, with changes being more evident in the 2-jaw surgery group. The alar base showed significant lateral movement in the 2-jaw surgery patients, caution should be exercised in patients who have a wide alar base. Soft tissues alterations in the lower third of the face were found in both surgery groups, but they were insignificant.

Sanders et al (2014) carried out a CBCT study to describe the features of facial and dental asymmetries in a normal, adolescent population consisting of 30 patients. The examination of asymmetry of this sample demonstrated either mild right-side predominance or a mild left-side deficiency in the auriculo-temporal and condylar regions. The glenoid fossa was more laterally displaced on the right side and, along with the Porion, was more superior in relation to the axial plane compared to the left side. Additionally, the condylar points were all more laterally displaced and the 2D and 3D measured ramus heights were greater on the right side. The frontal ramus inclination was also more obtuse on the right side compared to the left, and the PNS point was found to lie to the right of the midsagittal plane. Maxillary and mandibular arch lengths were the only measurements which were increased on the left side. CBCT analysis indicated minor asymmetries in all planes of space in an apparently normal symmetric population.

van Loon et al. (2015) used CBCT images to measure the maxillary translation and 3dMD images to measure the nasal volume, upper lip volume and the inter-alar width changes in patients who underwent a Le Fort I osteotomy, with or without a bilateral sagittal split osteotomy. According to the results, anterior translation and clockwise pitching of the maxilla resulted in a significant volume increase in the lip. Cranial translation of the maxilla led to an increase in the alar width. These results come in agreement with a previous study of Park et al (2011), who evaluated nasal morphologic and maxillary skeletal changes after bimaxillary surgery (Le Fort I advancement with impaction and mandibular setback). According to Park et al (2011), the upward and forward movement of maxilla appeared to cause anterosuperior shift of the nasal tip and widening of the alar base and nostrils.

Ryu et al (2015) analyzed the rotational patterns of dentofacial structures and their impact on Menton deviation in a skeletal Class III asymmetry group and a normal group. CBCT assessment revealed significantly larger measurements of mandibular roll and yaw in the asymmetry than the control group, implying that menton deviation in skeletal Class III deformity with mandibular asymmetry is influenced by rotation of mandibular posterior dentofacial structures.

Nur et al (2016) used CBCT analysis in 2 groups of symmetric and asymmetric patients to evaluate the facial asymmetry and compare the right and left facial hard and soft tissues volumetrically to find out if there are any compensations. The asymmetry analysis included linear, surface distance, angular, volumetric, and surface area measurements. In the asymmetric subjects, the gonial morphology showed 3D surface alterations and the authors suggested that multiple points (Gonion inferior, Gonion posterior, Gonion lateral) should be used in the Gonion area for a detailed diagnosis of asymmetry . Moreover, in the asymmetric group, asymmetry was more frequently identified in the lower rather than in the middle third of the face according to volumetric and surface area measurements. Even in the symmetry group, mild asymmetries were observed that were compensated for by surface modifications of the skeletal units or soft tissue adaptations. The authors reached the conclusion that the soft tissues may compensate for the skeletal asymmetry. A thin soft tissue layer such as in the menton region has less potential for compensation;

nevertheless, in areas with thicker layers, such as the gonial region the compensation effect is stronger. Skeletal transverse asymmetries were apparently identified at the gonial and occlusal levels, but no soft tissue transverse discrepancies could be detected at the same level, probably due to soft tissue thickness compensation. However, 3D right and left volumetric soft tissue evaluations confirmed the asymmetry. In this study, facial hard and soft tissue asymmetries were accurately quantified using CBCT.

Lin et al (2016) examined the true asymmetry of the mandible after mandibular deviation correction by a virtual bilateral sagittal split ramus osteotomy in a sample of 45 severe asymmetric cases with menton deviation more than 4mm. The residual asymmetry, characterized as the superimposition and boolean operation of the mirrored elongation side on the normal side, was quantified, including the volumetric differences and the length of transversal and vertical asymmetry discrepancy. For more specific evaluation, both sides of the hemi-mandible were divided into the three regions: 1) symphysis and parasymphysis (SP), 2) mandibular body (MB), and 3) mandibular angle (MA). After correction of Menton deviation mandibular asymmetry persisted: The average volumetric discrepancy after virtual Me point correction in the SP, MB, and MA regions were 407.8±64.8 mm^3, 2139.1±72.5 mm^3, and 422.5±36.9mm^3, respectively and all of them were of statistical significance. Results showed transverse discrepancy in the symphysis and parasymphysis region, vertical discrepancy in mandibular body and both vertical and transverse asymmetry of the mandibular angle. This study provides useful information for adjunctive, cosmetic, surgical procedures that should be performed concomitantly, perioperatively or at a distant time from the orthognathic surgery to address specific undesirable skeletal and soft tissue deviations.

Thiesen et al (2017) analyzed the symmetry of several mandibular and maxillary components related to different degrees of mandibular deviation. They investigated the CBCT images from 138 patients, who were classified into three groups according to the Gnathion deviation from the midsagittal plane: relative symmetry group had deviation up to 2mm, moderate asymmetry group had Gnathion displacement 2-4 mm and asymmetry group had deviation higher than 4mm. For

patients with moderate and severe mandibular asymmetry, there was a statistically significant difference in bilateral measurements for transverse and sagittal positioning of the Gonion, sagittal positioning of the condylar heads, mandibular body length, and ramus height, and transverse and vertical positioning of the Jugale point. In severe asymmetry group, a difference in the vertical positioning of the Gonion was observed between the deviated and the contralateral side. In addition in the severe asymmetry group, a highly relevant correlation of Gnathion lateral displacement with lower dental midline displacement and with the difference in height of the mandibular rami between the deviated and contralateral sides was found.

4.2.4.2.5.1 The Asymmetry Index

Apart from the asymmetry of the skeletofacial structures, CBCT has been employed to evaluate the asymmetry of the anatomical landmarks. For this reason, an Asymmetry Index has been developed, which is mainly an application of the geometric formula to calculate the distance of the points in space.

The Asymmetry Index was introduced by Katsumata et al (2005), in order to evaluate the asymmetry of anatomical points in three planes of space. After the reference planes were defined, the distances between each anatomical point and the theee planes were measured in millimeters and defined as dx, dy, and dz. The differences in the values of dx, dy, and dz between the right and left sides were considered as the elements of a 3D vector. The asymmetry index of each bilateral point, that is the length of 3D vector, was calculated using the following formula, where R = right and L = left:

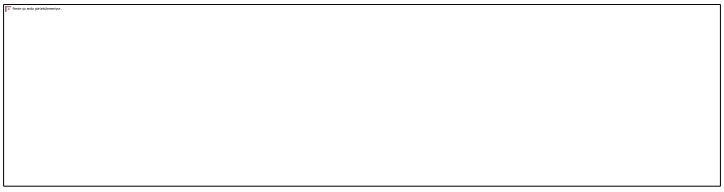

As there is no difference in the dy and dz values between the right and the left sides for solitary paramedial points in this instance, dx distance expresses the Asymmetry Index. For perfect symmetrical paired bilateral landmarks, the discrepancy in dx,dy, and dz should approach zero.

This formula is an extension of the Pythagorean theorem into three dimensions and gives the distance of two points in the 3d coordinate geometry. In 3d geometry the three coordinate planes divide space into eight parts, called octants. However, since Katsumata et al (2005) applied the absolute values dx, dy, dz for two points, which define the distances between each anatomical point and the three planes, the two bilateral points are reflected across the yz, xz, xy planes and interpreted into the first octant of the 3d coordinate system, where coordinates x,y,z of all points are positive. Perfectly symmetric bilateral points should coincide after the reflection. In the case that the points do not coincide, Katsumata ‘s formula gives the distance of the two bilateral reflected points in space, which can be used to evaluate the degree of their deviation and asymmetry.

Fig 4.1: The first octant, in the foreground, is determined by the positive axes.

Katsumata et al (2005) used a control group of symmetric patients to define a baseline for each point and evaluated the Asymmetry indices according to this. The baseline for each point was defined as the mean asymmetry indices plus the standard deviation in control subjects and was used as the threshold to define an anatomical point as asymmetric or not. For each anatomical landmark, the index was classified into one of 3 categories, “Symmetry”, “Asymmetry” and “Marked asymmetry”. “Symmetry” was defined as the index within the mean plus the standard deviation of normal subjects (baseline), “Asymmetry” was between the values of the baseline and twice the baseline, and “Marked asymmetry” was defined as the value beyond twice the baseline.

The Asymmetry Index designed by Katsumata et al (2005) has been been used in many reports in the evaluation of skeletal asymmetry (Maeda et al, 2006; Yanez Vico et al, 2011) and soft tissue asymmetry (Huang et al, 2013).

Maeda et al (2006) conducted a study based in the formula that Katsumata et al (2005) introduced, in order to characterize the symmetrical features of patients with facial deformities in comparison with normal subjects and to suggest a classification system for facial asymmetry based on 3D-CT evaluation. In this study, Menton showed marked asymmetry in the prognathic patients, whereas significant asymmetry was found in the region of area.

Yanez Vico et al (2011) utilized the asymmetry indices of craniometric landmarks to correlate them with the structures and craniofacial dimensions that possibly affect the facial asymmetry. The asymmetry index of the Menton correlated positively with asymmetry of the frontal ramal inclination and negatively with mandibular body length such that the greater the asymmetry of the menton, the greater the difference between the frontal inclinations of both ramuses (left and right) and the greater the symmetry between left and right mandibular body lengths.

Huang et al (2013) used the predefined Asymmetry Index to identify the right and left difference of the facial soft tissue landmarks three-dimensionally from the subjects of normal occlusion individuals. The authors found out that right and left difference values tended to increase according to the lower and lateral positioning of the landmarks in the face.

Hofman et al (2016) evaluated patients with oculoauriculovertebral spectrum malformations using Katsumata's asymmetry index and assessed the usefulness of the scores thus obtained in identifying degrees and sites of asymmetry. The conclusion of this study was that the Asymmetry index sheds light both on the presence and on the severity of asymmetries. Katsumata's asymmetry index is capable of yielding clearly structured and illustrative views of landmark distribution, thus, being a suitable diagnostic tool to evaluate asymmetry in cases of oculoauriculovertebral spectrum and to identify which skeletal regions are involved. Selecting an appropriately large and symmetrical control group is essential to the amount of information that can be derived from this index.

3. Treatment of Class III malocclusion

1. Treatment approaches

There are mainly three approaches for the treatment of a skeletal Class III deformity depending on the degree of skeletal discrepancy, the skeletal pattern, and the age of the patient, including:

1. Growth modification in early age, by the means of appliances as Functional Class III Regulator, Protaction face mask, Chin cup.

2. Dentoalveolar compensation (orthodontic camouflage) of the skeletal jaw discrepancy.

3. Combined orthodontic-orthognathic surgical correction of the skeletal disharmony.

Growth modification is suitable for growing patients. Maxillary protraction is indicated in Class III patients with deficient maxilla and normal mandible. However, this approach cannot be applied to patients with overdeveloped mandible or if mandible continues to develop excessively. Late relapse has been described and it is always a possibility (Hagg et al, 2003; Baccetti et al, 2004).

After growth spurt, either dental camouflage or surgical correction is possible. Camouflage orthodontic treatment aims to a functional occlusion and an aesthetic profile without correcting the jaw discrepancy. It may be performed in patients with a mild skeletal Class III discrepancy and no remaining growth by selective tooth extraction, the use of the multiple edgewise arch wire (MEAW) technique to induce generalized distal tipping of the mandibular posterior segment, or the application of mini-implants to distalize the entire mandibular dentition.

However, in patients with a severe skeletal discrepancy or continuous mandibular growth and facial asymmetry, a combined surgical/orthodontic approach should be considered (Baik, 2007). This treatment modality leads to an improved dentofacial harmony to enhance patient’ s function and appearance. Surgical

correction of Class III malocclusion can be accomplished by mandibular setback, maxillary advancement, or a combination of both operations (Rabie, et al 2008). Moreover, during the surgery the maxilla may be inferiorly (maxillary down graft) or superiorly positioned (maxillary impaction) in order to achieve the ideal spatial repositioning of the jaws.

Because the subject of this thesis is concerned with the orthognathic surgical approach; the first and third subjects will not be discussed further and all the focus will be on the treatment of Class III skeletal malocclusion through combined orthodontic-orthognathic surgical correction.

1. Maxillary orthognathic surgery

The Le Fort I osteotomy of the maxilla is the most commonly maxillary operation and it prevails in the maxillary orthognathic surgery. It allows down-fracture, impaction and/or advancement movement of maxilla, to correct anteroposterior, vertical and transverse discrepancies. It can be performed solely or combined mandibular surgery and it offers predictability and great stability (Proffit et al. 2003).

Except the radiographic examination, some clinical indications of performing maxillary advancement are: 1)decreased pharyngeal airway, 2) excessive submental adipose tissue, 3) decreased malar convexity, 4) increased nasolabial grooves upon smiling.

Impaction of maxilla is indicated to correct the maxillary vertical excess when the following clinical manifestations are present: 1) increased tooth-to-lip relation, 2) increased gingival display 3) increased interlabial gap, 4) relative mandibular deficiency, 5) anterior open bite.

Inferior maxillary repositioning (down-graft) can be performed in cases that present with: 1) decreased tooth –to- lip relation, 2) decreased gingival display, 3) a relative mandibular prognathism and /or prominent chin.

The surgical procedure starts with the soft tissue dissection, the exposure of the maxilla and the nasal aperture. The osteotomy of the lateral maxilla begins posteriorly at the zygomatic maxillary buttress, about 35 mm above the maxillary occlusal plane. The osteotomy advances through the thicker bone at the buttress and the thin bone of the lateral maxillary wall to the piriform rim where the bone thickens again. Then, the osteotomy is directed inferiorly and posteriorly, from the zygomatic buttress to the junction of the maxilla and pterygoid plate. At the nasal floor the cartilaginous septum is freed and the bony septum and the lateral nasal wall are sectioned. The maxilla is released from the pterygoid plates with osteotome malleting. Down fracture of the maxilla is performed by finger pressure on the anterior aspect. After maxillary mobilization, and the insertion of the occlusal splint the jaws are held together and the surgeon places the maxilla into the planned position according to the reference marks he had already made. The bony and cartilage structures of the osteotomy are adjusted according to the movement of the maxilla so that better bony contact and esthetic results are achieved. Bone plates are preferred for transosseous fixation while bone grafts for stabilization might be utilized according to the needs of the case. Finally, the wound closure is performed including a variety of techniques such as V-Y mucosal (single or double), alar base cinch suture etc. (Proffit et al, 2003).

2. Mandibular setback surgery

Currently, the most common mandibular surgical procedures to setback the mandible are bilateral sagittal split ramus osteotomy (BSSRO) and intraoral vertical ramus osteotomy (IVRO) can be performed. Technically, the IVRO is a much simpler, faster, and less morbid procedure, compared to BSSRO (Nanda, 2005). However, BSSRO dominates nowadays in the mandibular orthognathic surgery , because it presents with the following advantages (Proffit et al, 2003; Proffit et al, 2007):

1. Great flexibility in repositioning the lower jaw. The mandible can be moved forward or back as desired, and the tooth-bearing segment can be rotated down anteriorly if additional anterior face height is desired.

2. It is quite compatible with the use of rigid internal fixation.

3. Excellent and broad bone-to-bone contact after the osteotomy minimizes healing problems.

4. Minimal alterations in the position of the muscles of mastication and the temporomandibular joint.

The procedure starts with the incision and periosteal elevation. The purpose of the soft-tissue dissection is the sufficient access for the osteotomy. The basic osteotomy pattern includes cuts just through the cortical bone: on the medial side of the ramus above the lingula, down the anterior ramus onto the superior aspect of the body of the mandible and then curving inferiorly through the lateral cortical plate, including the inferior border. The horizontal osteotomy should extend posteriorly one half or two thirds the anteroposterior dimension of the ramus and anteriorly until the second molar area. Then, after the split of the ramus the mandible is placed on the desired position according to the surgical plan and stabilized and fixed. The option most effective today is the rigid internal fixation (Proffit et al. 2003; Reyneke, 2010; Posnick, 2013).

1. Adjunctive, cosmetic surgical procedures

Adjunctive, cosmetic surgical procedures are usually added to the original jaw repositioning so that the orthognathic intervention meets the specific aesthetic needs of the patient. Approaching the orthognathic patients with aesthetic concerns in mind maximizes the overall benefit of orthognathic surgery, by accomplishing the maximal aesthetic outcome achievable for the patient. These interventions may be performed concomitantly, perioperatively or at a distant time from the orthognathic operation addressing specific undesirable deformities that remained or created during

the orthognathic surgery. The decision for the type and the timing of the intervention depends strongly on the soft tissue predictability. If predictability is low, the supplemental procedures should be performed separately from the orthognathic surgery (Sarver and Rousso, 2004; Mohamed and Perenack, 2014).

Adjunctive cosmetic procedures can be divided according to the facial region of intervention into the following categories:

1. Upper face procedures, including forehead/brow augmentation, temple augmentation, hairline augmentation.

2. Midface procedures, including orbital augmentation, malar osteotomies/implants, piriform augmentation, soft tissue augmentation, lip augmentation/shortening and rhinoplasty.

3. Lower face procedures, including chin augmentation/reduction, mandibular angle modification, submental/ jowl liposculpting and lower face/neck rhytidectomy.

4. Skin procedures, such as skin resurfacing, treatment of lesions, laser hair removal.

1. Genioplasty

Genioplasty is the most commonly performed aesthetic surgical procedure at the time of orthognathic surgery. Inferior border osteotomy, also referred to as genioplasty, can be used to correct abnormality in the anterior or the body of mandible, by altering the form in the vertical, transverse or anteroposterior dimensions (Proffit et al, 2003). It may involve augmentation or reduction of the chin and correction of chin cant or asymmetry and it be used alone or in conjunction with maxillary or mandibular operations.

Surgeons have two options for chin augmentation: osteplastic genioplasty by inferior border osteotomy or an alloplastic genioplasty by placing chin implants.

Regardless of the method of augmentation, it can be performed in conjunction with orthognathic surgery, or independently as an alternative in patients who are not willing to undergo orthognathic surgery but desire a stronger chin (Proffit et al, 2003; Fattahi, 2007).

A horizontal sliding osteotomy is made inferiorly and anteriorly to the mental foramen of the mandible to avoid damage to the mental nerve and roots of the teeth. The ostotomised chin is then reduced or advanced to a desired position and fixed by the means of plates and/or screws (Trauner and Obwegeser, 1957).

The advantages of the inferior border osteotomy include predictability, stability, and chin-neck contour changes. Because the mentalis muscle remains attached to the bony chin, the soft tissues changes secondary to chin advancement occur in a 1:1 ratio to bony advancement. Another advantage to advancing the chin via inferior border osteotomy is that it also advances the genial tubercles. This results in an improvement in chin-neck contour because of a tightening of the suprahyoid musculare. A disadvantage of the technique is the possibility of trauma to the mental nerve in the area of mental foramen, which can cause diminished sensation on the surface of the chin and the lower lip (Profitt et al, 2003; Fattahi, 2007).

Alloplastic chin implants can be used for chin augmentation, with the major disadvantage, particularly for silicone implants, that there is a possibility of resorption of the anterior cortical plate of the mandible. Soft-tissue tension is always present against the implant material and it may be transmitted to the implant-bone interface, resulting in bone resorption. The advantages of chin implants include less risk of sensory loss, shorter recovery period postoperatively, and the possibility of removal if the patient is not happy with the result. Moreover, implants enable lateral augmentation to provide greater width to the lower face and improve the pre-jowl sulcus to obtain a more harmonious appearance of the lower face (Proffit et al, 2003; Fattahi, 2007).

Reduction genioplasty is approached either by inferior border osteotomy or osteoplasty. With either procedure the loss of hard tissue support results in loss of skin elasticity that can produce an undesirable soft tissue response. Loss of skin

elasticity is a greater problem with osteoplasty. Unpredictability is another disadvantage of osteoplasty (Proffit et al, 2003).

Correction of anterior mandibular inferior asymmetry presents complex problems. Following release of the inferior border of the mandible after osteotomy, the segment can be shifted either to left or right side and shortened or lengthened, advanced or retruded asymmetrically. Defects can be grafted as needed. Vertical reduction at the inferior border of the body of the mandible, usually unilateral, e.g. in hemimandibular hyperplasia, is more predictably done alone as a second surgery after mandibular repositioning. It is extremely difficult to plan the exact amount of bone removal at the inferior border until the mandible has been repositioned in the primary procedure and the soft tissues have adapted to the new position, a process requiring a minimum of six months (Profitt et al, 2003).

2. Rhinoplasty

Rhinoplasty is performed at the time of the orthognathic surgery or postoperatively, and aims to enhance the nose appearance, as well as improve its function (air flow) when combined with septoplasty (septorhinoplasty). Because of the central position of the nose relative to the face, even minor deformities or asymmetries are easily apparent. For this reason, addressing a nasal deformity is challenging and rhinoplasty is one of the most difficult cosmetic procedures (Fattahi, 2007; Mohamed and Perenack, 2014).

Mandibular orthognathic surgery has minimal impact on the nasal structures and morphology, however, advancement or setback of the mandible causes an increase or decrease of the chin prominence, respectively. A more or less prominent chin creates the impression of a smaller or larger nose, respectively. Therefore, when addressing a nasal deformity the mandibular and chin changes should be taken into consideration (Mohamed and Perenack, 2014).

Maxillary movements are more directly related to nasal changes. Maxillary advancements cause increases in nasiolabial angle, in alar base width, and in tip projection. Superior repositioning of maxilla increases the nasal projection and the superior rotation of the nasal tip, thus decreasing the appearance of a dorsal hump. Widening of the alar base and a decrease in nasiolabial angle also occurs (Mohamed and Perenack, 2014). It is really hard to predict the change of nasal tip in three planes of space, because apart from the maxillary position many factors affect the nasal tip projection. Predictability is worsened by long-term scar contracture and healing of the tip (Rosen, 1988).

It remains controversial whether rhinoplasty should be performed simultaneously or separately from the orthognathic surgery. Advocates of the simultaneous approach claim the advantages of a single planning and surgery, less postoperative discomfort, high patient satisfaction when addressing maxillomandibular discrepancies and nasoseptal deformities in a single operation (Fattahi, 2007; Colbert et al, 2011).

A disadvantage of performing a rhinoplasty at the time of orthognathic surgery is the need for an endotracheal tube change from a nasotracheal to an orotracheal tube at the completion of the orthognathic surgery. Although this change can be challenging, most experienced anesthesiologists and oral and maxillofacial surgeons can perform it safely. Perhaps the biggest drawback of the simultaneous orthognathic surgery and rhinoplasty is the poor control of the intraoperative swelling and edema around the nose, which can distort nasal architecture and affect negatively the overall final result of nasal surgery (Fattahi, 2007).

Moderate dorsal deformities and minor abnormalities of tip morphology and alar base are indications for simultaneous rhinoplasty. The contraindications include patient-directed minor changes in the nasal tip position and shape.

Waite et al (1988) performed 22 septrorhinoplasties in conjunction with orthognathic surgery, 15 cases were done with a LeFort I and 7 cases done with isolated sagittal split osteotomies. They followed the cases for one year and reported

high patient satisfaction and an aesthetic outcome. No significant difference could be established between the two groups.

Colbert et al (2011) carried out a retrospective study of 22 patients who underwent simultaneous orthognathic and nasal surgery. When asked, 94% of these 22 patients were in favor of having both surgeries together. 16% of the patient group would consider separate nasal surgery if it was not done at the time of the osteotomy. All the patients were satisfied with their postoperative results. None of the patients suffered any aesthetic or functional complications from the rhinoplasty.

3. Malarplasty

Patients with maxillary deficiency often have hypoplasia of the infraorbital rims or the tear troughs. Maxillary advancement without addressing the infraorbital rim hypoplasia, will definitely worsen the appearance of the midface. Therefore, "high" Le-Fort I osteotomy was introduced to advance the infraorbital rims along with the maxilla. Alternatively, standard Le-Fort I can be performed, supported by infraorbital rims or tear troughs augmentation by placing malar or submalar implants. Solid silicone implants have been used and it is reported that implant augmentation gives a harmonious appearance to the midface (Fattahi, 2007).

2. The effect of jaw repositioning on facial aesthetics

Virtually all LeFort I osteotomies, whether for retropositioning or advancement, result in widening of the alar bases (Schendel and Carlotti, 1991). This is most likely a result of the approach to the maxilla rather than being caused by movement of the bone itself. When the periosteum is elevated off the face of the maxilla, the regional muscles are detached from their insertions, leading to retraction and thus alar widening. The involved muscles include zygomaticus major, levator labiisuperiorus, levator labii superiorus alaeque nasi, and nasalis. A further result of the retraction of these muscles is shortening, flattening, and thinning of the upper lip (O' Ryan and Schendel, 1992). The movement of the underlying structure of the maxilla will have a greater effect on the lip than on the alar base.

Nasal tip support is provided by the various components of the nasal anatomy and their fibrous connections with one another. The nasal septum, the quality of the lower lateral cartilages, the attachment of the medial crural footplates to the septum, and the junction of the upper and lower lateral cartilages all contribute to tip support. These structures are in direct contact with the maxilla by way of the nasal spine and nasal crest. It follows logically that any movement of the maxilla should have a resultant effect on nasal tip projection and location (Altman and Oeltjen, 2007).

Reyneke (2010) summarized the effect of the orthognathic surgery on the facial aesthetics as follows:

Maxillary advancement

Frontal changes

1. Elevated nasal tip
2. Increased upper lip fullness
3. Increased upper lip vermilion exposure
4. Increased paranasal fullness

Profile changes

5. Increased paranasal area fullness
6. Elevated nasal tip (controllable)
7. Increased upper lip fullness
8. Decreased prominence of chin and nose (relative)

Maxillary down graft

Frontal changes

9. Increased lower-third face height

10. Increased upper lip length

11. Increased upper lip vermilion exposure

12. Increased maxillary tooth exposure

Profile changes

13. Increased upper lip prominence

14. More obtuse nasolabial angle

15. Less prominent mandible anteroposteriorly (autorotation)

Maxillary impaction

Frontal changes

16. Reduced maxillary incisor exposure

17. Reduced upper lip vermilion exposure

18. Reduced interlabial distance

19. Reduced upper lip length (controllable)

20. Reduced lower -third face height

21. Reduced gingival exposure when smiling

22. Increased alar base width (controllable)

Profile changes

23. Elevated nasal tip (controllable)

24. Reduced lower -third face height

25. Reduced interlabial distance

26. Increased mandibular anteroposterior prominence (autorotation)

27. Increased paranasal fullness

Mandibular setback

Frontal changes

28. Decrease in mandibular prominence

29. Upper lip vermilion becomes more prominent

30. Decrease in lower third face height

Profile changes

31. Decreased mandibular anteroposterior prominence

32. Reduced lower lip vermilion exposure

33. Reduced chin-throat length

34. Increased chin-throat angle

35. MATERIALS AND METHODS

1. Patient selection

This is a retrospective study performed on CBCT images of 20 skeletal Class III patients who underwent combined orthodontic and surgical treatment at the Department of Orthodontics, Faculty of Dentistry, Marmara University. Initially, the sample consisted of 23 patients; however, three of them were excluded because genioplasty was performed simultaneously during the surgery. All subjects presented completed growth and development and were skeletally mature.

Each one of the 20 patients had 2 sets of CBCT images which were taken before and 4 to 6 months after the surgery with the same machine (ILUMA CBCT, Imtec Imaging, Ardmore, OK).

The patients were selected according to following selection criteria:

1. Skeletal Class III patients with mild skeletal asymmetry 1-4mm, who underwent bimaxillary orthognathic surgery: mandibular setback combined with maxillary advancement, with or without maxillary impaction.

2. Available pre- and post-surgical CBCT images obtained before and 4 to 6 months after the surgery.

3. No craniofacial syndromes, systemic diseases and anomalies, including cleft lip and palate, or a history of trauma to the jaw.

4. No adjunctive, cosmetic surgical procedures were performed during the orthognathic surgery, including genioplasty and mandibular contouring.

The patients were separated into two groups according to the type of the maxillary surgical movement, which was either pure advancement or advancement combined with impaction. 10 subjects underwent mandibular setback and maxillary advancement, whereas 10 subjects underwent mandibular setback, maxillary

advancement and impaction (Table 1). For the Advancement group, the average amount of mandibular setback was 3,88±2,91 mm and the average amount of maxillary advancement was 3,74±1,88 mm. For the Impaction group, the average amount of mandibular setback was 2,88±2,34 mm, the average amount of maxillary advancement was 3,81±1,77 mm, the average amount of maxillary impaction was 3,81±1,77 mm (Table 1).

Table 1. Amount of surgical jaw movements.

	Impaction+ advancement group (n=10)	**Advancement group (n=10)**	**Sample (n=20)**
Mandibular setback	2,88±2,34	3,88±2,91	3,38±2,62
Maxillary advancement	3,81±1,77	3,74±1,88	3,77±1,78
Maxillary impaction	3,35±2,40	-	3,35±2,40

As part of the routine protocol in the Department of Orthodontics of Marmara University informed consent forms had been signed by all patients or their parents. This project was approved by the Ethical Committee of the Institute of Health Sciences of Marmara University (12.10.2017).

1. Collection of Data

The pre-operative CBCT evaluation was performed within a period of 1 week before surgery (T1). All the postsurgical CBCT scans were obtained between a period of 4-6 months after the surgery (T2). The CBCT images were taken with the ILUMA CBCT (Imtec Imaging, Ardmore, OK) at the NET Radiology and

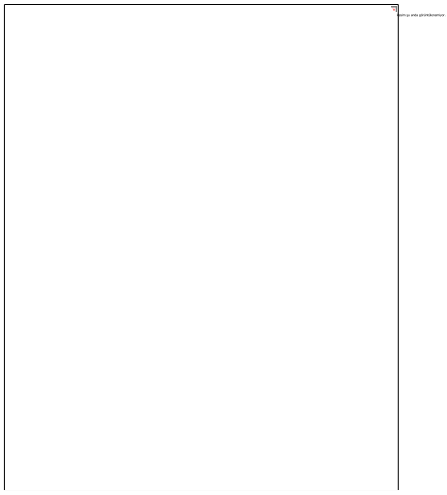

Fig. 5.1: The CBCT machine used in this study.

Diagnostic Center, Nisantasi, Istanbul. The scans were acquired while the patient was sitting upright with the Frankfort Horizontal plane parallel to the floor, at maximum intercuspation. The patient's head position was adjusted with the help of two laser beams, one parallel to the floor, coinciding with the Frankfort Horizontal plane, and one vertical beam passing through the patient's facial midline. At this position the head was supported on the occipital region and on the lateral sides of the forehead with the help of two cephalostats. The patients were asked not to swallow and not to move their heads or tongues during exposure. The technical properties of the Volumetric Cone Beam machine which was used included (Fig 5.1):

1. Brand Name: Iluma Imtec imaging a 3M company
2. X-ray tube is working with Cone–Beam technology
3. Focal Spot: 0.3 mm x 0.3 mm
4. X-ray tube is working with 120 KV
5. X-ray tube current: 1-4 mA
6. Detector size :19.5 x 24.5 cm
7. Scanning with 360 degrees rotation
8. Radiation: 58 microsieverts maximum
9. Scanning time 40 seconds maximum and 7.8 seconds minimum (180 degrees rotation angle option)
10. FOV –Field of View or Imaging area: 14.2 cm x 21.1 cm
11. Voxel Size: 0.0936 mm
12. Grey Scala: 14 bit

The data was exported in DICOM (Digital Imaging and Communications in Medicine) format.

1. CBCT Data processing in Mimics

1. Generation of the masks and three-dimensional images

Obtained 3D images in DICOM data format were transferred to a network computer workstation, where skeletal, dental and soft tissue parameters were measured using MIMICS 19.0 software launched by Materialise (Materialise Europe, World Headquarters, Leuven, Belgium).

Materialise Interactive Medical Image Control System (MIMICS) is an interactive tool for the visualization and segmentation of CT images as well as MRI images, STL images etc. and 3D rendering of objects. Therefore, in the medical field MIMICS can be used for diagnostic, operation-planning or rehearsal purposes. The software divides the screen into four views (Fig. 5.2):

Fig. 5.2: The main screen of the MIMICS. software

1. The axial view
2. The coronal view
3. The sagittal view
4. The 3-D view

All of the images were processed by the same operator (S.S.).

After installing each DICOM set of data of the subject in MIMICS 19.0 software, initial orientation (top, bottom, left, right, anterior, posterior) was verified (Fig.5.3).

Then, a predefined threshold representing the bone between 226-3071 Hounsfield Units (HU) was chosen in order to create a skeleton mask on the scan (Fig. 5.4).

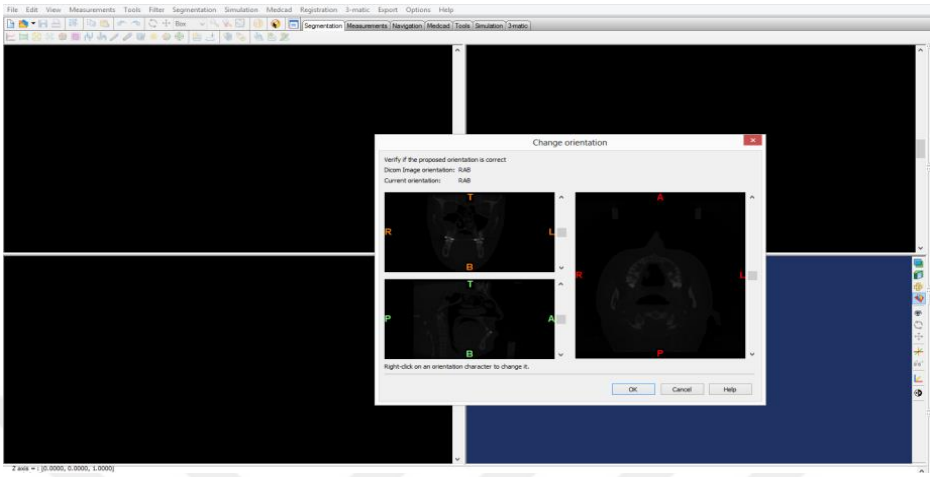

Fig. 5.3: Verification of the initial orientation.

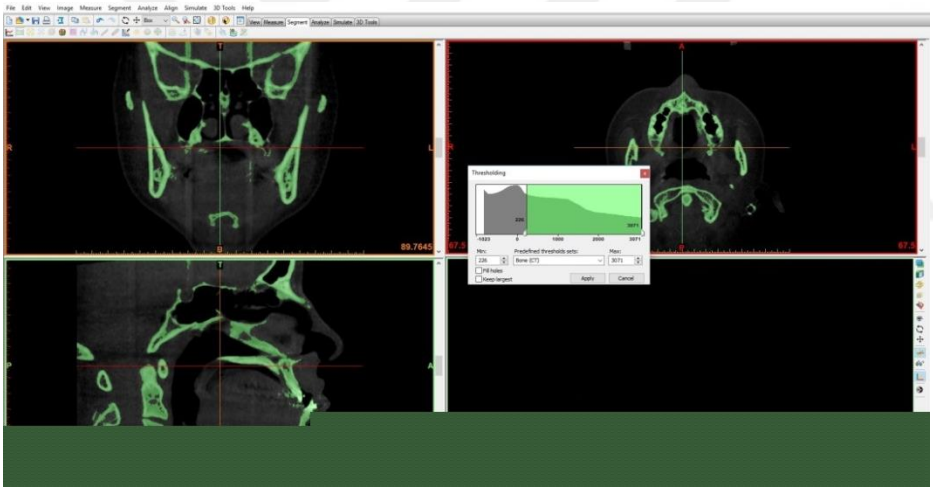

Fig. 5.4: Setting the threshold values to create a mask of the bone.

After the mask was created, using the "region growing" option the skeleton was selected, eliminating any existing irrelevant interferences and artifacts (Fig 5.5).

Fig. 5.5: Application of the “region growing” tool.

After this refined mask was created, a 3D reconstruction of the skeleton mask was created in high quality through the “Calculate 3D” function of MIMICS software (Fig 5.6, 5.7).

Fig. 5.6: Creating a high quality three-dimensional reconstruction of the selected mask.

Fig. 7: The 3D reconstruction of the skeleton mask.

Following the same steps by choosing a predefined threshold between -700 and 225 Hounsfield Units (HU) representing the soft tissue, the soft tissue mask and 3D model were created (Fig. 5.8).

Fig. 5.8: The soft tissue mask and 3D model created from the refined mask.

Afterwards the skeleton mask was segmented as follow:

The cervical vertebrae were segmented and eliminated, in order for the cranium to be depicted. To achieve this, the erasing tool of the Mimics software was employed and any connection between the first cervical vertebra and the occipital bone was cropped (Fig. 5.9). Then, by using the "region growing" option the cranium was selected and a new mask of the separated cranium was created. The 3D reconstruction model of the cranium was also generated through the 3D calculation option (Fig. 5.10).

Fig. 5.9: Segmentation of the cranium.

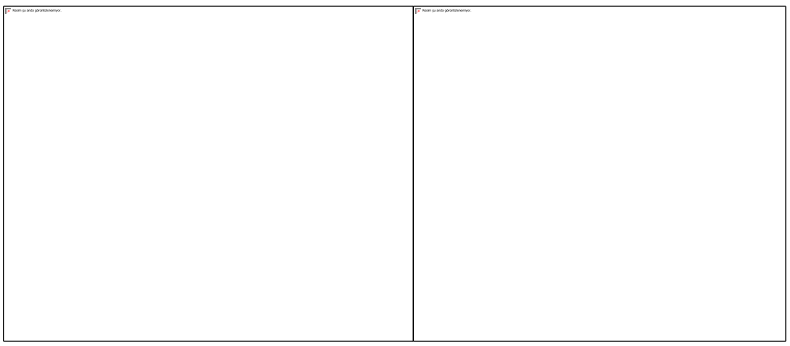

Fig. 5.10: The 3D reconstruction model of the cranium.

The next step was to segment the mandible from the craniofacial skeleton. The Split Tool provided by Mimics 19.0 software was utilized to automatically split the mandible from the craniofacial skeleton by marking the adjacent structures in a

few slices in all coronal, axial, sagittal views (Fig. 5.11). This resulted in the generation of two new masks and 3D models. One included the separated mandible and the other was consisted of the maxilla and the cranial vault (Fig. 5.12).

Fig. 11: Segmentation of mandible from the craniofacial skeleton.

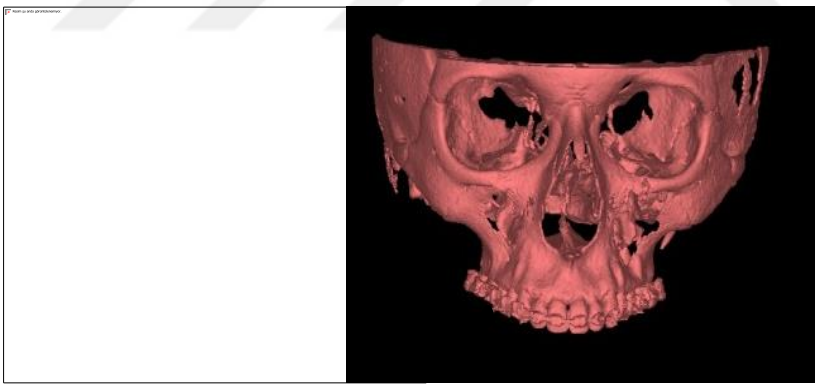

Fig.12: The mandible and the maxillofacial 3D models.

Till this point, the cranium, mandible, maxillofacial, soft tissue masks and 3D models were created. Exactly the same procedure was repeated for the postoperative CBCT images of each patient (Fig. 5.13).

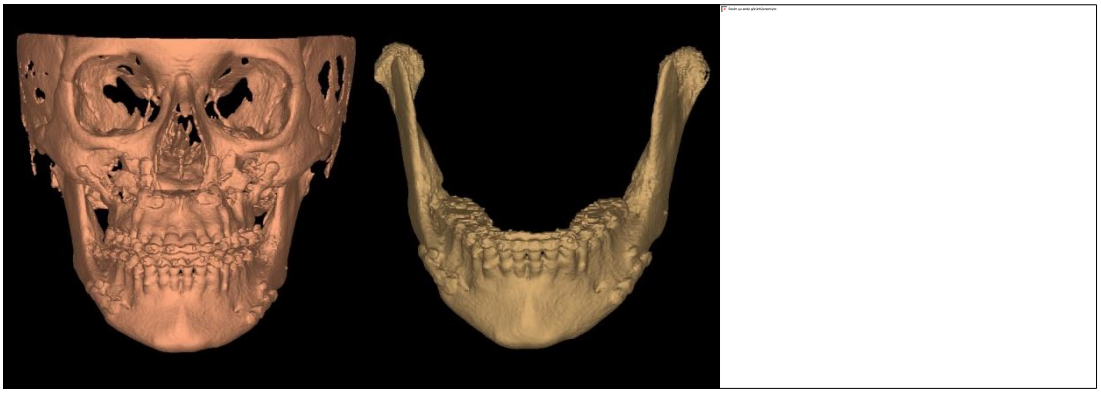

Fig. 13: The 3D reconstruction models of the postoperative CBCT: the cranium, the segmented mandible and the soft tissues.

1. Superimposition of the preoperative and postoperative images

The image registration and superimposition of the preoperative and the postoperative three dimensional masks was done with a global registration method based on the anterior cranial base. The cranial fossa and the ethmoid bone surfaces are considered as stable areas as their growth is completed before puberty (Belden, 1998; Melsen, 1969). First, the postoperative cranium, mandible, maxillofacial, soft tissue masks were merged into a new mask (fig 5.14), which was exported as STL file. This STL file was, subsequently, imported in the preoperative CBCT file of the patient. The postoperative merged three-dimensional mask was firstly registered to the preoperative skeletal mask manually. Then automatic registration was done in which the movable part was the postoperative 3D mask whereas the fixed part was the preoperative 3D mask. The distance threshold was 5 mm in the automatic distance threshold method. Registration was done again where the distance threshold method was set as manual and the distance threshold was set at 1 mm. The subsample percentage was gradually increased from 80 to 100% (Fig. 5.15).

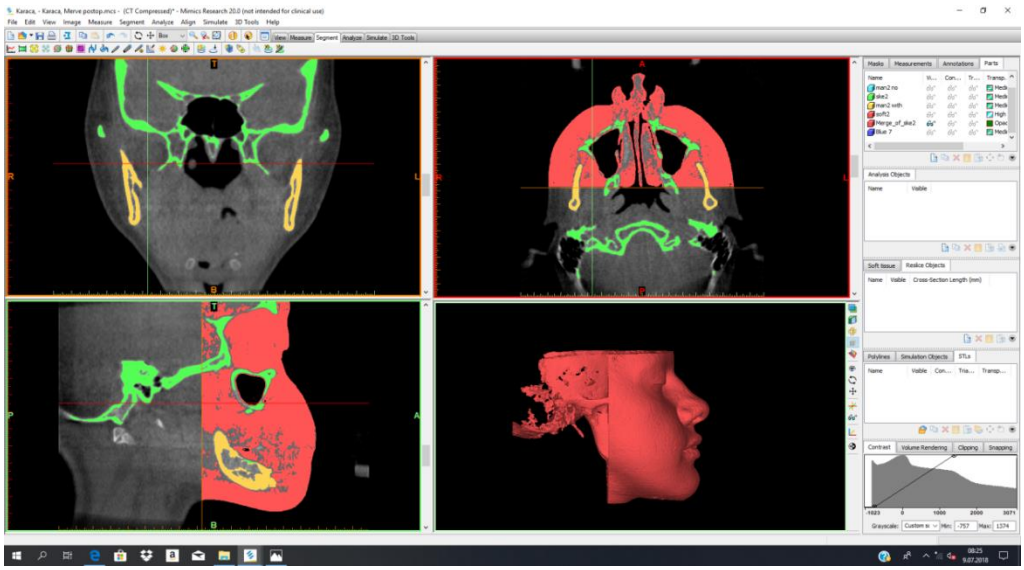

Fig. 5.14: Merge of the postoperative cranium, mandible, maxillofacial, soft tissue masks.

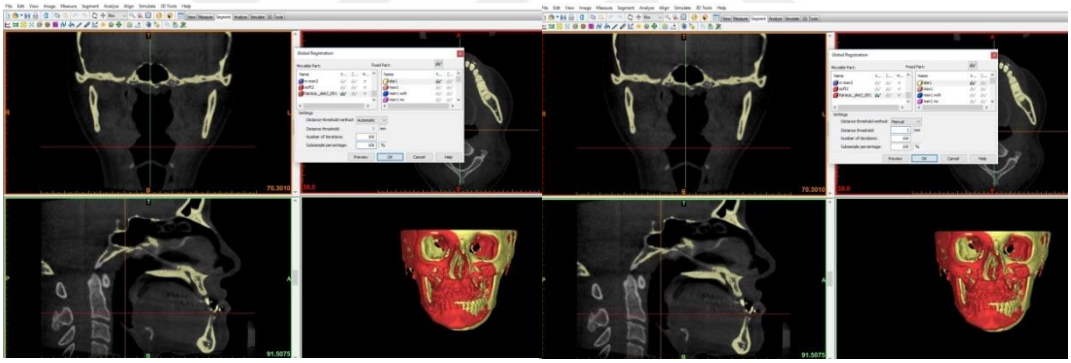

Fig. 5.15: The registration process of pre- and postoperative 3D masks.

In order to evaluate the quality of the superimposition procedure, a 3-matic image was created where the distance of the two 3D models in different points of the anterior cranial base complex bones was measured automatically by the program. Also superimposition was checked on axial and sagittal slices of anterior cranial base (Fig. 5.16). After registration of the preoperative and the postoperative volumes, they have the same coordinate system relative to the anterior cranial base, which in turn compensates for any discrepancies between before and after volumes when the reference planes are defined, and reduces the risks of projection and measurement errors.

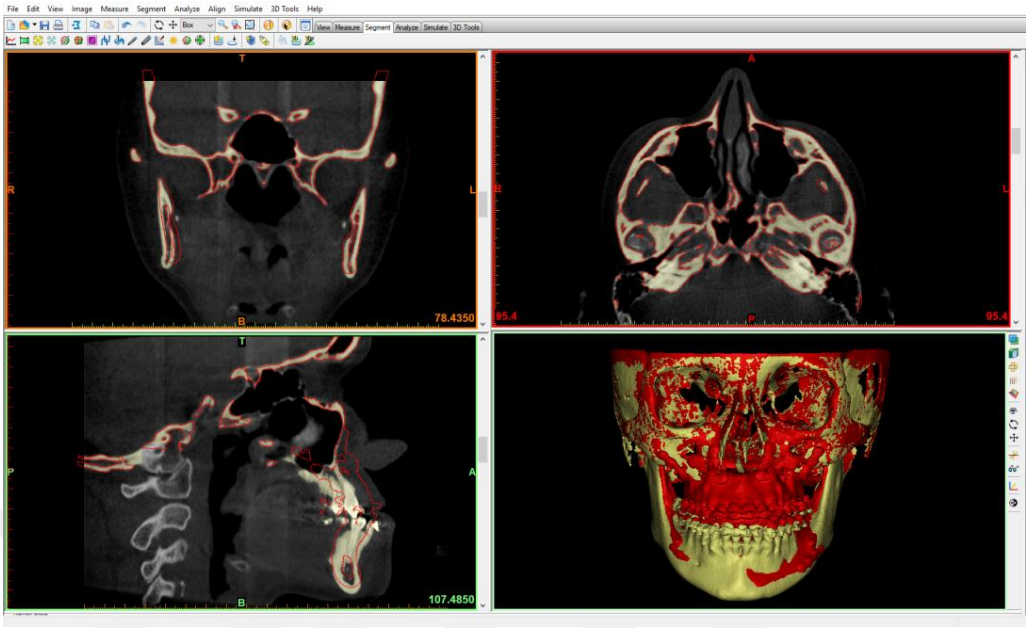

5.16: The registration of the preoperative and the postoperative volumes and 3D models.

The registration of postoperative merged 3D mask was followed by the splitting to the initial 3D masks: postoperative cranium, mandible, maxillofacial, soft tissue masks, which were already registered. After this last step the registration of process was completed, and the identification of the reference planes and the skeletal and soft tissue marks followed.

2. Three-dimensional Cephalometric Analysis and Measurements

The next step was the 3D tracing. For that purpose, a cephalometric analysis was predefined based on landmarks already described in the literature (Hajeer et al, 2004; You et al, 2010; Nur et al, 2016). This cephalometric analysis consisted of:

1. reference and auxiliary planes

2. skeletal, dental and soft tissue landmarks

3. skeletal, dental and soft tissue measurements

1. Definition of the reference planes

In order to evaluate the degree of asymmetry pre- and post-operatively, it was essential to define a reliable midsagittal plane. For this reason, surface-based Procrustes analysis was performed and symmetry plane was defined for each patient. The symmetry plane's position can be determined by superimposing the original and the mirror image obtained by a reflection along an initially arbitrary plane (Benz et al, 2002). After the fine registration, the symmetry plane can be assigned from the correlating points of the original and mirror image (Hartman et al, 2007).

This method was implemented in Mimics 19.0 software as follows: The preoperative cranium 3D model was mirrored along an arbitrary sagittal plane and the "mirrored" cranium 3D model was generated (Fig. 5.17). The original and the mirrored 3D models were then superimposed. Superimposition was done first manually and then automatically using "Global registration" based on the anterior cranial base. Initially, automatic global registration was done in which the movable part was the "mirrored" cranium 3D model whereas the fixed part was the original one. The distance threshold was 5 mm in the automatic distance threshold method. Registration was done again where the distance threshold method was set as manual and the distance threshold was set at 1 mm. The subsample percentage was gradually

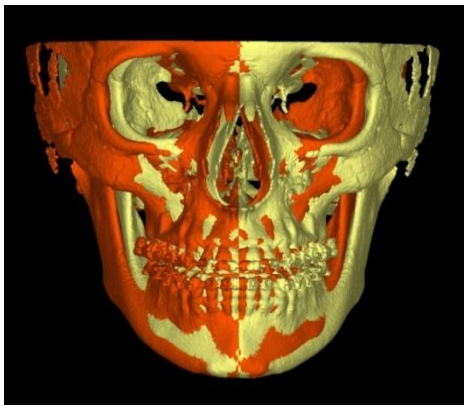

Fig. 5.17: Mirroring (orange) of the preoperative cranium 3D model (yellow).

increased from 80 to 100%. After superimposition was completed, the Mid-sagittal plane (MSP) was computed by means of the corresponding points of the original and the mirrored image of cranium (Fig. 5.18).

After verification of the MSP, the Horizontal Plane (HP) was defined as the plane perpendicular to the MSP and passing through the right Porion (PoR) and the right Orbitale (OrR).

Finally, the Coronal Plane (CP) was defined as the plane perpendicular to MSP and HP and passing through the right Porion (PoR) (Table 2, Fig. 5.19).

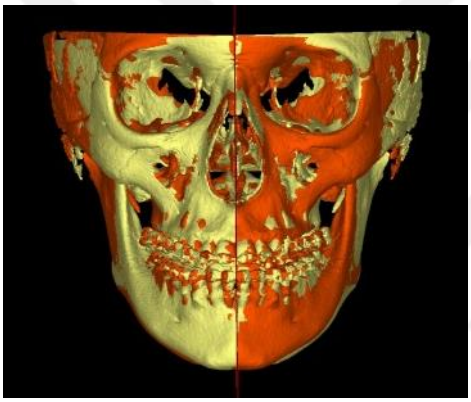

Fig. 5.18: Computation of the midsagittal plane.

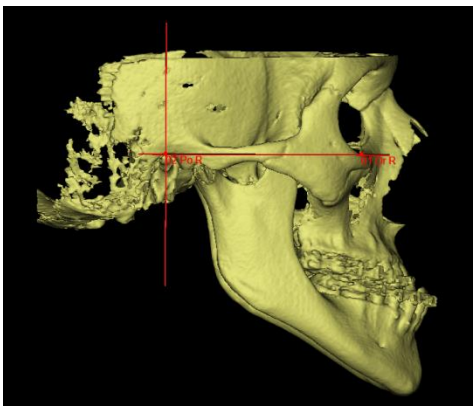

Fig. 5.19: The Coronal and the Horizontal Planes.

Table 2: The skeletal references planes.

Mid-sagittal Plane (MSP)	The symmetry plane computed by the superimposition of the original and the mirrored image of the cranial vault, assigned from the correlating points of the two images.
Horizontal Plane (HP)	Being perpendicular to the Mid-sagittal Plane and passing through the right Porion and the right Orbitale.
Coronal Plane (CP)	Being perpendicular to the Mid-sagittal Plane and the Horizontal Plane and passing through the right Porion.

1. Definition of the auxiliary planes

The following auxiliary planes were defined to assist the measurements of our study. Bilateral planes are noted with R or L to distinguish right and left side, and 1 or 2 follows, indicating planes that were determined on the preoperative and/or the postoperative CBCT image, respectively (Table 3).

Table 3: The auxiliary planes.

Occlusal Preoperative Plane (OP 1)	Passing through bilateral Maxillary first molar mesiobuccal cusp tip points and Incision superior frontale point on the preoperative CBCT image (Fig. 5.20).
Occlusal Postoperative Plane (OP 2)	Passing through bilateral Maxillary first molar mesiobuccal cusp tip points and Incision superior frontale point on the postoperative CBCT image.
Mandibular Preoperative Plane (MP 1)	Passing through bilateral Gonion points and Menton point on the preoperative CBCT image (Fig. 5.21).

Mandibular Postoperative Plane (MP 2)	Passing through bilateral Gonion points and Menton point on the postoperative CBCT image.
Left Ramal Preoperative Plane (RP L1)	Passing through bilateral Gonion points and left Condylion point on the preoperative CBCT image.
Right Ramal Preoperative Plane (RP R1)	Passing through bilateral Gonion points and right Condylion point on the preoperative CBCT image (Fig. 5.22).
Left Ramal Postoperative Plane (RP L2)	Passing through bilateral Gonion points and left Condylion point on the postoperative CBCT image.
Right Ramal Postoperative Plane (RP R2)	Passing through bilateral Gonion points and right Condylion point on the postoperative CBCT image.
Left Coronoid Preoperative Plane (CP L1)	Passing through left Condylion, left Gonion and left Coronoid points on the preoperative CBCT image (Fig. 5.23).
Right Coronoid Preoperative Plane (CP R1)	Passing through right Condylion, right Gonion and right Coronoid points on the preoperative CBCT image (Fig. 5.23).
Left Coronoid Postoperative Plane (CP L2)	Passing through left Condylion, left Gonion and left Coronoid points on the postoperative CBCT image.
Right Coronoid Postoperative Plane (CP R2)	Passing through right Condylion, right Gonion and right Coronoid points on the postoperative CBCT image.
Gonial Preoperative Plane (G1)	Being perpendicular to Mandibular Preoperative Plane and passing through bilateral Gonion points on the preoperative CBCT image (Fig. 5.24).
Gonial Postoperative Plane (G2)	Being perpendicular to Mandibular Postoperative Plane and passing through bilateral Gonion points on the postoperative CBCT image.

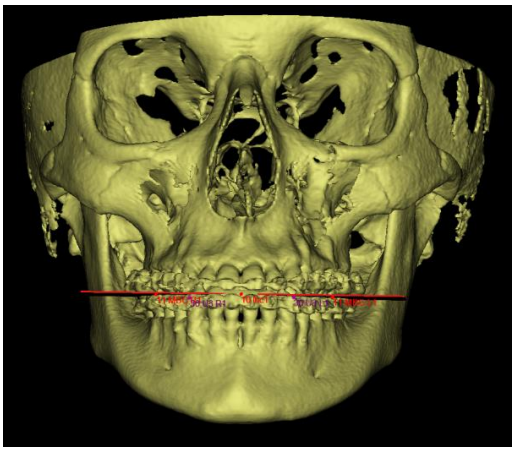

Fig. 5.20: The Occlusal Plane (preoperative) and the dental landmarks.

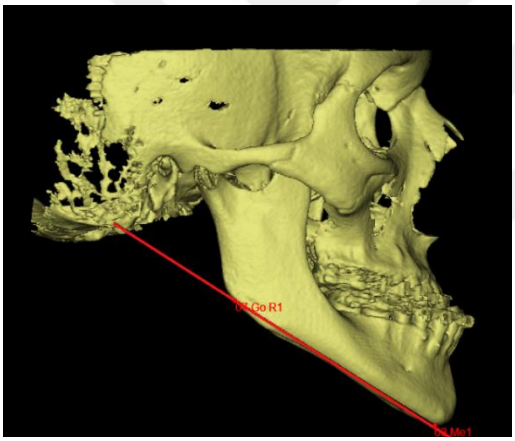

Fig. 5.21: The Mandibular Preoperative Plane.

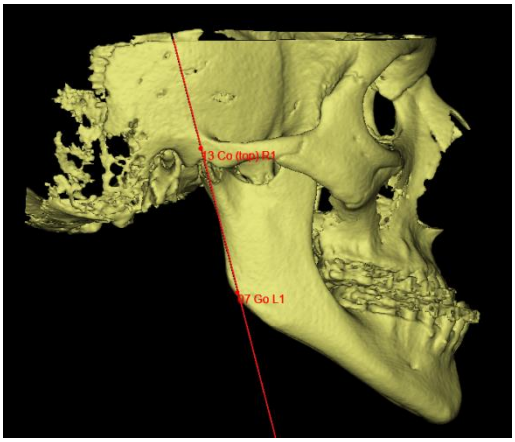

Fig. 5.22: The Right Preoperative Ramal Plane.

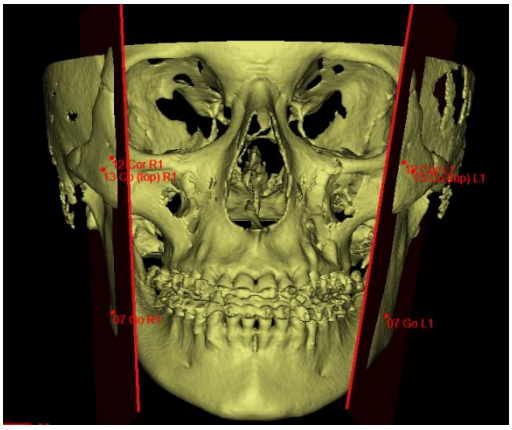

Fig. 5.23: The Right and Left Preoperative Coronoid Planes.

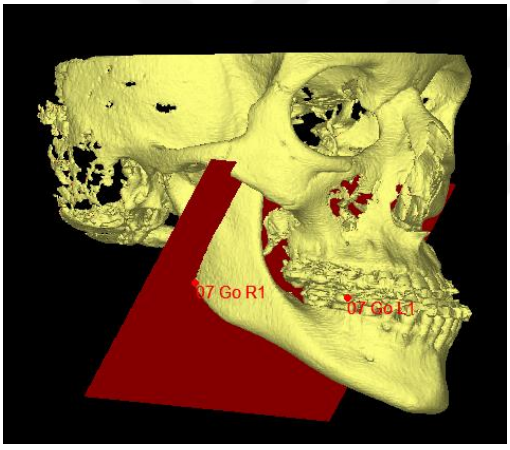

Fig. 5.24: The Gonial Preoperative Plane.

1. Definition of the skeletal, dental and soft tissue landmarks

In the present study, we used all three sectional images, in the midsagittal, horizontal, and coronal planes, and the 3D surface-rendered images for accurate landmark localization. If the positioning of any landmark was disturbed by the presence of artifacts, the threshold of the hard-tissue or the soft-tissue mask was readjusted until the unimpeded tracing was possible.

The definition of the skeletal, dental and soft tissue landmarks used in this study is presented in Tables 4, 5 and 6, respectively. Bilateral points are noted with deviated (dev) or opposite (opp) to distinguish the deviated and oppposite side. The side towards which Menton point was deviated according to the Midsagittal Plane was defined as the deviated side, while the other side is named the opposite nondeviated side. Then, 1 or 2 follows, indicating points that were determined on the preoperative and/or the postoperative CBCT image, respectively (Fig 5.20, 5.25, 5.26, 5.27).

Table 4: The skeletal landmarks.

Orbitale (Or) (Right)	The lowest point in the inferior margin of the orbit.
Porion (Po) (Right)	The most superior point of the external auditory meatus.
Menton (Me) (1/2)	The most inferior midline point on the mandibular symphysis.
A point (A) (1/2)	The point at the deepest midline concavity on the maxilla between the anterior nasal spine and prosthion.
B point (B) (1/2)	The point at the deepest midline concavity on the mandibular symphysis between infradentale and pogonion.

Genial tubercle (Gt) (dev/opp, 1/2)	The center of the genial tubercle, which is defined as a paired eminence on the mental protuberance of the mandible.
Gonion (Go) (dev/opp, 1/2)	The constructed point on the curvature of the mandibular angle by bisecting the angle formed by the ramus plane and the mandibular plane.
Jugale (J) (dev/opp, 1/2)	The most inferior midpoint of the concavity at the zygomaticomaxillary process.
Pogonion (Pog) (1/2)	The most anterior point of the bony chin in the median plane.
Coronoid (Cor) (dev/opp, 1/2)	The most superior point of the coronoid process.
Condyle top (Co top) (dev/opp, 1/2)	The most superior point of the head of the condyle.
Condyle medial (Co med) (dev/opp, 1/2)	The most medial point of the head of the condyle.
Condyle lateral (Co lat) (dev/opp, 1/2)	The most lateral point of the head of the condyle.

Table 5: The dental landmarks.

Incision superior frontale (Inc) (1/2)	The midpoint between the maxillary central incisors at the level of the incisal edges (Fig. 5.20).
Maxillary first molar (U6) (dev/opp, 1/2)	The tip of the mesiobuccal cusp of the maxillary first permanent molar (Fig. 5.20).
Maxillary canine (U3) (dev/opp, 1/2)	The cusp tip of the maxillary canine (Fig. 5.20).

Table 6: The soft tissue landmarks.

Pronasale (Pn) (1/2)	The most prominent point of the nasal tip.
Subnasale (Sn) (1/2)	The point where the lower border of the nose meets the outer contour of the upper lip.
Columella (C) (1/2)	The midpoint on columella at the level of the superior nostrils.
Alare(Al) (dev/opp, 1/2)	The most lateral point on each alar contour.
Alar base (Ab) (dev/opp, 1/2)	The most lateral point of the alar base.
Nostril Superior (NoS) (dev/opp, 1/2)	The most superior point of the nostril.
Nostril Inferior (NoI) (dev/opp, 1/2)	The most inferior point of the nostril.
Nostril lateral (NoL) (dev/opp, 1/2)	The most lateral point of the nostril.
Soft tissue Pogonion (Pog') (1/2)	The most anterior midpoint of the chin.
Soft tissue Gonion (Go') (dev/opp, 1/2)	The intersection of Mandibular and Gonial planes with the overlying cutaneous surface (Fig. 5.27).
Labrale Superius (Ls) (1/2)	The midpoint of the vermilion line of the upper lip.
Cheilion (Ch) (dev/opp, 1/2)	The point located at each labial commissure.
Endocanthion (En) (dev/opp, 1/2)	The point at the inner commissure of the eye fissure.

Exocanthion (Ex)

(dev/opp, 1/2)

The point at the outer commissure of the eye fissure.

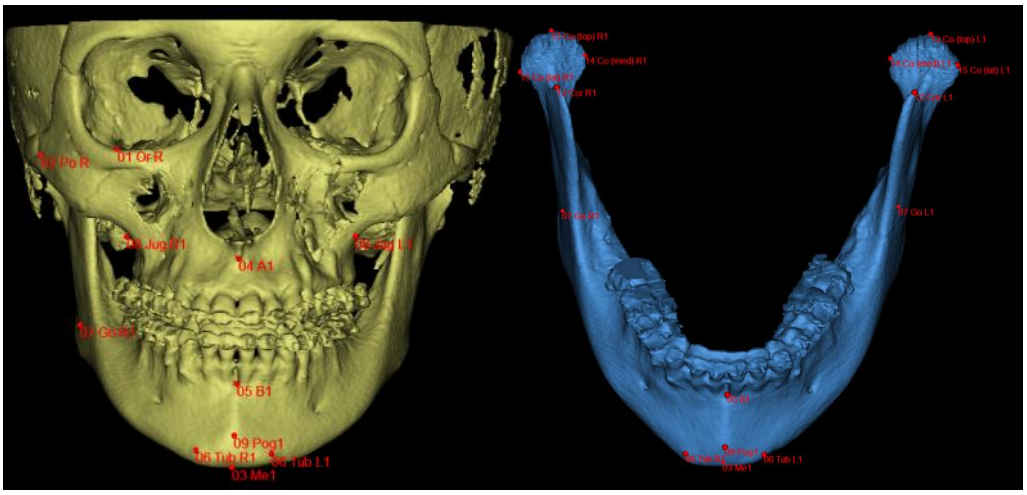

Fig. 5.25: The skeletal landmarks.

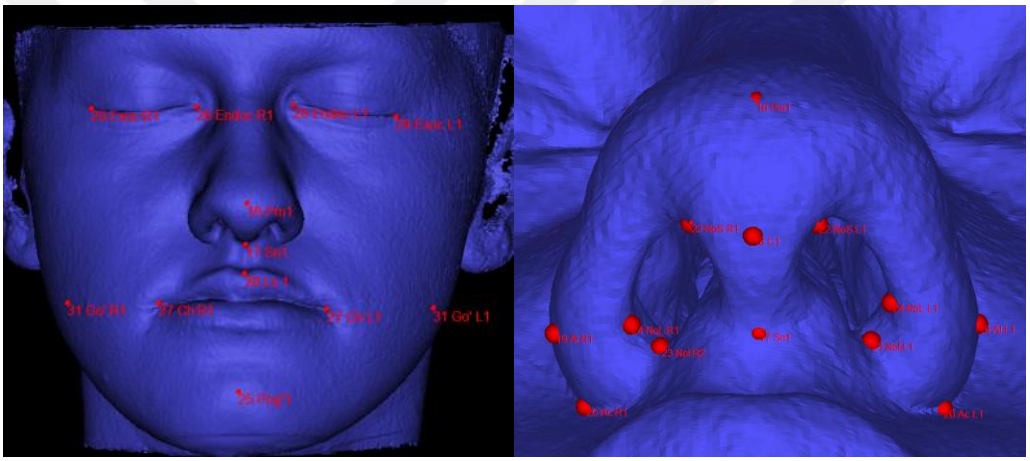

Fig. 5.26: The soft tissue landmarks.

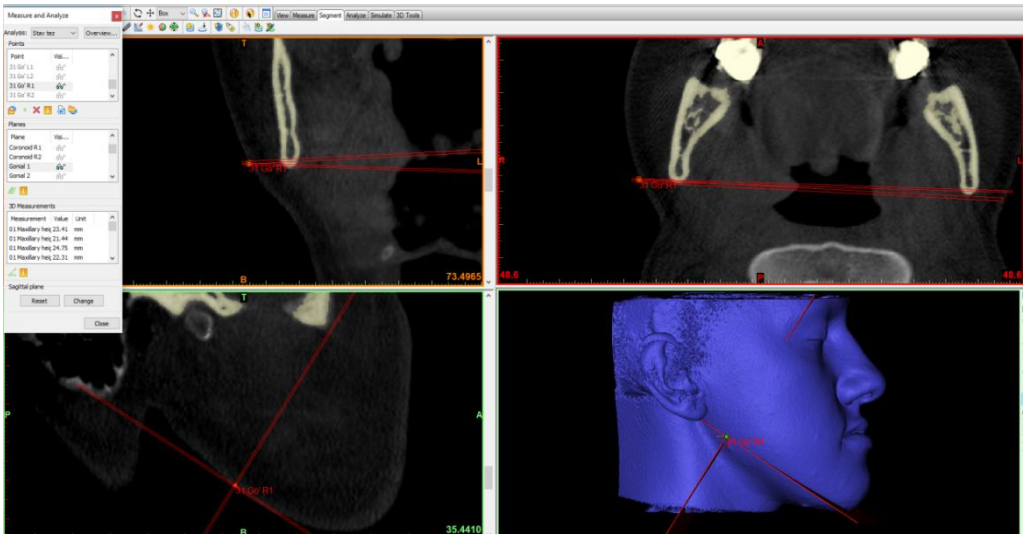

Fig. 5.27: The Soft Gonion Point at the intersection of Mandibular and Gonial planes with the overlying cutaneous surface.

2. Description of the skeletal, dental and soft tissue measurements

The measurements consisted of the distances of each point from the reference planes. These planes were defined by skeletal points that were not affected by the surgical skeletal movement. Furthermore, since the patients, whose images were used in this study, were not growing anymore, the spatial position of these skeletal landmarks could be considered unchanged between the initial and final CBCT acquisition. Each point was characterized by three measurements which were the distances from the Mid-sagittal Plane (MSP), the Horizontal Plane (HP) and the Coronal Plane (CP). In other words, a 3-dimensional coordinate system was constructed, in which, each point was characterized by three numbers. These numbers, which represented the coordinates of the landmark, defined the spatial position of each landmark.

If the distance from

1. the MSP was the x coordinate
2. the HP was the y coordinate
3. the CP was the z coordinate

for example, the A-point could be represented as A(x,y,z).

A descriptive analysis of factors contributing to craniofacial asymmetry was performed (Hwang et al, 2006). In order to assess asymmetry of the structures thoroughly the skeletal, dental and soft tissue measurements presented in Tables 7, 8 and 9 were carried out. All these measurements were correlated to Menton deviation, to assess their contribution to mandibular asymmetry.

Table 7. The skeletal measurements.

Menton deviation	Distance from Menton to Midsagittal Plane.

Maxillary rotation	Distance from A Point to Midsagittal Plane.
Maxillary height	Distance from Jugale to Horizontal Plane.
Maxillary width	Distance from Jugale to Midsagittal Plane.
Ramus length	Distance between Gonion and Condylion.
Mandibular body length	Distance between Gonion and Menton.
Gonial angle	Angle between the Ramal and the Mandibular Planes.
Gonion-HP	Distance from Gonion to Horizontal Plane.
Gonion-MSP	Distance from Gonion to Midsagittal Plane.
Gonion-CP	Distance from Gonion to Coronal Plane.
Bigonial width	Distance between bilateral Gonion points.
Condyle top-HP	Distance from Condyle top to Horizontal Plane.
Condyle top-MSP	Distance from Condyle top to Midsagittal Plane.
Condyle top-CHP	Distance from Condyle top to Coronal Plane.
Bicondylar width	Distance between bilateral Condyle top points.
Coronoid-HP	Distance from Coronoid to Horizontal Plane.
Coronoid-MSP	Distance from Coronoid to Midsagittal Plane.
Coronoid-CP	Distance from Coronoid to Coronal Plane.
Bicoronoid width	Distance between bilateral Coronoid points.
Frontal ramal inclination	Angle between the Coronoid and the Midsagittal Planes.
Lateral ramal inclination	Angle between the Ramal and the Horizontal Planes.
Genial tubercle-HP	Distance from Genial tubercle to Horizontal Plane.
Genial tubercle-MSP	Distance from Genial tubercle to Midsagittal Plane.

Genial tubercle-CP	Distance from Genial tubercle to Coronal Plane.

Table 8. The dental measurements.

Maxillary dental height	Distance from Maxillary First Molar to Horizontal Plane.
Maxillary canine height	Distance from Maxillary Canine to Horizontal Plane.
Maxillary dental width	Distance from Maxillary First Molar to Midsagittal Plane.
Occlusal cant	Angle between the Occlusal and the Horizontal Planes.

Table 9. The soft tissue measurements.

Soft tissue Pogonion deviation	Distance from Soft tissue Pogonion to Midsagittal plane.
Soft tissue Gonion-HP	Distance from Soft tissue Gonion to Horizontal Plane.
Soft tissue Gonion-MSP	Distance from Soft tissue Gonion to Midsagittal Plane.
Alar width	Distance from Alare to Midsagittal Plane.
Interalar width	Distance between bilateral Alare points.
Alar base width	Distance from Alar base to Midsagittal Plane.
Alar base width (total)	Distance between bilateral Alar base points.
Nostril length	Distance between the Nostil Superior and Nostil inferior points on each side.
Nostril width	Distance from Nostril lateral to Midsagittal plane.
Internostril width	Distance between bilateral Nostril lateral points.
Nasal protrusion	Distance between Pronasale and Subnasale.
Nasiolabial angle	Angle between the intersectiong lines from Subnasale to both the Columella and the Labrale Superius points.
Cheilion-MSP	Distance from Cheilion to Midsagittal plane.
Intercommissural width	Distance between bilateral Cheilion points.

Subsequently, for each point, an asymmetry index was calculated pre- and postoperatively. For solitary paramedial landmarks, for example Menton, Pogonion, A point, only the distance to Midsagittal plane was measured and was defined as the asymmetry index. The asymmetry indices of the bilateral landmarks, for example Gonion, Condylion, and Condyle top, were calculated using the following formula,

where R: right, L: left, dx: distance from Midsagittal Plane, dy: distance from Horizontal Plane, dz: distance from Coronal Plane (Katsumata et al, 2005, Maeda et al, 2006):

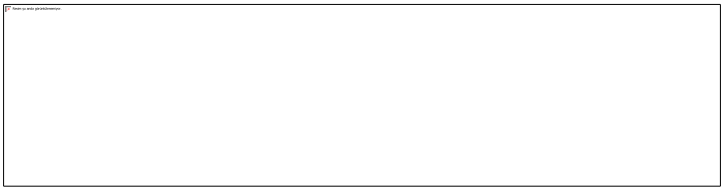

Finally, nasal morphology was assessed pre- and posteoperatively separately in each group and postoperative changes in nose area were compared between the Impaction and the Advancement group.

1. STATISTICAL ANALYSIS

6.1 POWER ANALYSIS

Initially, the sample size calculation was made with G* Power program using the the difference in ramal height between the contralateral side and the deviated side (Baek et al, 2007). The minimum number of subjects required for power: 0.80 and α: 0.05 when the effect size is d (effect size): 1.384 and SD: 3.49 was 20.

6.2 STATISTICAL METHOD

Statistical calculations were performed with IBM SPSS Statistics 22 (SPSS IBM, Turkey). For the analysis of reliability regarding parameter measurements, intraclass correlation coefficient (ICC) was calculated. Intra-observer method error was investigated by re-measuring the 40% of our sample, under the same conditions 2 weeks after the initial measuring. The results were evaluated within a 95% confidence interval. The normal distribution of the parameters was evaluated by the Shapiro Wilks test. Student t test was used to compare the two groups of parameters with normal distribution. Paired Sample t test was used for intra-group comparison of quantitative data showing normal distribution. Pearson's correlation analysis was used to determine the relationship between the parameters with normal distribution. Statistical significance level was established at $p<0.05$.

1. RESULTS

7.1 Reliability test

The results of the separately calculated method error for skeletal, dental and soft tissue parameters are shown in Table 10. Method of error was found to be within a 95% confidence interval for all the values measured. As seen in the table, Intraclass Correlation Coefficient (ICC) was found to be close to 1 for all measuments. All the measurements were found to be reliable. The errors were non-fatal and did not affect the results of our measurements. The measurements of skeletal, dental and soft tissues variables could be repeated with an insignificant error ($p>0.05$).

Table 10: Reliability of Measurements.

Variables	Intraclass Correlation Coefficient	95% Confidence Interval	
		Lower Bound	Upper Bound
SKELETAL			
Me1-CP	0,996	0,978	0,999
Me1-HP	0,996	0,981	0,999
Me1-MSP	0,994	0,970	0,999
Me2-CP	0,993	0,964	0,999
Me2-HP	0,999	0,993	1,000
Me2-MSP	0,982	0,915	0,996
A1-CP	0,993	0,964	0,999
A1-HP	0,997	0,983	0,999
A1-MSP	0,944	0,750	0,989
A2-CP	0,997	0,984	0,999
A2-HP	0,869	0,481	0,972
A2-MSP	0,976	0,884	0,995
B1-CP	0,998	0,991	1,000
B1-HP	0,998	0,992	1,000
B1-MSP	0,999	0,995	1,000
B2-CP	0,997	0,984	0,999
B2-HP	0,998	0,989	1,000
B2-MSP	0,992	0,958	0,998
Go L1-CP	0,972	0,867	0,994
Go L1-HP	0,976	0,884	0,995
Go L1-MSP	0,968	0,852	0,994
Go L2-CP	0,983	0,920	0,997
Go L2-HP	0,998	0,991	1,000
Go L2-MSP	0,986	0,930	0,997
Go R1-CP	0,986	0,931	0,997
Go R1-HP	0,982	0,911	0,996
Go R1-MSP	0,965	0,835	0,993

Go R2-CP	0,948	0,763	0,989
Go R2-HP	0,995	0,975	0,999
Go R2-MSP	0,961	0,819	0,992
Pog1-CP	0,999	0,993	1,000
Pog1-HP	1,000	0,998	1,000
Pog1-MSP	0,998	0,988	1,000
Pog2-CP	0,998	0,989	1,000
Pog2-HP	0,997	0,984	0,999
Pog2-MSP	0,998	0,990	1,000
J L1-CP	0,976	0,885	0,995
J L1-HP	0,997	0,986	0,999
J L1-MSP	0,997	0,984	0,999
J L2-CP	0,985	0,928	0,997
J L2-HP	0,996	0,980	0,999
J L2-MSP	0,922	0,665	0,984
J R1-CP	0,997	0,985	0,999
J R1-HP	0,953	0,787	0,990
J R1-MSP	0,989	0,947	0,998
J R2-CP	0,998	0,991	1,000
J R2-HP	0,976	0,886	0,995
J R2-MSP	0,954	0,791	0,991
Gt L1-CP	0,999	0,994	1,000
Gt L1-HP	1,000	0,998	1,000
Gt L1-MSP	0,999	0,997	1,000
Gt L2-CP	0,998	0,988	1,000
Gt L2-HP	0,999	0,995	1,000
Gt L2-MSP	0,996	0,978	0,999
Gt R1-CP	0,999	0,996	1,000
Gt R1-HP	0,999	0,997	1,000
Gt R1-MSP	0,999	0,994	1,000
Gt R2-CP	0,999	0,994	1,000
Gt R2-HP	0,996	0,978	0,999
Gt R2-MSP	0,998	0,992	1,000
Cor L1-CP	0,927	0,683	0,985
Cor L1-HP	0,998	0,989	1,000
Cor L1-MSP	0,975	0,883	0,995
Cor L2-CP	0,919	0,653	0,983
Cor L2-HP	0,999	0,995	1,000
Cor L2-MSP	0,996	0,979	0,999
Cor R1-CP	0,939	0,727	0,987
Cor R1-HP	0,996	0,981	0,999
Cor R1-MSP	0,989	0,946	0,998
Cor R2-CP	0,996	0,979	0,999
Cor R2-HP	0,997	0,983	0,999
Cor R2-MSP	0,912	0,627	0,982
Co med L1-CP	0,933	0,706	0,986
Co med L1-HP	0,995	0,977	0,999
Co med L1-MSP	0,966	0,842	0,993
Co med L2-CP	0,898	0,576	0,979
Co med L2-HP	0,996	0,982	0,999

Co med L2-MSP	0,954	0,791	0,991
Co med R1-CP	0,963	0,830	0,993
Co med R1-HP	0,984	0,921	0,997
Co med R1-MSP	0,970	0,861	0,994
Co med R2-CP	0,949	0,770	0,990
Co med R2-HP	0,955	0,793	0,991
Co med R2-MSP	0,962	0,824	0,992
Co lat L1-CP	0,783	0,243	0,952
Co lat L1-HP	0,992	0,959	0,998
Co lat L1-MSP	0,985	0,928	0,997
Co lat L2-CP	0,849	0,421	0,968
Co lat L2-HP	0,992	0,960	0,998
Co lat L2-MSP	0,982	0,912	0,996
Co lat R1-CP	0,995	0,973	0,999
Co lat R1-HP	0,988	0,942	0,998
Co lat R1-MSP	0,988	0,939	0,997
Co lat R2-CP	0,994	0,969	0,999
Co lat R2-HP	0,998	0,991	1,000
Co lat R2-MSP	0,978	0,894	0,996
Co top L1-CP	0,752	0,172	0,945
Co top L1-HP	0,913	0,628	0,982
Co top L1-MSP	0,967	0,844	0,993
Co top L2-CP	0,760	0,190	0,947
Co top L2-HP	0,992	0,960	0,998
Co top L2-MSP	0,962	0,824	0,992
Co top R1-CP	0,949	0,768	0,990
Co top R1-HP	0,986	0,934	0,997
Co top R1-MSP	0,930	0,692	0,986
Co top R2-CP	0,977	0,892	0,995
Co top R2-HP	0,984	0,924	0,997
Co top R2-MSP	0,840	0,394	0,966
Maxillary height L1	0,997	0,986	0,999
Maxillary height L2	0,996	0,980	0,999
Maxillary height R1	0,953	0,787	0,990
Maxillary height R2	0,976	0,886	0,995
Maxillary dental height L1	0,998	0,989	1,000
Maxillary dental height L2	0,993	0,963	0,998
Maxillary dental height R1	0,999	0,995	1,000
Maxillary dental height R2	0,987	0,938	0,997
Maxillary width L1	0,997	0,984	0,999
Maxillary width L2	0,922	0,665	0,984
Maxillary width R1	0,989	0,947	0,998
Maxillary width R2	0,954	0,791	0,991
Maxillary dental width L1	0,986	0,930	0,997
Maxillary dental width L2	0,987	0,937	0,997

Maxillary dental width R1	0,967	0,845	0,993
Maxillary dental width R2	0,978	0,894	0,996
Ramus length L1	0,953	0,784	0,990
Ramus length L2	0,999	0,993	1,000
Ramus length R1	0,973	0,872	0,995
Ramus length R2	0,993	0,966	0,999
Body length L1	0,976	0,884	0,995
Body length L2	0,989	0,948	0,998
Body length R1	0,972	0,869	0,994
Body length R2	0,987	0,937	0,997
Gonial angle L1	0,985	0,929	0,997
Gonial angle L2	0,993	0,968	0,999
Gonial angle R1	0,981	0,907	0,996
Gonial angle R2	0,992	0,961	0,998
Bigonial width 1	0,990	0,950	0,998
Bigonial width 2	0,995	0,977	0,999
Bicondylar width 1	0,999	0,006	1,000
Bicondylar width 2	0,998	0,992	1,000
Bicoronoid width 1	0,992	0,961	0,998
Bicoronoid width 1	0,984	0,923	0,997
Frontal ramal inclination L1	0,795	0,273	0,955
Frontal ramal inclination L2	0,990	0,951	0,998
Frontal ramal inclination R1	0,937	0,720	0,987
Frontal ramal inclination R2	0,978	0,896	0,996
Lateral ramal inclination L1	0,998	0,989	1,000
Lateral ramal inclination L2	0,998	0,990	1,000
Lateral ramal inclination R1	0,990	0,950	0,998
Lateral ramal inclination R2	0,995	0,974	0,999
DENTAL			
Inc1-CP	0,985	0,927	0,997
Inc1-HP	0,996	0,978	0,999
Inc1-MSP	0,980	0,905	0,996
Inc2-CP	0,987	0,935	0,997
Inc2-HP	0,966	0,839	0,993
Inc2-MSP	0,974	0,878	0,995
U6 L1-CP	0,986	0,934	0,997
U6 L1-HP	0,998	0,989	1,000
U6 L1-MSP	0,986	0,930	0,997
U6 L2-CP	0,993	0,965	0,999
U6 L2-HP	0,993	0,963	0,998
U6 L2-MSP	0,956	0,799	0,991
U6 R1-CP	0,997	0,984	0,999

U6 R1-HP	0,999	0,995	1,000
U6 R1-MSP	0,840	0,394	0,966
U6 R2-CP	0,988	0,941	0,998
U6 R2-HP	0,987	0,938	0,997
U6 R2-MSP	0,830	0,365	0,963
U3 L1-CP	0,994	0,972	0,999
U3 L1-HP	0,999	0,995	1,000
U3 L1-MSP	0,997	0,985	0,999
U3 L2-CP	0,994	0,969	0,999
U3 L2-HP	0,999	0,997	1,000
U3 L2-MSP	0,797	0,279	0,956
U3 R1-CP	0,997	0,987	0,999
U3 R1-HP	0,999	0,993	1,000
U3 R1-MSP	0,953	0,785	0,990
U3 R2-CP	0,971	0,865	0,994
U3 R2-HP	0,999	0,994	1,000
U3 R2-MSP	0,999	0,997	1,000
Occlusal cant 1	0,983	0,920	0,997
Occlusal cant 2	0,998	0,989	1,000
SOFT TISSUE			
Pn1-CP	0,989	0,948	0,998
Pn1-HP	0,972	0,866	0,994
Pn1-MSP	0,863	0,462	0,971
Pn2-CP	0,990	0,951	0,998
Pn2-HP	0,984	0,922	0,997
Pn2-MSP	0,850	0,423	0,968
Sn1-CP	0,980	0,905	0,996
Sn1-HP	0,968	0,850	0,994
Sn1-MSP	0,921	0,658	0,984
Sn2-CP	0,994	0,972	0,999
Sn2-HP	0,950	0,774	0,990
Sn2-MSP	0,947	0,761	0,989
C1-CP	0,992	0,960	0,998
C1-HP	0,992	0,960	0,998
C1-MSP	0,926	0,679	0,985
C2-CP	0,994	0,971	0,999
C2-HP	1,000	0,998	1,000
C2-MSP	0,895	0,565	0,978
Pog'1-CP	1,000	0,997	1,000
Pog'1-HP	0,849	0,421	0,968
Pog'1-MSP	0,998	0,990	1,000
Pog'2-CP	0,999	0,997	1,000
Pog'2-HP	0,997	0,985	1,000
Pog'2-MSP	0,999	0,994	1,000
Go'L1-CP	0,979	0,900	0,996
Go'L1-HP	0,999	0,995	1,000
Go'L1-MSP	0,976	0,884	0,995
Go'L2-CP	0,979	0,901	0,996
Go'L2-HP	0,999	0,996	1,000
Go'L2-MSP	0,977	0,888	0,995

Go'R1-CP	0,999	0,994	1,000
Go'R1-HP	1,000	0,999	1,000
Go'R1-MSP	0,973	0,870	0,994
Go'R2-CP	0,999	0,993	1,000
Go'R2-HP	1,000	0,999	1,000
Go'R2-MSP	0,986	0,931	0,997
Ls1-CP	0,993	0,966	0,999
Ls1-HP	0,995	0,977	0,999
Ls1-MSP	0,945	0,753	0,989
Ls2-CP	0,995	0,976	0,999
Ls2-HP	0,994	0,971	0,999
Ls2-MSP	0,956	0,799	0,991
Al L1-CP	0,989	0,946	0,998
Al L1-HP	0,999	0,993	1,000
Al L1-MSP	0,996	0,982	0,999
Al L2-CP	0,975	0,879	0,995
Al L2-HP	0,973	0,873	0,995
Al L2-MSP	0,997	0,984	0,999
Al R1-CP	0,995	0,973	0,999
Al R1-HP	0,974	0,877	0,995
Al R1-MSP	0,992	0,961	0,998
Al R2-CP	0,993	0,966	0,999
Al R2-HP	0,873	0,494	0,973
Al R2-MSP	0,986	0,932	0,997
Ab L1-CP	0,988	0,940	0,998
Ab L1-HP	0,998	0,990	1,000
Ab L1-MSP	0,996	0,980	0,999
Ab L2-CP	0,985	0,925	0,997
Ab L2-HP	0,988	0,940	0,998
Ab L2-MSP	0,983	0,918	0,997
Ab R1-CP	0,995	0,977	0,999
Ab R1-HP	0,996	0,982	0,999
Ab R1-MSP	0,988	0,942	0,998
Ab R2-CP	0,996	0,979	0,999
Ab R2-HP	0,997	0,985	0,999
Ab R2-MSP	0,989	0,948	0,998
NoS L1-CP	0,942	0,740	0,988
NoS L1-HP	0,998	0,987	1,000
NoS L1-MSP	0,961	0,818	0,992
NoS L2-CP	0,885	0,532	0,976
NoS L2-HP	0,994	0,968	0,999
NoS L2-MSP	0,964	0,833	0,993
NoS R1-CP	0,994	0,969	0,999
NoS R1-HP	0,982	0,914	0,996
NoS R1-MSP	0,977	0,889	0,995
NoS R2-CP	0,993	0,964	0,999
NoS R2-HP	0,987	0,938	0,997
NoS R2-MSP	0,965	0,837	0,993
NoI L1-CP	0,990	0,951	0,998
NoI L1-HP	0,999	0,993	1,000

NoI L1-MSP	0,995	0,976	0,999
NoI L2-CP	0,988	0,942	0,998
NoI L2-HP	0,999	0,994	1,000
NoI L2-MSP	0,994	0,972	0,999
NoI R1-CP	0,993	0,967	0,999
NoI R1-HP	0,997	0,986	0,999
NoI R1-MSP	0,995	0,975	0,999
NoI R2-CP	0,994	0,972	0,999
NoI R2-HP	0,999	0,994	1,000
NoI R2-MSP	0,989	0,946	0,998
NoL L1-CP	0,988	0,943	0,998
NoL L1-HP	0,999	0,997	1,000
NoL L1-MSP	0,994	0,972	0,999
NoL L2-CP	0,994	0,969	0,999
NoL L2-HP	0,998	0,988	1,000
NoL L2-MSP	0,968	0,851	0,994
NoL R1-CP	0,995	0,977	0,999
NoL R1-HP	0,997	0,986	0,999
NoL R1-MSP	0,989	0,945	0,998
NoL R2-CP	0,992	0,963	0,998
NoL R2-HP	0,990	0,949	0,998
NoL R2-MSP	0,956	0,799	0,991
Ch L1-CP	0,995	0,974	0,999
Ch L1-HP	0,983	0,917	0,997
Ch L1-MSP	0,852	0,428	0,968
Ch L2-CP	0,992	0,959	0,998
Ch L2-HP	0,998	0,991	1,000
Ch L2-MSP	0,943	0,744	0,988
Ch R1-CP	0,999	0,993	1,000
Ch R1-HP	0,999	0,997	1,000
Ch R1-MSP	0,988	0,940	0,998
Ch R2-CP	0,999	0,994	1,000
Ch R2-HP	0,999	0,003	1,000
Ch R2-MSP	0,781	0,238	0,952
En L1-CP	0,943	0,745	0,988
En L1-HP	0,963	0,802	0,994
En L1-MSP	0,937	0,722	0,987
En L2-CP	0,984	0,924	0,997
En L2-HP	0,991	0,957	0,998
En L2-MSP	0,743	0,351	0,943
En R1-CP	0,974	0,875	0,995
En R1-HP	0,956	0,798	0,991
En R1-MSP	0,846	0,411	0,967
En R2-CP	0,974	0,876	0,995
En R2-HP	0,975	0,881	0,995
En R2-MSP	0,943	0,744	0,988
Ex L1-CP	0,911	0,624	0,982
Ex L1-HP	0,964	0,831	0,993
Ex L1-MSP	0,998	0,991	1,000

Ex L2-CP	0,917	0,646	0,983
Ex L2-HP	0,998	0,990	1,000
Ex L2-MSP	0,996	0,981	0,999
Ex R1-CP	0,991	0,954	0,998
Ex R1-HP	0,983	0,920	0,997
Ex R1-MSP	0,995	0,973	0,999
Ex R2-CP	0,998	0,988	1,000
Ex R2-HP	0,899	0,579	0,979
Ex R2-MSP	0,998	0,989	1,000
Alar width L1	0,996	0,982	0,999
Alar width L2	0,997	0,984	0,999
Alar width R1	0,992	0,961	0,998
Alar width R2	0,986	0,932	0,997
Alar base width L1	0,996	0,980	0,999
Alar base width L2	0,983	0,918	0,997
Alar base width R1	0,988	0,942	0,998
Alar base width R2	0,989	0,948	0,998
Nostril length L1	0,849	0,247	0,970
Nostril length L2	0,747	0,265	0,949
Nostril length R1	0,989	0,946	0,998
Nostril length R2	0,996	0,981	0,999
Internostril width 1	0,996	0,982	0,999
Internostril width 2	0,998	0,990	1,000
Nasal protrusion 1	0,967	0,844	0,993
Nasal protrusion 2	0,876	0,504	0,974
Nasiolabial angle 1	0,973	0,871	0,994
Nasiolabial angle 2	0,988	0,943	0,998
Intercommissural width 1	0,995	0,977	0,999
Intercommissural width 2	0,903	0,594	0,980
Intercanthal width 1	0,997	0,985	0,999
Intercanthal width 2	0,994	0,969	0,999
Biocular width 1	0,998	0,992	1,000
Biocular width 2	0,998	0,991	1,000

7.2 Demographics

All subjects were Caucasian and from the same geographic area (Turkey). Our sample consisted of 5 male (25%) and 15 (75%) female patients (Table 11). The ages of the women ranged from 18 to 40 and their average was 22.4 ± 5.82 years. The ages of the males ranged from 18 to 26, with an average of 22.2 ± 2.86 years. In the total sample, age ranges from 18 to 40, with an average of 22.35 ± 5.16 years. All the patients were referred to NET Radiology and Diagnostic Center, Nisantasi, Istanbul and the pre-operative CBCT evaluation was performed within a period of 1

week before surgery (T1). All the postsurgical CBCT scans were obtained between a period of 4-6 months after the surgery (T2).

Table 11: Gender and age distribution of the sample.

Sex	N	%	Mean±SD	Minimum	Maksimum
Male	5	25	22,2±2,86	18	26
Female	15	75	22,4±5,82	18	40
Total	20	100	22,35±5,16	18	40

7.3 Comparison of preoperative skeletal morphological variables between groups and sides

The preoperative skeletal morphological variables were compared between the Impaction and the Advancement group. For bilateral charecteristics, the measurements of the deviated and the opposite side were compared for each group and the difference found by subtracting the opposite side measurements from the deviated side ones was used to evaluate the degree of asymmetry (Table 12).

Table 12: Comparison of the skeletal morphological variables between groups and sides, preoperatively.

	Impaction group (n=10)	Advancement group (n=10)	Total sample (n=20)	p
	Ort±SS	Ort±SS	Ort±SS	
Me1 deviation	1,86±2,8	1,67±1,36	1,76±2,15	**0,852**
Me1-CP	84,86±8,66	86,68±11,31	85,77±9,85	**0,690**
Me1-HP	96,56±6,85	91,11±5,23	93,83±6,56	**0,061**
Me1-MSP	1,86±2,8	1,67±1,36	1,76±2,15	**0,852**
A1-CP	85,69±4,44	85±4,62	85,34±4,42	**0,736**
A1-HP	28,8±3,48	29,72±2,46	29,26±2,97	**0,506**
A1-MSP	0,54±0,33	0,45±0,37	0,5±0,34	**0,581**

Maxillary width 1				
Deviated side	30,66±2,71	30,81±1,87	30,73±2,27	**0,887**
Opposite side	30,32±3,15	31,21±1,86	30,76±2,56	**0,454**
^{2}p	0,462	0,414		
Difference	0,34±1,38	-0,4±1,48	-0,03±1,44	**0,265**
Maxillary height 1				
Deviated side	26,85±4,21	23,56±1,51	25,2±3,51	**0,040***
Opposite side	25,48±3,37	23,99±1,62	24,73±2,68	**0,231**
Difference	1,37±2,21	-0,43±0,9	0,47±1,89	**0,028***
^{2}p	0,081	0,166		
J 1-CP				
Deviated side	60,55±3,76	59,02±4,95	59,79±4,35	**0,446**
Opposite side	60,78±3,66	59,33±5,02	60,06±4,34	**0,469**
Difference	-0,23±3,13	-0,31±2,95	-0,27±2,96	**0,954**
^{2}p	0,822	0,748		
J 1-HP				
Deviated side	26,85±4,21	23,56±1,51	25,2±3,51	**0,040***
Opposite side	25,48±3,37	23,99±1,62	24,73±2,68	**0,231**
Difference	1,37±2,21	-0,43±0,9	0,47±1,89	**0,028***
^{2}p	0,081	0,166		
J 1-MSP				
Deviated side	30,66±2,71	30,81±1,87	30,73±2,27	**0,887**
Opposite side	30,32±3,15	31,21±1,86	30,76±2,56	**0,454**
Difference	0,34±1,38	-0,4±1,48	-0,03±1,44	**0,265**
^{2}p	0,462	0,414		
B1-CP	88,92±7,46	90,64±9,37	89,78±8,29	**0,654**
B1-HP	72,62±5,42	68,38±5,78	70,5±5,87	**0,108**
B1-MSP	1,62±2,69	1,54±1,08	1,58±2	**0,933**
Pog 1-CP	89,98±8,64	92,43±10,52	91,21±9,46	**0,576**
Pog 1-HP	89,82±7,18	84,24±5,91	87,03±7,01	**0,074**
Pog 1-MSP	1,91±3,05	1,55±1,4	1,73±2,32	**0,741**
Bigonial distance 1	92,76±3,5	92,92±6,63	92,84±5,16	**0,946**
Bicondylar distance 1	115,35±4,09	117,56±6,3	116,46±5,29	**0,366**
Intercoronoid	95,32±5,35	95,15±4,2	95,23±4,68	**0,938**

distance 1				
Ramus length 1				
Deviated side	57,29±4,41	58,88±4,83	58,09±4,57	**0,451**
Opposite side	60,05±4,56	58,68±5,07	59,37±4,74	**0,532**
Difference	-2,76±4,27	0,21±3,2	-1,28±3,98	**0,096**
^{2}p	0,071	0,844		
Body length 1				
Deviated side	87,67±6,06	86,02±4,31	86,84±5,19	**0,491**
Opposite side	88,36±5,64	86,76±5,41	87,56±5,44	**0,525**
Difference	-0,69±2,23	-0,74±1,91	-0,72±2,02	**0,958**
^{2}p	0,352	0,250		
Gonial angle 1				
Deviated side	47,89±4,23	50,13±6,09	49,01±5,23	**0,353**
Opposite side	48,85±4,13	49,19±4,79	49,02±4,35	**0,868**
Difference	-0,96±3,19	0,93±3,34	-0,01±3,32	**0,211**
^{2}p	0,366	0,399		
Go 1-CP				
Deviated side	21,93±4,78	23,14±6,03	22,54±5,33	**0,625**
Opposite side	22,17±4,24	23,76±6,25	22,97±5,26	**0,515**
Difference	-0,24±3,48	-0,62±2,4	-0,43±2,92	**0,780**
^{2}p	0,830	0,434		
Go 1-HP				
Deviated side	55,97±3,95	56,53±3,92	56,25±3,84	**0,753**
Opposite side	56,91±4,69	55,81±4,82	56,36±4,67	**0,610**
Difference	-0,94±3,53	0,73±2,67	-0,11±3,16	**0,249**
^{2}p	0,421	0,411		
Go 1-MSP				
Deviated side	46,89±1,7	47,1±3,68	46,99±2,79	**0,870**
Opposite side	45,75±2,07	45,75±3,27	45,75±2,67	**0,997**
Difference	1,14±1,59	1,35±2,07	1,24±1,8	**0,802**
^{2}p	0,060	0,070		
Co (top) 1-CP				
Deviated side	12,33±1,56	12,08±1,3	12,21±1,4	**0,701**
Opposite side	13,12±1,46	11,79±1,71	12,45±1,69	**0,079**
Difference	-0,79±1,5	0,29±1,55	-0,25±1,58	**0,133**
^{2}p	0,132	0,572		

Co (top) 1-HP				
Deviated side	1,91±1,92	1,48±1,15	1,7±1,56	**0,553**
Opposite side	2,21±0,89	1,47±0,95	1,84±0,98	**0,090**
Difference	-0,3±2,35	0,01±1,38	-0,15±1,88	**0,722**
^{2}p	0,695	0,982		
Co (top) 1-MSP				
Deviated side	48,89±2,64	49,83±3,27	49,36±2,93	**0,490**
Opposite side	48,36±2,45	49,09±2,61	48,72±2,49	**0,525**
Difference	0,54±3,18	0,74±2,92	0,64±2,98	**0,884**
^{2}p	0,608	0,446		
Co (med) 1-CP				
Deviated side	12,69±2,4	11,73±2,05	12,21±2,23	**0,350**
Opposite side	13,49±2,62	12,31±1,67	12,9±2,22	**0,245**
Difference	-0,8±1,73	-0,58±1,68	-0,69±1,66	**0,775**
^{2}p	0,178	0,307		
Co (med) 1-HP				
Deviated side	6,3±3,31	5,81±1,9	6,05±2,64	**0,691**
Opposite side	4,15±2,01	4,49±1,38	4,32±1,68	**0,657**
Difference	2,15±3,17	1,32±2,35	1,73±2,75	**0,511**
^{2}p	0,060	0,111		
Co (med) 1-MSP				
Deviated side	37,91±1,83	39,84±3,02	38,88±2,62	**0,102**
Opposite side	38,85±1,98	39,35±1,78	39,1±1,85	**0,559**
Difference	-0,93±1,4	0,49±2,21	-0,22±1,94	**0,103**
^{2}p	0,065	0,501		
Co (lat) 1-CP				
Deviated side	16,03±1,76	15,61±2,25	15,82±1,98	**0,650**
Opposite side	16,56±1,02	15,82±2,39	16,19±1,83	**0,376**
Difference	-0,54±2,17	-0,21±1,9	-0,37±1,99	**0,722**
^{2}p	0,454	0,738		
Co (lat) 1-HP				
Deviated side	7,11±2,47	5,86±2,17	6,48±2,35	**0,246**
Opposite side	6,52±1,81	5,26±1,79	5,89±1,87	**0,135**
Difference	0,59±2,17	0,6±1,59	0,59±1,85	**0,985**
^{2}p	0,415	0,263		

Co (lat) 1-MSP				
Deviated side	56,83±2,78	58,63±3,95	57,73±3,45	**0,253**
Opposite side	58,49±1,86	58,9±2,97	58,69±2,42	**0,716**
Difference	-1,66±2,4	-0,27±3,02	-0,96±2,75	**0,268**
^{2}p	0,057	0,788		
Cor 1-CP				
Deviated side	46,72±2,23	44,29±2,43	45,5±2,59	**0,032***
Opposite side	47,85±3,04	44,8±2,48	46,33±3,12	**0,024***
Difference	-1,14±1,83	-0,51±1,26	-0,83±1,56	**0,387**
^{2}p	0,081	0,232		
Cor 1-HP				
Deviated side	5,57±4,25	4,71±4,38	5,14±4,22	**0,660**
Opposite side	4,47±3,54	5,2±3,57	4,84±3,48	**0,652**
Difference	1,1±1,3	-0,49±2,79	0,3±2,27	**0,118**
^{2}p	0,025*	0,589		
Cor 1-MSP				
Deviated side	47,84±2,49	47,76±2,03	47,8±2,21	**0,935**
Opposite side	47,42±3,11	47,33±2,34	47,38±2,68	**0,948**
Difference	0,42±1,78	0,42±1,18	0,42±1,47	**0,998**
^{2}p	0,471	0,287		
Gt 1-CP				
Deviated side	87,67±8,35	88,21±12,37	87,94±10,27	**0,910**
Opposite side	87,15±8,25	88,18±12,75	87,66±10,47	**0,832**
Difference	0,53±1,49	0,03±0,88	0,28±1,22	**0,378**
^{2}p	0,295	0,920		
Gt 1-HP				
Deviated side	92,99±7,1	87,67±5,23	90,33±6,65	**0,073**
Opposite side	93,18±6,82	88,04±5,21	90,61±6,47	**0,074**
Difference	-0,19±1,12	-0,37±1,08	-0,28±1,07	**0,726**
^{2}p	0,604	0,310		
Gt 1-MSP				
Deviated side	12,43±2,83	13,65±3,88	13,04±3,36	**0,433**
Opposite side	9,88±4,93	10,03±4,79	9,96±4,73	**0,945**
Difference	2,55±6,34	3,62±3,72	3,08±5,09	**0,652**
^{2}p	0,235	0,013*		
Frontal ramal				

inclination 1				
Deviated side	5,23±4,5	6,67±3,75	5,95±4,1	**0,447**
Opposite side	4,88±2,8	5,06±3,02	4,97±2,83	**0,893**
Difference	0,34±4,04	1,61±5,75	0,98±4,88	**0,577**
[2]p	0,794	0,400		
Lateral ramal inclination 1				
Deviated side	80,26±4,39	79,41±5,73	79,83±4,99	**0,715**
Opposite side	81,22±3,89	78,79±6,02	80,01±5,09	**0,298**
Difference	-0,96±3,19	0,62±3,29	-0,17±3,26	**0,290**
[2]p	0,364	0,568		

[1]Student t test *[2]Paired Sample t Test* **p<0.05*

According to Table 12, no statistically significant difference was found among groups as regard the measurements Me1 deviation, Me1-CP, Me1-HP, Me1-MSP, A1-CP, A1-HP, A1-MSP, B1-CP, B1-HP, B1-MSP, Pog 1-CP, Pog 1-HP, Pog 1-MSP, Bigonial distance 1, Bicondylar distance 1, Intercoronoid distance 1 (p>0.05).

No statistically significantdifference was found among groups and sides for Maxillary width 1, J 1-CP, J 1-MSP, Ramus length 1, Body length 1, Gonial angle 1, Go 1-CP, Go 1-HP, Go 1-MSP, Co (top) 1-CP, Co (top) 1-HP, Co (top) 1-MSP, Co (med) 1-CP, Co (med) 1-HP, Co (med) 1-MSP, Co (lat) 1-CP, Co (lat) 1-HP, Co (lat) 1-MSP, Cor 1-MSP, Gt 1-CP, Gt 1-HP, Gt 1-MSP, Frontal and Lateral ramal inclination 1 (p>0.05).

Maxillary height on the deviated side showed a significant difference between groups before surgery, which gives the reason of surgical movement performed (p:0.028; p<0.05).

Cor-CP showed a significant difference between groups on both sides before surgery (p<0.05).

In Impaction group, a significant difference of Cor-HP was found among two sides (p: 0.025; p<0.05).

In Advancement group, a significant difference of Gt-MSP between the deviated and opposite side has been shown (p: 0.013; p<0.05).

The preoperative dental morphological variables were compared between the Impaction and the Advancement group. For bilateral charecteristics, the measurements of the deviated and the opposite side were compared for each group and their difference was used to evaluate the degree of asymmetry (Table 13).

Table 13: Comparison of the dental morphological variables between groups and sides, preoperatively.

	Impaction group (n=10)	**Advancement group (n=10)**	**Total sample (n=20)**	**p**
	Ort±SS	**Ort±SS**	**Ort±SS**	
Occlusal cant 1	9,66±3,86	8,67±2,96	9,17±3,39	**0,529**
Inc1-CP	91,26±6,48	89,41±5,57	90,33±5,96	**0,500**
Inc1-HP	53,54±5,42	50,52±3,24	52,03±4,61	**0,149**
Inc1-MSP	1,4±1,01	1,17±1,03	1,28±1	**0,628**
Maxillary dental width 1				
Deviated side	26,68±1,84	26,1±1,92	26,39±1,85	**0,498**
Opposite side	25,53±2,11	26,32±1,7	25,93±1,91	**0,370**
Difference	1,15±1,8	-0,22±1,6	0,46±1,8	**0,089**
^{2}p	0,074	0,669		
Maxillary dental height 1				
Deviated side	49,36±4,34	46,47±1,8	47,92±3,55	**0,076**
Opposite side	48,86±4,54	46,63±1,88	47,75±3,57	**0,168**
Difference	0,5±2,03	-0,16±0,68	0,17±1,51	**0,356**
^{2}p	0,460	0,482		
U6 1-CP				
Deviated side	64,43±3,86	63,29±5,06	63,86±4,42	**0,579**

Opposite side	64,01±5,13	63,52±5,08	63,76±4,98	**0,831**
Difference	0,42±3,47	-0,22±2,12	0,1±2,82	**0,622**
[2]p	0,710	0,746		
U6 1-HP				
Deviated side	49,36±4,34	46,47±1,8	47,92±3,55	**0,076**
Opposite side	48,86±4,54	46,63±1,88	47,75±3,57	**0,168**
Difference	0,5±2,03	-0,16±0,68	0,17±1,51	**0,356**
[2]p	0,460	0,482		
U6 1-MSP				
Deviated side	26,68±1,84	26,1±1,92	26,39±1,85	**0,498**
Opposite side	25,53±2,11	25,92±1,73	25,73±1,89	**0,658**
Difference	1,15±1,8	0,18±2,49	0,66±2,17	**0,331**
[2]p	0,074	0,828		
U3 (1)-CP				
Deviated side	83,07±6,19	81,34±5,87	82,21±5,94	**0,531**
Opposite side	81,79±7,36	80,61±5,34	81,2±6,29	**0,686**
Difference	1,28±2,67	0,74±1,53	1,01±2,14	**0,586**
[2]p	0,165	0,162		
U3 (1)-HP				
Deviated side	52,8±5,06	49,71±2,96	51,26±4,34	**0,113**
Opposite side	52,3±5,16	50,19±3,19	51,25±4,31	**0,284**
Difference	0,5±1	-0,48±1,08	0,01±1,13	**0,051**
[2]p	0,151	0,196		
U3 (1) -MSP				
Deviated side	16,6±1,46	16,96±1,89	16,78±1,65	**0,646**
Opposite side	16,48±2	17,01±1,33	16,75±1,68	**0,493**
Difference	0,12±3,1	-0,06±2,71	0,03±2,84	**0,892**
[2]p	0,903	0,949		

[1]Student t test *[2]Paired Sample t Test*

As shown in Table 13, there was no statistically significant difference of dental variables between the two groups and between the deviated and opposite side of each group ($p<0.05$).

The preoperative soft tissue morphological variables were compared between the Impaction and the Advancement group. For bilateral charecteristics, the measurements of the deviated and the opposite side were compared for each group and their difference was used to evaluate the degree of asymmetry (Table 14).

Table 14: Comparison of the soft tissue morphological variables between groups and sides, preoperatively.

	Impaction group (n=10)	Advancement group (n=10)	Total sample (n=20)	p
	Ort±SS	Ort±SS	Ort±SS	
Pog'1-CP	100,87±7,44	103,18±10,55	102,02±8,96	**0,578**
Pog'1-HP	84,38±7,02	79,58±5,7	81,98±6,7	**0,111**
Pog'1-MSP	1,71±1,99	1,33±1,08	1,52±1,57	**0,601**
Pn1-CP	118,35±5,25	117,44±4,15	117,89±4,63	**0,671**
Pn1-HP	16,52±3,5	19,27±2,82	17,89±3,4	**0,068**
Pn1-MSP	1,57±1,53	1,17±0,51	1,37±1,13	**0,452**
Sn1-CP	102,69±4,83	101,29±4,13	101,99±4,43	**0,494**
Sn1-HP	28,11±3,75	30,25±2,53	29,18±3,3	**0,153**
Sn1-MSP	1,34±1,36	0,87±0,51	1,1±1,03	**0,328**
C1-CP	110,88±4,21	110,93±4,19	110,91±4,09	**0,979**
C1-HP	25,87±3,42	28,16±3,1	27,02±3,39	**0,134**
C1-MSP	1,42±1,54	1,08±0,49	1,25±1,12	**0,521**
Ls 1-CP	104,09±5,47	104,07±6,44	104,08±5,81	**0,995**
Ls 1-HP	40,91±4,63	42,57±3,65	41,74±4,15	**0,385**
Ls 1-MSP	1,17±0,92	0,54±0,4	0,86±0,76	**0,069**
Alar base width (total) 1	29,44±2,83	30,44±2,61	29,94±2,7	**0,423**
Nasal projection 1	19,56±1,77	19,57±1,71	19,56±1,69	**0,988**
Nasiolabial angle 1	119,06±11,68	110,77±12,96	114,92±12,74	**0,150**
Intercommısural width 1	47,07±3,06	51,76±4,77	49,41±4,58	**0,017***
Interalar width 1	33,52±2,9	35,13±2,69	34,32±2,85	**0,216**
Internostril width 1	21,98±2,57	24,21±1,93	23,09±2,49	**0,042***
Alar width 1				
Deviated side	16,53±1,98	17,29±1,49	16,91±1,75	**0,347**
Opposite side	16,91±2,2	17,71±1,73	17,31±1,97	**0,379**
Difference	-0,38±2,99	-0,42±1,94	-0,4±2,45	**0,971**
^{2}p	0,697	0,509		
Alar base width 1				
Deviated side	14,64±2,19	15,04±1,43	14,84±1,81	**0,635**
Opposite side	14,76±1,65	15,37±1,72	15,07±1,67	**0,428**
Difference	-0,12±2,63	-0,34±1,8	-0,23±2,2	**0,836**

^{2}p	0,885	0,570		
Go' 1-CP				
Deviated side	21,76±4,97	23,14±5,98	22,45±5,4	**0,581**
Opposite side	22,27±4,37	23,23±6,39	22,75±5,35	**0,698**
Difference	-0,51±4,51	-0,09±3,34	-0,3±3,87	**0,816**
^{2}p	0,731	0,935		
Go' 1-HP				
Deviated side	55,59±4,13	56,63±4,15	56,11±4,06	**0,580**
Opposite side	56,91±5	55,13±5,32	56,02±5,11	**0,450**
Difference	-1,32±4,57	1,5±3,5	0,09±4,22	**0,138**
^{2}p	0,384	0,208		
Go' 1-MSP				
Deviated side	58,14±3,12	58,88±4,63	58,51±3,86	**0,681**
Opposite side	57,67±3,01	58,7±3,95	58,18±3,46	**0,519**
Difference	0,47±1,57	0,18±1,45	0,33±1,48	**0,669**
^{2}p	0,365	0,704		
Nostril length 1				
Deviated side	13,61±0,99	14,95±1,39	14,28±1,36	**0,023***
Opposite side	13,2±1,19	14,5±1,16	13,85±1,32	**0,024***
Difference	0,41±0,75	0,45±0,68	0,43±0,7	**0,897**
^{2}p	0,119	0,065		
Ch 1-CP				
Deviated side	93,92±6,38	91,52±7,67	92,72±6,97	**0,457**
Opposite side	93,36±5,95	91,76±7,34	92,56±6,56	**0,599**
Difference	0,56±1,77	-0,24±1,32	0,16±1,58	**0,268**
^{2}p	0,344	0,581		
Ch 1-HP				
Deviated side	51,58±4,51	49,43±3,39	50,5±4,03	**0,243**
Opposite side	51,7±4,69	50,05±3,7	50,87±4,2	**0,393**
Difference	-0,12±1,07	-0,62±0,87	-0,37±0,98	**0,267**
^{2}p	0,730	0,051		
Ch 1-MSP				
Deviated side	23,36±1,57	26,08±2,5	24,72±2,46	**0,009***
Opposite side	23,04±2,11	25,25±2,58	24,15±2,56	**0,049***
Difference	0,32±1,53	0,82±1,37	0,57±1,44	**0,445**
^{2}p	0,532	0,090		

En 1-CP				
Deviated side	80,41±2,38	79,24±2,85	79,83±2,62	**0,329**
Opposite side	80,52±2,62	79,28±2,93	79,9±2,78	**0,332**
Difference	-0,1±1,13	-0,04±0,72	-0,07±0,92	**0,887**
^{2}p	0,782	0,860		
En 1-HP				
Deviated side	15,4±1,78	15,58±1,14	15,49±1,45	**0,794**
Opposite side	15,78±1,61	15,59±1,18	15,68±1,38	**0,762**
Difference	-0,38±0,57	-0,01±0,54	-0,19±0,58	**0,154**
^{2}p	0,065	0,964		
En 1-MSP				
Deviated side	16,16±1,27	16,76±1,44	16,46±1,36	**0,336**
Opposite side	16,05±0,82	16,33±1,82	16,19±1,38	**0,670**
Difference	0,11±0,85	0,43±1,31	0,27±1,09	**0,516**
^{2}p	0,701	0,323		
Ex 1-CP				
Deviated side	72,31±2,01	71,19±3,61	71,75±2,9	**0,402**
Opposite side	73,38±3,12	71,45±3,03	72,42±3,15	**0,178**
Difference	-1,07±1,96	-0,26±1,82	-0,67±1,89	**0,353**
^{2}p	0,119	0,659		
Ex 1-HP				
Deviated side	12,55±2,09	12,78±1,4	12,66±1,74	**0,775**
Opposite side	13,18±1,47	13,16±1,64	13,17±1,52	**0,977**
Difference	-0,63±1,87	-0,38±1,27	-0,51±1,56	**0,729**
^{2}p	0,312	0,367		
Ex 1-MSP				
Deviated side	48,86±3,25	47,69±2,11	48,28±2,73	**0,354**
Opposite side	47,42±1,88	47,51±1,73	47,47±1,76	**0,914**
Difference	1,43±2,22	0,18±1,64	0,81±2	**0,168**
^{2}p	0,071	0,735		
Al 1-CP				
Deviated side	97,64±3,42	95,81±4,55	96,73±4,03	**0,323**
Opposite side	96,84±4,23	96,88±4,08	96,86±4,05	**0,985**
Difference	0,8±1,8	-1,07±2,48	-0,13±2,32	**0,070**
^{2}p	0,192	0,207		
Al 1-HP				

Deviated side	21,05±3,58	22,39±1,8	21,72±2,85	**0,307**
Opposite side	21,24±3,03	22,33±2,57	21,78±2,79	**0,397**
Difference	-0,19±1,32	0,07±1,85	-0,06±1,57	**0,726**
^{2}p	0,662	0,911		
Al 1-MSP				
Deviated side	16,53±1,98	17,29±1,49	16,91±1,75	**0,347**
Opposite side	16,91±2,2	17,71±1,73	17,31±1,97	**0,379**
Difference	-0,38±2,99	-0,42±1,94	-0,4±2,45	**0,971**
^{2}p	0,697	0,509		
Ab 1-CP				
Deviated side	90,76±3,84	89,78±4,67	90,27±4,19	**0,614**
Opposite side	90,89±4,15	90,23±4,21	90,56±4,08	**0,730**
Difference	-0,13±1,13	-0,46±1,2	-0,29±1,15	**0,538**
^{2}p	0,722	0,258		
Ab 1-HP				
Deviated side	24,72±3,56	25,71±1,85	25,21±2,81	**0,445**
Opposite side	24,74±3,8	26,14±1,69	25,44±2,95	**0,305**
Difference	-0,02±1,17	-0,43±0,66	-0,23±0,95	**0,344**
^{2}p	0,962	0,067		
Ab 1-MSP				
Deviated side	14,64±2,19	15,04±1,43	14,84±1,81	**0,635**
Opposite side	14,76±1,65	15,37±1,72	15,07±1,67	**0,428**
Difference	-0,12±2,63	-0,34±1,8	-0,23±2,2	**0,836**
^{2}p	0,885	0,570		
NoS 1-CP				
Deviated side	109,64±4,06	109,54±4,38	109,59±4,11	**0,958**
Opposite side	109,69±4,15	109,4±4,31	109,55±4,12	**0,882**
Difference	-0,05±0,79	0,14±0,61	0,04±0,69	**0,564**
^{2}p	0,845	0,500		
NoS 1-HP				
Deviated side	22,84±4,28	25,89±2,94	24,36±3,9	**0,079**
Opposite side	23,02±3,2	25,63±2,81	24,32±3,22	**0,069**
Difference	-0,18±1,78	0,27±1,3	0,04±1,53	**0,529**
^{2}p	0,755	0,533		
NoS 1-MSP				
Deviated side	4,62±1,6	5,36±1,3	4,99±1,47	**0,272**

Opposite side	5,22±2,47	5,79±1,62	5,5±2,06	**0,544**
Difference	-0,6±3,8	-0,44±2,67	-0,52±3,2	**0,915**
^{2}p	0,632	0,617		
NoI 1-CP				
Deviated side	97,22±4,6	95,49±4,08	96,35±4,32	**0,386**
Opposite side	97,29±4,58	95,89±3,87	96,59±4,19	**0,469**
Difference	-0,07±0,72	-0,4±0,85	-0,23±0,78	**0,369**
^{2}p	0,767	0,174		
NoI 1-HP				
Deviated side	25,36±3,16	25,62±1,71	25,49±2,48	**0,823**
Opposite side	24,66±3,42	25,96±1,8	25,31±2,74	**0,308**
Difference	0,7±0,89	-0,34±0,8	0,18±0,98	**0,013***
^{2}p	0,034*	0,217		
NoI 1-MSP				
Deviated side	9,03±1,95	9,97±0,99	9,5±1,58	**0,191**
Opposite side	9,05±2,26	10,33±1,61	9,69±2,02	**0,161**
Difference	-0,02±3,7	-0,36±2,1	-0,19±2,94	**0,801**
^{2}p	0,988	0,599		
NoL 1-CP				
Deviated side	100,71±3,78	99,74±4,85	100,22±4,26	**0,624**
Opposite side	100,66±3,95	99,64±3,93	100,15±3,87	**0,567**
Difference	0,05±0,99	0,11±1,59	0,08±1,29	**0,922**
^{2}p	0,886	0,839		
NoL 1-HP				
Deviated side	22,79±3,54	24,18±1,85	23,49±2,84	**0,289**
Opposite side	22,44±3,64	24,29±2,02	23,36±3,02	**0,180**
Difference	0,36±0,71	-0,11±0,72	0,12±0,73	**0,164**
^{2}p	0,148	0,645		
NoL 1-MSP				
Deviated side	10,8±1,88	11,79±1,36	11,3±1,68	**0,194**
Opposite side	11,15±2,4	12,35±1,66	11,75±2,1	**0,209**
Difference	-0,35±3,46	-0,56±2,34	-0,45±2,88	**0,874**
^{2}p	0,760	0,470		

^{1}Student t test *^{2}Paired Sample t Test* **p<0.05*

According to Table 14, no significant difference between the two groups was found for Interalar width 1, Pog'1-CP, Pog'1-HP, Pog'1-MSP, Pn1-CP, Pn1-HP, Pn1-MSP, Sn1-CP, Sn1-HP, Sn1-MSP, C1-CP, C1-HP, C1-MSP, Ls 1-CP, Ls 1-HP, Ls 1-MSP, Alar base width (total) 1, Nasal projection 1, Nasiolabial angle 1 ($p>0.05$).

No significant difference was shown among groups and sides for Alar width 1, Alar base width 1, Go' 1-CP, Go' 1-HP, Go' 1-MSP, Ch 1-CP, Ch 1-HP, En 1-CP, En 1-HP, En 1-MSP, Ex 1-CP, Ex 1-HP, Ex 1-MSP, Al 1-CP, Al 1-HP, Al 1-MSP, Ab 1-CP, Ab 1-HP, Ab 1-MSP, NoS 1-CP, NoS 1-HP, NoS 1-MSP, NoI 1-CP, NoI 1-MSP, NoL 1-CP, NoL 1-HP, NoL 1-MSP ($p>0.05$).

As shown in Table 14, there was a statistically significant difference of Intercommisural width, Internostril width. Nostril length 1 and Ch 1-MSP between the two groups ($p<0.05$). NoI 1-HP differed significantly between the deviated and opposite side in Impaction group (p: 0.034; $p<0.05$).

7.4 Comparison of postoperative skeletal, dental and soft tissue morphological variables between groups and sides

The postoperative skeletal morphological variables were compared between the Impaction and the Advancement group. For bilateral charecteristics, the measurements of the deviated and the opposite side were compared for each group and their difference was used to evaluate the degree of asymmetry (Table 15).

Table 15: Comparison of the skeletal morphological variables between groups and sides, postoperatively.

	Impaction group (n=10)	**Advancement group (n=10)**	**Total sample (n=20)**	**p**
	Ort±SS	**Ort±SS**	**Ort±SS**	
Me2 deviation	1,57±2,09	1,1±0,92	1,33±1,59	**0,527**
Me2-CP	85,61±7,84	83,95±8,44	84,78±7,98	**0,655**
Me2-HP	92,54±6,42	89,28±4,41	90,91±5,61	**0,202**
Me2-MSP	1,57±2,09	1,1±0,92	1,33±1,59	**0,527**
A2-CP	89,5±4,96	88,87±5,41	89,19±5,06	**0,789**

A2-HP	26,34±3,72	29,84±2,67	28,09±3,62	**0,026***
A2-MSP	1,41±0,83	0,56±0,39	0,99±0,77	**0,012***
Maxillary width 2				
Deviated side	32,05±2,27	29,63±2,18	30,84±2,5	**0,025***
Opposite side	31,26±3,43	30,46±1,83	30,86±2,7	**0,524**
Difference	0,79±1,71	-0,84±1,51	-0,02±1,78	**0,036***
^{2}p	0,177	0,113		
Maxillary height 2				
Deviated side	23,26±4,17	23,54±1,97	23,4±3,17	**0,853**
Opposite side	22,75±3,46	23,79±1,72	23,27±2,71	**0,411**
Difference	0,51±1,64	-0,25±1,45	0,13±1,56	**0,283**
^{2}p	0,349	0,595		
Jug 2-CP				
Deviated side	64,6±4,16	63,4±5,15	64±4,6	**0,574**
Opposite side	65,08±4,67	64,17±4,77	64,62±4,62	**0,673**
Difference	-0,48±2,21	-0,77±2,57	-0,62±2,34	**0,786**
^{2}p	0,512	0,367		
Jug 2-HP				
Deviated side	23,26±4,17	23,54±1,97	23,4±3,17	**0,853**
Opposite side	22,75±3,46	23,79±1,72	23,27±2,71	**0,411**
Difference	0,51±1,64	-0,25±1,45	0,13±1,56	**0,283**
^{2}p	0,349	0,595		
Jug 2-MSP				
Deviated side	32,05±2,27	29,63±2,18	30,84±2,5	**0,025***
Opposite side	31,26±3,43	30,46±1,83	30,86±2,7	**0,524**
Difference	0,79±1,71	-0,84±1,51	-0,02±1,78	**0,036***
^{2}p	0,177	0,113		
B2-CP	87,54±6,53	86,77±7,56	87,16±6,89	**0,810**
B2-HP	70,09±6,25	67,32±3,78	68,7±5,22	**0,246**
B2-MSP	1,54±1,77	1,52±0,78	1,53±1,33	**0,976**
Pog 2-CP	91,26±7,7	89,5±7,9	90,38±7,65	**0,621**
Pog 2-HP	85,81±6,98	83,3±5,04	84,55±6,07	**0,369**
Pog 2-MSP	1,67±1,95	1,28±0,92	1,47±1,5	**0,576**
Bigonial distance 2	92,5±3,38	92,55±7,54	92,53±5,69	**0,984**
Bicondylar distance 2	115,04±4,4	116,35±5,98	115,69±5,15	**0,584**
Intercoronoid distance 2	101,7±3,93	101,06±5,26	101,38±4,53	**0,762**

Ramus length 2				
Deviated side	56,99±4,25	59,51±5,34	58,25±4,87	**0,258**
Opposite side	59,88±5,4	58,53±4,86	59,21±5,05	**0,564**
Difference	-2,89±4,78	0,98±2,82	-0,96±4,3	**0,041***
^{2}p	0,088	0,303		
Body length 2				
Deviated side	86,29±5,92	82,6±5,37	84,44±5,82	**0,161**
Opposite side	86,8±4,7	84,01±5,1	85,4±4,98	**0,219**
Difference	-0,51±4,1	-1,41±1,89	-0,96±3,14	**0,537**
^{2}p	0,703	0,043*		
Gonial angle 2				
Deviated side	50,04±6,1	50,38±6,21	50,21±5,99	**0,901**
Opposite side	51,76±5,26	50,58±6,6	51,17±5,84	**0,663**
Difference	-1,73±4,9	-0,2±4,55	-0,96±4,67	**0,479**
^{2}p	0,295	0,895		
Go 2-CP				
Deviated side	22,23±4,8	23,92±5,55	23,08±5,13	**0,475**
Opposite side	22,11±4,88	23,07±5,88	22,59±5,28	**0,696**
Difference	0,12±3,59	0,86±2,96	0,49±3,22	**0,623**
^{2}p	0,916	0,382		
Go 2-HP				
Deviated side	55,55±4,19	57,1±4,93	56,32±4,52	**0,458**
Opposite side	56,97±5,59	55,76±4,99	56,36±5,2	**0,616**
Difference	-1,42±3,84	1,34±2,74	-0,04±3,54	**0,081**
^{2}p	0,272	0,156		
Go 2-MSP				
Deviated side	46,26±2,23	46,7±4,12	46,48±3,23	**0,770**
Opposite side	46,06±1,97	45,76±4,03	45,91±3,09	**0,836**
Difference	0,2±2,42	0,94±3,05	0,57±2,71	**0,556**
^{2}p	0,802	0,357		
Co (top) 2-CP				
Deviated side	12,18±1,85	12,19±1,55	12,18±1,66	**0,985**
Opposite side	12,7±1,3	12,11±2,11	12,41±1,74	**0,463**
Difference	-0,53±1,5	0,08±2,05	-0,23±1,77	**0,460**
^{2}p	0,294	0,907		
Co (top) 2-HP				

Deviated side	1,81±1,43	1,52±1,08	1,66±1,24	**0,616**
Opposite side	1,88±0,88	1,36±1	1,62±0,96	**0,230**
Difference	-0,07±1,75	0,16±1,34	0,04±1,52	**0,740**
^{2}p	0,897	0,713		
Co (top) 2-MSP				
Deviated side	47,28±2,06	49,58±3,37	48,43±2,97	**0,082**
Opposite side	48,71±2,52	49,49±2,57	49,1±2,51	**0,502**
Difference	-1,44±2,1	0,09±3,15	-0,68±2,72	**0,218**
^{2}p	0,058	0,931		
Co (med) 2-CP				
Deviated side	12,63±2,31	11,25±1,88	11,94±2,17	**0,161**
Opposite side	12,89±2,18	11,48±1,8	12,19±2,08	**0,132**
Difference	-0,26±1,6	-0,23±2,15	-0,24±1,84	**0,969**
^{2}p	0,618	0,745		
Co (med) 2-HP				
Deviated side	6,58±2,76	6,02±1,75	6,3±2,27	**0,594**
Opposite side	4,48±2,8	5,03±1,73	4,76±2,28	**0,609**
Difference	2,1±3,03	0,99±2,09	1,54±2,6	**0,356**
^{2}p	0,056	0,168		
Co (med) 2-MSP				
Deviated side	38,1±1,89	39,83±2,85	38,97±2,52	**0,129**
Opposite side	38,89±2,07	39,61±1,9	39,25±1,97	**0,429**
Difference	-0,78±1,4	0,22±2,41	-0,28±1,99	**0,270**
^{2}p	0,111	0,779		
Co (lat) 2-CP				
Deviated side	16,52±2,16	16,14±2,79	16,33±2,44	**0,739**
Opposite side	16,6±0,91	15,38±2,32	15,99±1,83	**0,150**
Difference	-0,08±2,33	0,76±3,1	0,34±2,7	**0,503**
^{2}p	0,919	0,457		
Co (lat) 2-HP				
Deviated side	3,51±2,48	3,51±2,64	3,51±2,49	**0,997**
Opposite side	4,61±3,02	3,8±2,78	4,2±2,86	**0,540**
Difference	-1,1±4,49	-0,29±5,11	-0,69±4,7	**0,712**
^{2}p	0,459	0,862		
Co (lat) 2-MSP				
Deviated side	56,6±2,93	58,25±3,92	57,43±3,47	**0,300**

Opposite side	58,39±2,12	58,03±2,67	58,21±2,35	**0,744**
Difference	-1,79±2,62	0,22±3,06	-0,78±2,96	**0,132**
^{2}p	0,059	0,825		
Cor 2-CP				
Deviated side	46,68±2,52	44,33±2,28	45,5±2,63	**0,042***
Opposite side	47,67±2,99	44,58±2,6	46,12±3,16	**0,024***
Difference	-0,99±1,38	-0,25±1,38	-0,62±1,4	**0,244**
^{2}p	0,049*	0,586		
Cor 2-HP				
Deviated side	5,92±4,51	4,38±4,72	5,15±4,56	**0,466**
Opposite side	4,71±3,89	5,45±4,05	5,08±3,88	**0,680**
Difference	1,21±2,7	-1,07±2,22	0,07±2,68	**0,054**
^{2}p	0,191	0,161		
Cor 2-MSP				
Deviated side	47,86±3,97	45,76±4,08	46,81±4,06	**0,257**
Opposite side	47,09±3,22	46,09±2,05	46,59±2,68	**0,418**
Difference	0,77±2,4	-0,33±2,86	0,22±2,63	**0,361**
^{2}p	0,335	0,722		
Gt-CP				
Deviated side	88,46±7,09	85,71±9,97	87,09±8,54	**0,485**
Opposite side	87,91±7,12	85,7±10,21	86,8±8,64	**0,581**
Difference	0,56±1,83	0,01±1,59	0,28±1,69	**0,490**
^{2}p	0,364	0,978		
Gt2-HP				
Deviated side	88,55±6,74	85,93±4,72	87,24±5,82	**0,328**
Opposite side	88,4±6,68	85,92±4,37	87,16±5,64	**0,339**
Difference	0,15±1,13	0,01±1,37	0,08±1,23	**0,809**
^{2}p	0,680	0,975		
Gt 2-MSP				
Deviated side	12,07±3,35	12,24±3,51	12,15±3,34	**0,915**
Opposite side	10,39±4,67	10,85±4,43	10,62±4,43	**0,823**
Difference	1,68±6,53	1,38±3,55	1,53±5,12	**0,901**
^{2}p	0,437	0,249		
Frontal ramal inclination 2				
Deviated side	6,87±4,45	8,51±5,2	7,69±4,79	**0,458**

Opposite side	5,94±4,12	8,2±3,43	7,07±3,87	**0,200**
Difference	0,93±5,1	0,32±5,75	0,62±5,3	**0,805**
[2]p	0,580	0,865		
Lateral ramal inclination 2				
Deviated side	79,41±4,96	78,97±5,56	79,19±5,13	**0,854**
Opposite side	81,13±4,41	79,29±6,43	80,21±5,45	**0,464**
Difference	-1,72±4,9	-0,32±4,44	-1,02±4,61	**0,510**
[2]p	0,294	0,825		

[1]Student t test *[2]Paired Sample t Test* **p<0.05*

According to Table 15, no significant difference was found among groups for Me2 deviation, Me2-CP, Me2-HP, Me2-MSP, A2-CP, B2-CP, B2-HP, B2-MSP, Pog 2-CP, Pog 2-HP, Pog 2-MSP, Bigonial distance 2, Bicondylar distance 2, Intercoronoid distance 2 ($p>0.05$).

Moreover no significant difference between sides and groups was shown for measurements Maxillary height 2, Jug 2-CP, Jug 2-HP, Gonial angle 2, Go 2-CP, Go 2-HP, Go 2-MSP, Co (top) 2-CP, Co (top) 2-HP, Co (top) 2-MSP, Co (med) 2-CP, Co (med) 2-HP, Co (med) 2-MSP, Co (lat) 2-CP, Co (lat) 2-HP, Co (lat) 2-MSP, Cor 2-HP, Cor 2-MSP, Gt 2-CP, Gt 2-HP, Gt 2-MSP, Frontal and Lateral ramal inclination 2 ($p>0.05$).

In table 15, it is demonstrated that A2-HP, A2-MSP, Jug 2-MSP had significant differences among the groups ($p<0.05$).

Cor 2-CP had a significant difference between the groups and between the deviated and the opposite side in the Impaction group (p: 0.049; $p<0.05$).

Body length 2 showed a significant difference between the two sides of the Advancement group (p:0.043; $p<0.05$).

Moreover, the skeletal postoperative measurements were evaluated in comparison to the preoperative and the changes that occurred during the surgery were evaluated separately in each group, as shown in Table 16.

Table 16: Evaluation of the preoperative and postoperative skeletal measurements, separately in each group.

	Impaction group (n=10)			Advancement group (n=10)		
	Preop	Postop	p	Preop	Postop	p
	Ort±SS	Ort±SS		Ort±SS	Ort±SS	
Me deviatıon	1,86±2,8	1,57±2,09	**0,454**	1,67±1,36	1,1±0,92	**0,368**
Me-CP	84,86±8,66	85,61±7,84	**0,567**	86,68±11,31	83,95±8,44	**0,062**
Me-HP	96,56±6,85	92,54±6,42	**0,000***	91,11±5,23	89,28±4,41	**0,037***
Me-MSP	1,86±2,8	1,57±2,09	**0,454**	1,67±1,36	1,1±0,92	**0,368**
A-CP	85,69±4,44	89,5±4,96	**0,000***	85±4,62	88,87±5,41	**0,000***
A-HP	28,8±3,48	26,34±3,72	**0,047***	29,72±2,46	29,84±2,67	**0,499**
A-MSP	0,54±0,33	1,41±0,83	**0,021***	0,45±0,37	0,56±0,39	**0,416**
Maxillary width						
Deviated side	30,66±2,71	32,05±2,27	**0,032***	30,81±1,87	29,63±2,18	**0,129**
Opposite side	30,32±3,15	31,26±3,43	**0,178**	31,21±1,86	30,46±1,83	**0,110**
Maxillary height						
Deviated side	26,85±4,21	23,26±4,17	**0,000***	23,56±1,51	23,54±1,97	**0,920**
Opposite side	25,48±3,37	22,75±3,46	**0,000***	23,99±1,62	23,79±1,72	**0,243**
J-CP						
Deviated side	60,55±3,76	64,6±4,16	**0,000***	59,02±4,95	63,4±5,15	**0,000***
Opposite side	60,78±3,66	65,08±4,67	**0,009***	59,33±5,02	64,17±4,77	**0,000***
J -HP						
Deviated side	26,85±4,21	23,26±4,17	**0,000***	23,56±1,51	23,54±1,97	**0,920**
Opposite side	25,48±3,37	22,75±3,46	**0,000***	23,99±1,62	23,79±1,72	**0,243**
J -MSP						
Deviated side	30,66±2,71	32,05±2,27	**0,032***	30,81±1,87	29,63±2,18	**0,129**
Opposite side	30,32±3,15	31,26±3,43	**0,178**	31,21±1,86	30,46±1,83	**0,110**
B-CP	88,92±7,46	87,54±6,53	**0,252**	90,64±9,37	86,77±7,56	**0,002***
B-HP	72,62±5,42	70,09±6,25	**0,026***	68,38±5,78	67,32±3,78	**0,459**
B-MSP	1,62±2,69	1,54±1,77	**0,868**	1,54±1,08	1,52±0,78	**0,972**
Pog -CP	89,98±8,64	91,26±7,7	**0,262**	92,43±10,52	89,5±7,9	**0,043***
Pog -HP	89,82±7,18	85,81±6,98	**0,001***	84,24±5,91	83,3±5,04	**0,157**
Pog -MSP	1,91±3,05	1,67±1,95	**0,608**	1,55±1,4	1,28±0,92	**0,677**
Bigonial distance	92,76±3,5	92,5±3,38	**0,678**	92,92±6,63	92,55±7,54	**0,711**

Bicondylar distance	115,35±4,09	115,04±4,4	**0,427**	117,56±6,3	116,35±5,98	**0,125**
Intercoronoid distance	95,32±5,35	101,7±3,93	**0,000***	95,15±4,2	101,06±5,26	**0,001***
Ramus length						
Deviated side	57,29±4,41	56,99±4,25	**0,753**	58,88±4,83	59,51±5,34	**0,142**
Opposite side	60,05±4,56	59,88±5,4	**0,845**	58,68±5,07	58,53±4,86	**0,685**
Body length						
Deviated side	87,67±6,06	86,29±5,92	**0,391**	86,02±4,31	82,6±5,37	**0,029***
Opposite side	88,36±5,64	86,8±4,7	**0,222**	86,76±5,41	84,01±5,1	**0,118**
Gonial angle						
Deviated side	47,89±4,23	50,04±6,1	**0,34**	50,13±6,09	50,38±6,21	**0,886**
Opposite side	48,85±4,13	51,76±5,26	**0,191**	49,19±4,79	50,58±6,6	**0,446**
Go-CP						
Deviated side	21,93±4,78	22,23±4,8	**0,818**	23,14±6,03	23,92±5,55	**0,555**
Opposite side	22,17±4,24	22,11±4,88	**0,959**	23,76±6,25	23,07±5,88	**0,611**
Go-HP						
Deviated side	55,97±3,95	55,55±4,19	**0,639**	56,53±3,92	57,1±4,93	**0,316**
Opposite side	56,91±4,69	56,97±5,59	**0,948**	55,81±4,82	55,76±4,99	**0,869**
Go-MSP						
Deviated side	46,89±1,7	46,26±2,23	**0,26**	47,1±3,68	46,7±4,12	**0,621**
Opposite side	45,75±2,07	46,06±1,97	**0,584**	45,75±3,27	45,76±4,03	**0,984**
Co (top) -CP						
Deviated side	12,33±1,56	12,18±1,85	**0,675**	12,08±1,3	12,19±1,55	**0,722**
Opposite side	13,12±1,46	12,7±1,3	**0,214**	11,79±1,71	12,11±2,11	**0,295**
Co (top) -HP						
Deviated side	1,91±1,92	1,81±1,43	**0,654**	1,48±1,15	1,52±1,08	**0,817**
Opposite side	2,21±0,89	1,88±0,88	**0,094**	1,47±0,95	1,36±1	**0,450**
Co (top) -MSP						
Deviated side	48,89±2,64	47,28±2,06	**0,107**	49,83±3,27	49,58±3,37	**0,533**
Opposite side	48,36±2,45	48,71±2,52	**0,077**	49,09±2,61	49,49±2,57	**0,098**
Co (med) -CP						
Deviated side	12,69±2,4	12,63±2,31	**0,838**	11,73±2,05	11,25±1,88	**0,183**
Opposite side	13,49±2,62	12,89±2,18	**0,167**	12,31±1,67	11,48±1,8	**0,016***
Co (med) -HP						
Deviated side	6,3±3,31	6,58±2,76	**0,382**	5,81±1,9	6,02±1,75	**0,351**
Opposite side	4,15±2,01	4,48±2,8	**0,407**	4,49±1,38	5,03±1,73	**0,245**

Co (med) -MSP						
Deviated side	37,91±1,83	38,1±1,89	**0,548**	39,84±3,02	39,83±2,85	**0,980**
Opposite side	38,85±1,98	38,89±2,07	**0,894**	39,35±1,78	39,61±1,9	**0,440**
Co (lat) -CP						
Deviated side	16,03±1,76	16,52±2,16	**0,372**	15,61±2,25	16,14±2,79	**0,395**
Opposite side	16,56±1,02	16,6±0,91	**0,891**	15,82±2,39	15,38±2,32	**0,559**
Co (lat) -HP						
Deviated side	7,11±2,47	3,51±2,48	**0,005***	5,86±2,17	3,51±2,64	**0,042***
Opposite side	6,52±1,81	4,61±3,02	**0,035***	5,26±1,79	3,8±2,78	**0,056**
Co (lat) -MSP						
Deviated side	56,83±2,78	56,6±2,93	**0,465**	58,63±3,95	58,25±3,92	**0,312**
Opposite side	58,49±1,86	58,39±2,12	**0,528**	58,9±2,97	58,03±2,67	**0,251**
Cor -CP						
Deviated side	46,72±2,23	46,68±2,52	**0,899**	44,29±2,43	44,33±2,28	**0,888**
Opposite side	47,85±3,04	47,67±2,99	**0,368**	44,8±2,48	44,58±2,6	**0,520**
Cor -HP						
Deviated side	5,57±4,25	5,92±4,51	**0,659**	4,71±4,38	4,38±4,72	**0,564**
Opposite side	4,47±3,54	4,71±3,89	**0,794**	5,2±3,57	5,45±4,05	**0,689**
Cor -MSP						
Deviated side	47,84±2,49	47,86±3,97	**0,974**	47,76±2,03	45,76±4,08	**0,100**
Opposite side	47,42±3,11	47,09±3,22	**0,581**	47,33±2,34	46,09±2,05	**0,070**
Gt -CP						
Deviated side	87,67±8,35	88,46±7,09	**0,514**	88,21±12,37	85,71±9,97	**0,085**
Opposite side	87,15±8,25	87,91±7,12	**0,49**	88,18±12,75	85,7±10,21	**0,070**
Gt-HP						
Deviated side	92,99±7,1	88,55±6,74	**0,001***	87,67±5,23	85,93±4,72	**0,031***
Opposite side	93,18±6,82	88,4±6,68	**0,000***	88,04±5,21	85,92±4,37	**0,023***
Gt -MSP						
Deviated side	12,43±2,83	12,07±3,35	**0,345**	13,65±3,88	12,24±3,51	**0,076**
Opposite side	9,88±4,93	10,39±4,67	**0,282**	10,03±4,79	10,85±4,43	**0,273**
Frontal ramal incl						
Deviated side	5,23±4,5	6,87±4,45	**0,294**	6,67±3,75	8,51±5,2	**0,234**
Opposite side	4,88±2,8	5,94±4,12	**0,183**	5,06±3,02	8,2±3,43	**0,003***
Lateral ramal incl						
Deviated side	80,26±4,39	79,41±4,96	**0,582**	79,41±5,73	78,97±5,56	**0,707**

Opposite side	81,22±3,89	81,13±4,41	**0,953**	78,79±6,02	79,29±6,43	**0,675**

According to Table 16, the measurements Gt-HP, Co (lat) –HP, J-CP, A-CP, Me-HP and Intercoronoid distance showed a significant difference between the postoperative and preoperative values in both groups ($p<0.05$).

In Impaction group, Pog-HP, B-HP, A-HP, A-MSP, Maxillary height, J -MSP (deviated side) also showed a statistical significant change after the orthognathic surgery ($p<0.05$).

In Advancement group, postoperative measurements of B-CP, Pog-CP, Body length (deviated), Co (med)-CP (opposite), Frontal ramal inclination (opposite side) differed significantly ($p<0.05$).

The postoperative dental morphological variables were compared between the Impaction and the Advancement group. For bilateral charecteristics, the measurements of the deviated and the opposite side were compared for each group and their difference was used to evaluate the degree of asymmetry (Table 17).

Table 17: Comparison of the dental morphological variables between groups and sides, postoperatively.

	Impaction group (n=10)	Advancement group (n=10)	Total sample (n=20)	p
	Ort±SS	Ort±SS	Ort±SS	
Occlusal cant 2	9,27±4,94	8,21±3,43	8,74±4,17	**0,584**
Inc2-CP	±6	94,57±7,23	95,43±6,53	**0,568**
Inc2-HP	51,82±5,45	51,17±3,38	51,49±4,42	**0,750**
Inc2-MSP	0,87±0,53	0,91±0,68	0,89±0,6	**0,883**
Maxillary dental width 2				
Deviated side	27,46±2,05	26,3±2,02	26,88±2,07	**0,217**
Opposite side	24,8±1,63	25,24±2,06	25,02±1,82	**0,600**
Difference	2,66±2,15	1,05±2,7	1,86±2,52	**0,159**
^{2}p	0,004*	0,250		
Maxillary dental height 2				
Deviated side	47,98±4,49	47,33±2,04	47,66±3,41	**0,682**
Opposite side	47,92±5,16	47,19±2,15	47,55±3,86	**0,685**
Difference	0,06±1,6	0,14±1,1	0,1±1,34	**0,903**
^{2}p	0,349	0,595		
U6 2-CP				
Deviated side	71,72±4,37	67,98±5,81	69,85±5,36	**0,121**
Opposite side	71,24±5,24	68,45±5,2	69,84±5,28	**0,247**
Difference	0,49±2,99	-0,47±2,27	0,01±2,63	**0,434**
^{2}p	0,620	0,534		
U6 2-HP				
Deviated side	47,98±4,49	47,33±2,04	47,66±3,41	**0,682**
Opposite side	47,92±5,16	47,19±2,15	47,55±3,86	**0,685**
Difference	0,06±1,6	0,14±1,1	0,1±1,34	**0,903**
^{2}p	0,902	0,696		
U6 2-MSP				
Deviated side	26,67±1,48	26,72±2,1	26,69±1,77	**0,952**

Opposite side	25,18±1,5	25,72±1,76	25,45±1,61	**0,470**
Difference	1,48±1,29	0,99±1,99	1,24±1,65	**0,522**
^{2}p	0,005*	0,148		
U3 (2)-CP				
Deviated side	89,23±5,56	85,27±6,33	87,25±6,14	**0,154**
Opposite side	87,55±6,52	85,52±6,44	86,54±6,39	**0,493**
Difference	1,68±2,64	-0,25±1,69	0,71±2,38	**0,067**
^{2}p	0,076	0,646		
U3 (2)-HP				
Deviated side	51,1±6,49	50,56±2,49	50,83±4,79	**0,808**
Opposite side	50,67±6,34	50,75±3,34	50,71±4,93	**0,974**
Difference	0,42±1,1	-0,19±1,34	0,12±1,23	**0,276**
^{2}p	0,254	0,661		
U3 (2) -MSP				
Deviated side	17,7±1,74	17,51±1,98	17,61±1,82	**0,823**
Opposite side	17,61±1,4	17,16±0,69	17,38±1,1	**0,379**
Difference	0,1±2,57	0,35±2,41	0,22±2,43	**0,820**
^{2}p	0,909	0,655		

^{1}Student t test *^{2}Paired Sample t Test*

As regard the postoperative dental morphological variables no statistically significant difference was afound among groups for Occlusal cant 2, Inc2-CP, Inc2-HP, Inc2-MSP, and among groups and sides for Maxillary dental width 2, Maxillary dental height 2, U6 2-CP, U6 2-HP, U6 2-MSP, U3 (2)-CP, U3 (2)-HP, U3 (2) –MSP ($p>0.05$)

According to Table 17, U6 2-MSP (p: 0.005; $p<0.05$) and Maxillary dental width 2 (p: 0.004; $p<0.05$) showed significant difference between the two sides of the Impaction group.

The postoperative soft tissue morphological variables were compared between the Impaction and the Advancement group. For bilateral charecteristics, the measurements of the deviated and the opposite side were compared for each group and their difference was used to evaluate the degree of asymmetry (Table 17).

Table 18: Comparison of the soft tissue morphological variables between groups and sides, postoperatively.

	Impaction group (n=10)	Advancement group (n=10)	Total sample (n=20)	p
	Ort±SS	Ort±SS	Ort±SS	
Pog'2-CP	102,83±7,09	100,42±8,61	101,63±7,77	**0,502**
Pog'2-HP	81,68±8,06	79,93±4,8	80,81±6,52	**0,562**
Pog'2-MSP	1,4±1,41	1,52±1,14	1,46±1,25	**0,836**
Pn2-CP	120,08±5,22	119,24±4,55	119,66±4,79	**0,706**
Pn2-HP	15,81±3,65	17,76±3,17	16,78±3,48	**0,218**
Pn2-MSP	1,89±1,46	1,34±0,64	1,62±1,13	**0,296**
Sn2-CP	105,06±5,02	104,3±5,11	104,68±4,94	**0,743**
Sn2-HP	27,73±3,75	29,88±1,91	28,81±3,1	**0,124**
Sn2-MSP	1,74±1,27	1,17±0,58	1,45±1	**0,223**
C2-CP	113,3±4,55	112,54±5,51	112,92±4,93	**0,743**
C2-HP	24,15±3,55	26,96±3,42	25,56±3,69	**0,088**
C2-MSP	1,83±1,52	1,33±0,62	1,58±1,16	**0,360**
Ls 2-CP	108,2±5,54	107,05±6,81	107,62±6,07	**0,685**
Ls 2-HP	40,38±4,22	43,2±3,54	41,79±4,06	**0,123**
Ls 2-MSP	1,34±0,71	0,98±0,71	1,16±0,72	**0,274**
Alar base width (total) 2	34,45±2,89	33,96±3,27	34,2±3,02	**0,728**
Nasal projection 2	19,26±1,52	19,38±1,66	19,32±1,55	**0,867**
Nasiolabial angle 2	113,72±9,4	116,84±11,1	115,28±10,14	**0,505**
Intercommısural width 2	48,99±3,05	52±4,05	50,49±3,82	**0,077**
Interalar width 2	37,72±2,47	37,48±3,18	37,6±2,77	**0,855**
Internostril width 2	24,93±2,12	26,26±2,16	25,6±2,19	**0,181**
Alar width 2				
Deviated side	18,83±2,06	18,87±2,01	18,85±1,98	**0,965**
Opposite side	18,76±1,88	18,57±1,96	18,67±1,87	**0,827**
Difference	0,07±3,12	0,3±2,41	0,18±2,72	**0,856**
^{2}p	0,946	0,704		
Alar base width 2				
Deviated side	16,87±2,41	17,02±1,9	16,95±2,11	**0,882**
Opposite side	17,49±2,04	16,9±2,11	17,2±2,04	**0,532**
Difference	-0,62±3,43	0,12±2,32	-0,25±2,88	**0,581**
^{2}p	0,582	0,877		
Go' 2-CP				
Deviated side	22,99±5,11	22,89±5,93	22,94±5,38	**0,967**
Opposite side	22,25±5,19	22,86±5,94	22,55±5,44	**0,809**
Difference	0,75±5,74	0,03±3,93	0,39±4,8	**0,748**

	^{2}p	0,691	0,982		
Go' 2-HP					
	Deviated side	55,26±4,53	56,29±5,29	55,77±4,82	**0,647**
	Opposite side	56,67±5,79	55,23±5,76	55,95±5,67	**0,585**
	Difference	-1,41±4,86	1,06±4,52	-0,17±4,74	**0,256**
	^{2}p	0,385	0,478		
Go' 2-MSP					
	Deviated side	57,94±2,82	58,32±4,55	58,13±3,69	**0,825**
	Opposite side	58,24±3,28	57,96±4,2	58,1±3,67	**0,868**
	Difference	-0,3±2,03	0,36±1,66	0,03±1,84	**0,433**
	^{2}p	0,649	0,507		
Nostril length 2					
	Deviated side	12,36±1,37	13,94±1,28	13,15±1,53	**0,016***
	Opposite side	12,09±1,49	13,93±1,61	13,01±1,78	**0,016***
	Difference	0,27±1,43	0,01±1,34	0,14±1,36	**0,684**
	^{2}p	0,569	0,980		
Ch 2-CP					
	Deviated side	94,34±6,78	90,88±7,33	92,61±7,1	**0,288**
	Opposite side	94,35±6,61	91,3±7,36	92,82±6,98	**0,341**
	Difference	-0,01±2,13	-0,42±1,18	-0,21±1,69	**0,607**
	^{2}p	0,986	0,295		
Ch 2-HP					
	Deviated side	50,89±4,1	51,36±2,72	51,12±3,4	**0,762**
	Opposite side	50,57±4,09	51,82±3,74	51,2±3,87	**0,484**
	Difference	0,32±1,01	-0,46±1,75	-0,07±1,45	**0,241**
	^{2}p	0,350	0,428		
Ch 2-MSP					
	Deviated side	24,43±2,17	26,67±2,93	25,55±2,76	**0,069**
	Opposite side	23,7±2,56	25,4±1,83	24,55±2,34	**0,105**
	Difference	0,73±2,21	1,27±2,72	1±2,43	**0,634**
	^{2}p	0,324	0,175		
En 2-CP					
	Deviated side	80,62±2,29	79±3,18	79,81±2,82	**0,208**
	Opposite side	80,47±2,55	79,28±3,27	79,88±2,92	**0,376**
	Difference	0,15±1,01	-0,28±0,93	-0,07±0,97	**0,335**
	^{2}p	0,653	0,362		
En 2-HP					
	Deviated side	15,16±2,13	15,54±1,37	15,35±1,75	**0,636**
	Opposite side	15,62±1,68	15,28±1,19	15,45±1,43	**0,606**
	Difference	-0,46±1,11	0,26±0,5	-0,1±0,91	**0,074**
	^{2}p	0,218	0,127		
En 2-MSP					

	Deviated side	16,27±1,64	17,1±1,47	16,69±1,58	**0,248**
	Opposite side	16,13±0,69	16,48±1,76	16,31±1,32	**0,575**
	Difference	0,14±1,29	0,62±0,75	0,38±1,06	**0,314**
	^{2}p	0,746	0,28		
Ex 2-CP					
	Deviated side	72,6±1,85	71,36±4,14	71,98±3,19	**0,405**
	Opposite side	73,43±2,67	71,76±3,16	72,59±2,97	**0,217**
	Difference	-0,83±1,85	-0,39±1,85	-0,61±1,82	**0,607**
	^{2}p	0,191	0,518		
Ex 2-HP					
	Deviated side	12,59±2,3	13,13±1,3	12,86±1,84	**0,525**
	Opposite side	13,22±1,74	13,2±1,52	13,21±1,59	**0,971**
	Difference	-0,63±1,78	-0,06±1,11	-0,35±1,47	**0,402**
	^{2}p	0,291	0,863		
Ex 2-MSP					
	Deviated side	48,74±3,33	47,56±2,09	48,15±2,77	**0,356**
	Opposite side	47,54±2	47,2±1,81	47,37±1,86	**0,693**
	Difference	1,2±2,27	0,36±1,51	0,78±1,92	**0,345**
	^{2}p	0,129	0,464		
Al 2-CP					
	Deviated side	99,96±3,92	98,33±4,32	99,15±4,1	**0,389**
	Opposite side	99,33±4,3	99,13±3,89	99,23±3,99	**0,916**
	Difference	0,63±2,38	-0,8±1,2	-0,08±1,98	**0,107**
	^{2}p	0,422	0,065		
Al 2-HP					
	Deviated side	20,19±2,78	21,6±1,84	20,89±2,4	**0,197**
	Opposite side	19,35±3,02	21,76±2,09	20,55±2,81	**0,053**
	Difference	0,84±1,99	-0,16±1,22	0,34±1,69	**0,193**
	^{2}p	0,213	0,696		
Al 2-MSP					
	Deviated side	18,83±2,06	18,87±2,01	18,85±1,98	**0,965**
	Opposite side	18,76±1,88	18,57±1,96	18,67±1,87	**0,827**
	Difference	0,07±3,12	0,3±2,41	0,18±2,72	**0,856**
	^{2}p	0,946	0,704		
Ab 2-CP					
	Deviated side	95,14±4,41	93,17±5,23	94,16±4,81	**0,376**
	Opposite side	94,89±4,62	93,41±4,41	94,15±4,46	**0,475**
	Difference	0,25±2,2	-0,24±1,46	0±1,83	**0,565**
	^{2}p	0,728	0,615		
Ab 2-HP					
	Deviated side	23,59±3,47	24,9±2,24	24,25±2,92	**0,332**
	Opposite side	22,96±3,64	25,41±2,13	24,18±3,17	**0,083**
	Difference	0,64±0,91	-0,51±0,85	0,06±1,04	**0,009***

	^{2}p	0,055	0,090		
Ab 2-MSP					
	Deviated side	16,87±2,41	17,02±1,9	16,95±2,11	**0,882**
	Opposite side	17,49±2,04	16,9±2,11	17,2±2,04	**0,532**
	Difference	-0,62±3,43	0,12±2,32	-0,25±2,88	**0,581**
	^{2}p	0,582	0,877		
NoS 2-CP					
	Deviated side	112±4,81	111,4±5	111,7±4,78	**0,785**
	Opposite side	111,85±4,64	111,27±4,82	111,56±4,62	**0,789**
	Difference	0,15±0,59	0,12±0,77	0,14±0,67	**0,923**
	^{2}p	0,436	0,628		
NoS 2-HP					
	Deviated side	21,9±3,64	24,04±3,4	22,97±3,6	**0,191**
	Opposite side	21,56±3,15	23,02±3,61	22,29±3,38	**0,349**
	Difference	0,33±0,77	1,01±4,29	0,67±3,02	**0,628**
	^{2}p	0,203	0,474		
NoS 2-MSP					
	Deviated side	5,17±2,1	5,67±1,85	5,42±1,94	**0,580**
	Opposite side	5,59±2,56	5,72±1,51	5,65±2,04	**0,896**
	Difference	-0,42±4,43	-0,05±3,19	-0,24±3,76	**0,831**
	^{2}p	0,770	0,963		
NoI 2-CP					
	Deviated side	100,96±4,91	98,77±4,9	99,87±4,9	**0,332**
	Opposite side	100,91±4,87	98,99±4,77	99,95±4,79	**0,385**
	Difference	0,05±1,16	-0,22±0,77	-0,08±0,97	**0,555**
	^{2}p	0,895	0,399		
NoI 2-HP					
	Deviated side	23,93±3,03	24,91±1,89	24,42±2,51	**0,397**
	Opposite side	23,71±3,04	25,45±1,99	24,58±2,65	**0,148**
	Difference	0,22±0,46	-0,54±0,69	-0,16±0,69	**0,010***
	^{2}p	0,168	0,036*		
NoI 2-MSP					
	Deviated side	9,95±2,64	10,8±1,71	10,38±2,21	**0,404**
	Opposite side	9,85±1,82	10,76±1,68	10,3±1,76	**0,261**
	Difference	0,1±4,31	0,04±2,43	0,07±3,4	**0,971**
	^{2}p	0,943	0,956		
NoL 2-CP					
	Deviated side	104,01±4,62	101,92±4,62	102,96±4,62	**0,326**
	Opposite side	103,85±4,3	102,41±4,66	103,13±4,43	**0,482**
	Difference	0,16±1,17	-0,49±1,7	-0,16±1,46	**0,333**
	^{2}p	0,675	0,387		
NoL 2-HP					

Deviated side	21,03±3,66	22,59±2,92	21,81±3,32	**0,304**
Opposite side	20,84±3,31	23,12±2,5	21,98±3,08	**0,099**
Difference	0,19±0,69	-0,53±1,47	-0,17±1,18	**0,181**
^{2}p	0,407	0,287		
NoL 2-MSP				
Deviated side	11,9±2,39	12,98±1,54	12,44±2,03	**0,245**
Opposite side	13±1,69	13,2±1,82	13,1±1,71	**0,802**
Difference	-1,1±3,53	-0,22±2,68	-0,66±3,08	**0,538**
^{2}p	0,350	0,802		

^{1}Student t test *^{2}Paired Sample t Test* **p<0.05*

No statistically significant difference was found among the groups as regards the measurements Pog'2-CP, Pog'2-HP, Pog'2-MSP, Pn2-CP, Pn2-HP, Pn2-MSP, Sn2-CP, Sn2-HP, Sn2-MSP, C2-CP, C2-HP, C2-MSP, Ls 2-CP, Ls 2-HP, Ls 2-MSP,Alar base width (total) 2, Nasal projection 2, Nasiolabial angle 2, Intercommısural width 2, Interalar width 2, Internostril width 2 (p>0.05).

No statistically significant differencewas found between the sides of each group and between the two groups for Alar width 2, Alar base width 2, Go' 2-CP, Go' 2-HP, Go' 2-MSP, Ch 2-CP, Ch 2-HP, Ch 2-MSP, En 2-CP, En 2-HP, En 2-MSP, Ex 2-CP, Ex 2-HP, Ex 2-MSP, Al 2-CP, Al 2-HP, Al 2-MSP, Ab 2-CP, Ab 2-MSP, NoS 2-CP, NoS 2-HP, NoS 2-MSP, NoI 2-CP, NoI 2-HP, NoI 2-MSP, NoL 2-CP, NoL 2-MSP(p>0.05).

According to Table 18, Nostril length 2, NoI 2-HP and Ab 2-HP differed significantly among the groups (p<0.05). In the Advancement group, NoI 2-HP differed significantly between the deviated andthe opposite side (p:0.036, p<0.05).

7.5 Calculation of asymmetry indices of the skeletal, dental, soft tissue landmarks, preoperatively and postoperatively

For each skeletal point, an asymmetry index was calculated pre- and postoperatively and the difference between the groups, as well as the change after the orthognathic surgery was evaluated by subtracting the preoperative values from the postoperative ones (Table 19).

Table 19: Asymmetry indices of the skeletal landmarks.

		Impaction group (n=10)	**Advancement group (n=10)**	***Total Sample (n=20)***	**[1]p**
		Mean±SD	**Mean±SD**	***Mean±SD***	
Me	**Preop**	1,86±2,8	1,67±1,36	*1,76±2,15*	0,852
	Postop	1,57±2,09	1,1±0,92	*1,33±1,59*	0,527
	Difference	-0,29±1,18	-0,57±1,9	*-0,43±1,55*	0,698
	[2]p	0,454	0,368		
A	**Preop**	0,54±0,33	0,45±0,37	*0,5±0,34*	0,581
	Postop	1,19±0,97	0,56±0,39	*0,87±0,79*	0,082
	Difference	0,65±1,15	0,11±0,39	*0,38±0,88*	0,186
	[2]p	0,109	0,416		
B	**Preop**	1,62±2,69	1,54±1,08	*1,58±2*	0,933
	Postop	1,54±1,77	1,52±0,78	*1,53±1,33*	0,976
	Difference	-0,08±1,44	-0,02±1,64	*-0,05±1,5*	0,933
	[2]p	0,868	0,972		
Go	**Preop**	4,36±2,91	4,12±1,15	*4,24±2,15*	0,813
	Postop	5,32±2,08	4,52±2,58	*4,92±2,32*	0,451
	Difference	0,96±3,3	0,39±2,05	*0,68±2,69*	0,647
	[2]p	0,380	0,560		
Pog	**Preop**	1,91±3,05	1,55±1,4	*1,73±2,32*	0,741
	Postop	1,67±1,95	1,28±0,92	*1,47±1,5*	0,576
	Difference	-0,24±1,42	-0,27±1,99	*-0,26±1,68*	0,967
	[2]p	0,608	0,677		
J	**Preop**	3,77±1,75	3,11±1,2	*3,44±1,5*	0,336
	Postop	3,03±1,26	3,22±0,98	*3,12±1,1*	0,701
	Difference	-0,75±1,32	0,11±0,77	*-0,32±1,14*	0,093
	[2]p	0,106	0,663		
Gt	**Preop**	4,72±5,15	4,37±3,03	*4,55±4,12*	0,856
	Postop	4,75±5,07	3,53±2,3	*4,14±3,88*	0,496
	Difference	0,03±2,09	-0,84±2,63	*-0,4±2,36*	0,421
	[2]p	0,960	0,338		
Cor	**Preop**	2,67±1,8	2,9±1,46	*2,79±1,6*	0,758
	Postop	3,52±2,15	3,53±1,61	*3,52±1,85*	0,990
	Difference	0,85±1,04	0,63±1,17	*0,74±1,08*	0,664
	[2]p	0,030*	0,123		

Co med	**Preop**	3,52±2,83	3,44±1,63	*3,48±2,25*	0,940
	Postop	3,52±2,35	3,26±2,05	*3,39±2,15*	0,797
	Difference	0±0,95	-0,18±1,49	*-0,09±1,22*	0,752
	[2]p	0,995	0,716		
Co lat	**Preop**	3,73±1,86	3,3±1,92	*3,51±1,86*	0,617
	Postop	5,48±1,98	5,68±3,16	*5,58±2,57*	0,868
	Difference	1,76±1,2	2,39±2,6	*2,07±2*	0,499
	[2]p	0,001*	0,017*		
Co top	**Preop**	3,19±2,77	3,13±1,63	*3,16±2,22*	0,950
	Postop	2,92±1,69	3,54±1,42	*3,23±1,55*	0,385
	Difference	-0,27±2,36	0,42±1,01	*0,07±1,8*	0,410
	[2]p	0,727	0,225		

[1]Student t test *[2]Paired Sample t Test* ** p<0.05*

According to Table 19, there was no statistically significant difference between groups in terms of preoperative and postoperative asymmetry indices of the skeletal landmarks (p> 0.05). There was no statistically significant difference between the groups in terms of the change of the asymmetry indices, postoperatively (p> 0.05).

In the Impaction group there was no statistically significant change of the asymmetry indices of the skeletal landmarks, postoperatively (p> 0.05). Only the point Cor showed a statistically significant change (p:0.030; p<0.05), as well as the Co lat point (p:0.001; p<0.05).

In the Advancement group there was no statistically significant change of the asymmetry indices of the skeletal landmarks, postoperatively (p> 0.05). Only the Co lat point showed statistically significant change (p:0.017; p<0.05).

Among the skeletal landmarks, Gt presented the highest asymmetry preoperatively in both groups, followed by Go. Postoperatively, Co lat presented the highest asymmetry in both groups, followed by Go.

For each dental point, an asymmetry index was calculated pre- and postoperatively and the difference between the groups, as well as the difference after the orthognathic surgery was evaluated (Table 20).

Table 20: Asymmetry indices of the dental landmarks.

		Impaction group (n=10)	**Advancement group (n=10)**	***Total Sample (n=20)***	**[1]p**
		Mean±SD	**Mean±SD**	***Mean±SD***	
INC	**Preop**	1,4±1,01	1,17±1,03	*1,28±1,0*	0,628
	Postop	0,87±0,53	0,91±0,68	*0,89±0,59*	0,883
	Difference	-0,53±0,76	-0,26±0,95	*-0,39±0,85*	0,498
	[2]p	0,055	0,410		
U6	**Preop**	3,98±1,94	2,78±1,64	*3,38±1,85*	0,152
	Postop	3,59±1,24	2,81±1,7	*3,20±1,50*	0,256
	Difference	-0,39±1,63	0,04±1,1	*-0,17±1,37*	0,505
	[2]p	0,472	0,919		
U3	**Preop**	3,75±2,05	2,82±1,7	*3,28±1,89*	0,283
	Postop	3,66±1,8	2,75±1,51	*3,21±1,68*	0,239
	Difference	-0,09±1,7	-0,06±1,94	*-0,07±1,77*	0,974
	[2]p	0,871	0,920		

[1]Student t test *[2]Paired Sample t Test* ** p<0.05*

According to Table 20, there was no statistically significant difference between groups in terms of preoperative and postoperative asymmetry indices of the dental landmarks (p> 0.05). There was no statistically significant difference between the groups in terms of the change of the asymmetry indices, postoperatively (p> 0.05).

In the Impaction group there was no statistically significant change of the asymmetry indices of the dental landmarks, postoperatively (p> 0.05).

In the Advancement group there was no statistically significant change of the asymmetry indices of the dental landmarks, postoperatively (p> 0.05).

Preoperatively, U6 presented the highest asymmetry in Impaction group and U3 in Advancement group. Postoperatively, U3 presented the highest asymmetry in Impaction group and U6 in Advancement group.

For each soft tissue point, an asymmetry index was calculated pre- and postoperatively and the difference between the groups, as well as the difference after the orthognathic surgery was evaluated (Table 21).

Table 21: Asymmetry indices of the soft tissue landmarks.

		Impaction group (n=10)	**Advancement group (n=10)**	***Total Sample (n=20)***	**[1]p**
		Mean±SD	**Mean±SD**	***Mean±SD***	
Pn	**Preop**	1,57±1,53	1,17±0,51	1,37±1,13	0,452
	Postop	1,89±1,46	1,34±0,64	1,62±1,13	0,296
	Difference	0,32±0,84	0,17±0,43	0,25±0,65	0,620
	[2]p	0,252	0,230		
Sn	**Preop**	1,34±1,36	0,87±0,51	1,1±1,03	0,328
	Postop	1,74±1,27	1,17±0,58	1,45±1	0,223
	Difference	0,4±0,92	0,3±0,62	0,35±0,77	0,773
	[2]p	0,202	0,161		
C	**Preop**	1,42±1,54	1,08±0,49	1,25±1,12	0,521
	Postop	1,83±1,52	1,33±0,62	1,58±1,16	0,360
	Difference	0,41±0,88	0,25±0,45	0,33±0,69	0,625
	[2]p	0,176	0,111		
Pog'	**Preop**	1,71±1,99	1,33±1,08	1,52±1,57	0,601
	Postop	1,4±1,41	1,52±1,14	1,46±1,25	0,836
	Difference	-0,31±1,38	0,19±1,79	-0,06±1,57	0,491
	[2]p	0,493	0,744		
Go'	**Preop**	5,28±3,9	4,7±1,87	4,99±2,99	0,677
	Postop	6,64±3,82	5,38±2,82	6,01±3,33	0,410
	Difference	1,36±5,41	0,68±2,32	1,02±4,07	0,717
	[2]p	0,447	0,382		
Ls	**Preop**	1,17±0,92	0,54±0,4	0,86±0,76	0,069
	Postop	1,34±0,71	0,98±0,71	1,16±0,72	0,274
	Difference	0,16±0,75	0,44±0,72	0,3±0,73	0,421
	[2]p	0,508	0,088		
Al	**Preop**	3,04±2,15	3,23±1,78	3,13±1,92	0,829
	Postop	3,95±1,83	2,83±0,84	3,39±1,5	0,104
	Difference	0,91±0,98	-0,4±1,93	0,26±1,63	0,077
	[2]p	0,017*	0,528		
Ab	**Preop**	2,51±1,62	1,96±1,2	2,23±1,42	0,393
	Postop	3,64±1,91	2,72±0,65	3,18±1,47	0,177
	Difference	1,13±1,75	0,76±1,23	0,94±1,48	0,595
	[2]p	0,073	0,081		
NoS	**Preop**	3,19±2,72	2,67±1,24	2,93±2,08	0,595
	Postop	3,67±2,44	4±3,54	3,84±2,96	0,807
	Difference	0,48±1,4	1,34±3,07	0,91±2,36	0,433

	[2]p	0,305	0,202		
Nol	**Preop**	2,85±2,56	2,07±1,22	2,46±1,99	0,398
	Postop	3,5±2,56	2,44±0,85	2,97±1,94	0,240
	Difference	0,65±2,42	0,37±1,41	0,51±1,94	0,753
	[2]p	0,416	0,428		
NoL	**Preop**	2,69±2,39	2,47±1,47	2,58±1,93	0,804
	Postop	3,06±2,30	3,1±1,49	3,08±1,89	0,965
	Difference	0,37±1,18	0,63±2,04	0,5±1,63	0,729
	[2]p	0,349	0,355		
Ch	**Preop**	2,46±0,61	1,98±1,11	2,22±0,91	0,250
	Postop	3,02±1,03	3,18±1,68	3,1±1,36	0,790
	Difference	0,55±1,04	1,2±1,56	0,88±1,33	0,287
	[2]p	0,125	0,038*		
En	**Preop**	1,27±0,84	1,44±0,64	1,36±0,73	0,618
	Postop	1,6±1,15	1,4±0,32	1,5±0,83	0,602
	Difference	0,33±0,51	-0,05±0,48	0,14±0,52	0,111
	[2]p	0,073	0,771		
Ex	**Preop**	3,1±2,37	2,44±1,13	2,77±1,84	0,442
	Postop	2,85±2,35	2,31±1,16	2,58±1,82	0,523
	Difference	-0,25±0,6	-0,13±0,41	-0,19±0,5	0,620
	[2]p	0,225	0,346		

[1]Student t test *[2]Paired Sample t Test* ** p<0.05*

According to Table 21, there was no statistically significant difference between groups in terms of preoperative and postoperative asymmetry indices of the soft tissue landmarks (p> 0.05). There was no statistically significant difference between the groups in terms of the change of the asymmetry indices, postoperatively (p> 0.05).

In the Impaction group there was no statistically significant change of the asymmetry indices of the soft tissue landmarks, postoperatively (p> 0.05). Only the Al point present statistically significant change (p: 0.017; p<0.05).

In the Advancement group there was no statistically significant change of the asymmetry indices of the soft tissue landmarks, postoperatively (p> 0.05). Only Ch showed statistically significant difference (p:0,038; p<0.05) postoperatively.

Among the soft tissue landmarks, Go' presented the highest asymmetry in both groups, preoperatively and postoperatively.

7.6 Correlation of asymmetry of morphological variables with Menton deviation

The preoperative skeletal variables and their asymmetry were correlated to the Menton deviation for the total sample, to evaluate their connectıon to the mandibular asymmetry (Table 22).

Table 22: Correlation of asymmetry of skeletal morphological variables with Menton deviation, preoperatively.

Preop		**Me1 (preop) deviation**	
		R	**p**
Me-CP		-0,032	0,895
Me-HP		0,058	0,808
Me-MSP		**1,000**	**0,000***
A-CP		0,048	0,840
A-HP		-0,116	0,626
A-MSP		-0,244	0,299
Maxillary width	**Deviated side**	-0,219	0,354
	Opposite side	-0,163	0,493
	Difference	-0,055	0,819
Maxillary height	**Deviated side**	-0,086	0,720
	Opposite side	-0,163	0,493
	Difference	0,072	0,762
J-CP	**Deviated side**	-0,034	0,887
	Opposite side	-0,260	0,268
	Difference	0,331	0,154
J-HP	**Deviated side**	-0,086	0,720
	Opposite side	-0,163	0,493
	Difference	0,072	0,762
J-MSP	**Deviated side**	-0,219	0,354
	Opposite side	-0,163	0,493
	Difference	-0,055	0,819
B-CP		-0,021	0,930
B-HP		0,103	0,664
B-MSP		**0,972**	**0,000***
Pog -CP		-0,035	0,885

Pog -HP		0,05	0,836
Pog -MSP		**0,988**	**0,000***
Bigonial distance		-0,100	0,675
Bicondylar distance		-0,353	0,127
Intercoronoid distance		-0,026	0,914
Ramus length	**Deviated side**	**-0,473**	**0,035***
	Opposite side	0,135	0,571
	Difference	**-0,705**	**0,001***
Body length	**Deviated side**	0,141	0,553
	Opposite side	0,099	0,679
	Difference	0,096	0,688
Gonial angle	**Deviated side**	0,244	0,299
	Opposite side	-0,066	0,783
	Difference	**0,471**	**0,036***
Go-CP	**Deviated side**	-0,369	0,110
	Opposite side	0,025	0,916
	Difference	**-0,720**	**0,000***
Go-HP	**Deviated side**	-0,346	0,135
	Opposite side	0,147	0,537
	Difference	**-0,637**	**0,003***
Go-MSP	**Deviated side**	-0,070	0,769
	Opposite side	-0,164	0,491
	Difference	0,134	0,574
Co (top)-CP	**Deviated side**	-0,233	0,324
	Opposite side	-0,025	0,918
	Difference	-0,180	0,448
Co (top)-HP	**Deviated side**	0,195	0,411
	Opposite side	-0,031	0,896
	Difference	0,177	0,455
Co (top)-MSP	**Deviated side**	-0,031	0,898
	Opposite side	-0,108	0,649
	Difference	0,061	0,800
Co (med)-CP	**Deviated side**	0,100	0,675
	Opposite side	-0,085	0,721
	Difference	0,248	0,291
Co (med)-HP	**Deviated side**	0,186	0,433

	Opposite side	0,055	0,818
	Difference	0,144	0,544
Co (med)-MSP	**Deviated side**	-0,385	0,093
	Opposite side	-0,108	0,650
	Difference	-0,416	0,068
Co (lat)-CP	**Deviated side**	-0,308	0,187
	Opposite side	0,092	0,698
	Difference	-0,391	0,088
Co (lat)-HP	**Deviated side**	-0,198	0,402
	Opposite side	0,104	0,662
	Difference	-0,358	0,122
Co (lat)-MSP	**Deviated side**	**-0,569**	**0,009***
	Opposite side	0,038	0,873
	Difference	**-0,749**	**0,000***
Cor-CP	**Deviated side**	-0,059	0,803
	Opposite side	0,265	0,258
	Difference	**-0,628**	**0,003***
Cor-HP	**Deviated side**	-0,135	0,570
	Opposite side	0,08	0,738
	Difference	-0,374	0,104
Cor-MSP	**Deviated side**	0,051	0,831
	Opposite side	-0,114	0,631
	Difference	0,286	0,222
Gt-CP	**Deviated side**	-0,054	0,821
	Opposite side	0,002	0,992
	Difference	**-0,475**	**0,034***
Gt-HP	**Deviated side**	0,021	0,931
	Opposite side	0,096	0,688
	Difference	**-0,448**	**0,047***
Gt-MSP	**Deviated side**	**0,607**	**0,005***
	Opposite side	**-0,514**	**0,021***
	Difference	**0,879**	**0,000***
	Deviated side	-0,072	0,764
Frontal ramal inclination	**Opposite side**	-0,225	0,340
	Difference	0,071	0,767
Lateral ramal inclination	**Deviated side**	0,276	0,238

	Opposite side	-0,028	0,905
	Difference	**0,468**	**0,038***

Pearson Correlation Analysis **p<0.05*

According to Table 22, no signicant correlation was found between Menton deviation and the measurements Me-CP, Me –HP, A-CP, A-HP, A-MSP, Maxillary , Maxillary height, J-CP, J-HP, J-MSP, B-CP, B-HP, Pog –CP, Pog –HP, Bigonial distance, Bicondylar distance, Intercoronoid distance, Body length, Go-MSP, Co (top)-CP, Co (top)-HP, Co (top)-MSP, Co (med)-CP, Co (med)-HP, Co (med)-MSP, Co (lat)-CP, Co (lat)-HP, Cor-HP, Cor-MSP, Gt-MSP, Frontal ramal inclination, Lateral ramal inclination (p>0.05).

Menton deviation was significantly correlated with B-MSP, Pog-MSP (p:0.000; p<0.05).

In ramus region, Co (lat)-MSP difference between the two sides was statistically significantly correlated with Menton deviation (p:0.000; p<0.05). A significant correlation was found between Menton deviation and Ramus length and Co (lat)-MSP on the deviated side, as well as the Ramus length (p:0.001; p<0.05), Lateral Ramal inclination (p:0.038; p<0.05) and Cor-CP difference between the deviated and the opposite side (p:0.003; p<0.05).

In Gonial angle region Go-CP difference between the deviated and opposite side were statistically significantly correlated with Menton deviation (p:0.000; p<0.05). Gonial angle difference (p:0.036; p<0.05) and Go-HP difference between the two sides (p:0.003; p<0.05) also showed a significant correlation with Menton deviation.

Gt-MSP difference had a stastically significant correlation with Menton deviation (p:0.000; p<0.05). Gt-CP (p:0.034; p<0.05) and Gt-HP difference between sides (p:0.047; p<0.05), as well as Gt-MSP on the deviated and on the opposite side correlated significanty with Menton deviatin (p<0.05).

The preoperative dental variables and their asymmetry were correlated to the Menton deviation for the total sample, to evaluate their connection to the mandibular asymmetry (Table 23).

Table 22: Correlation of asymmetry of dental morphological variables with Menton deviation, preoperatively.

Preop	**Me1 (preop) deviation**	
	r	**p**

Occlusal cant		-0,168	0,479
Maxillary dental width	**Deviated side**	0,008	0,972
	Opposite side	-0,218	0,356
	Difference	0,239	0,309
Maxillary dental height	**Deviated side**	-0,100	0,675
	Opposite side	-0,016	0,945
	Difference	-0,196	0,408
Inc-CP		0,010	0,966
Inc-HP		-0,111	0,642
Inc-MSP		-0,191	0,419
U6-CP	**Deviated side**	0,105	0,661
	Opposite side	-0,108	0,650
	Difference	0,355	0,125
U6-HP	**Deviated side**	-0,100	0,675
	Opposite side	-0,016	0,945
	Difference	-0,196	0,408
U6-MSP	**Deviated side**	0,008	0,972
	Opposite side	-0,145	0,542
	Difference	0,133	0,577
U3-CP	**Deviated side**	-0,001	0,998
	Opposite side	-0,167	0,482
	Difference	**0,489**	**0,028***
U3-HP	**Deviated side**	-0,056	0,815
	Opposite side	-0,016	0,948
	Difference	-0,156	0,513
U3-MSP	**Deviated side**	0,265	0,259
	Opposite side	0,325	0,162
	Difference	-0,038	0,875

Pearson Correlation Analysis *$p<0.05$

According to Table 23, Occlusal cant, Maxillary dental width, Maxillary dental height, Inc-CP, Inc-HP, Inc-MSP, U6-CP, U6-HP, U6-MSP, U3-HP, U3-MSP did not presented a statistically significant correlation to Menton deviation ($p>0.05$)

U3-CP difference between the deviated and opposite side showed a statistically significant correlation with Menton deviation (p:0.028; p<0.05).

The preoperative soft tıssue variables and their asymmetry were correlated to the Menton deviation for the total sample, to evaluate their connectıon to the mandibular asymmetry (Table 24).

Table 24: Correlation of asymmetry of soft tissue morphological variables with Menton deviation, preoperatively.

Preop		Me1 (preop) deviation	
		r	p
Pog'-CP		-0,017	0,943
Pog'-HP		0,164	0,490
Pog'-MSP		**0,933**	**0,000***
Pn-CP		0,119	0,618
Pn-HP		-0,020	0,933
Pn-MSP		-0,001	0,998
Sn-CP		0,126	0,596
Sn-HP		-0,141	0,552
Sn-MSP		0,054	0,822
C-CP		-0,016	0,945
C-HP		0,005	0,984
C-MSP		0,054	0,822
Ls -CP		0,012	0,961
Ls -HP		-0,105	0,658
Ls -MSP		0,314	0,178
Alar base width (total)		-0,11	0,643
Nasal protrusion		-0,151	0,524
Nasiolabial angle		0,118	0,621
Intercommısural width		-0,087	0,715
Interalar width		-0,187	0,431
Internostril width		-0,414	0,070
Alar width	**Deviated side**	0,167	0,483

	Opposite side	-0,397	0,083
	Difference	0,437	0,054
Alar base width	**Deviated side**	0,142	0,551
	Opposite side	-0,334	0,151
	Difference	0,370	0,108
Go'-CP	**Deviated side**	-0,417	0,067
	Opposite side	0,085	0,720
	Difference	**-0,700**	**0,001***
Go'-HP	**Deviated side**	-0,399	0,082
	Opposite side	0,196	0,408
	Difference	**-0,620**	**0,004***
Go'-MSP	**Deviated side**	0,122	0,607
	Opposite side	0,050	0,836
	Difference	0,204	0,388
Nostril length	**Deviated side**	-0,182	0,441
	Opposite side	-0,156	0,511
	Difference	-0,060	0,802
Ch-CP	**Deviated side**	0,013	0,956
	Opposite side	-0,006	0,979
	Difference	0,085	0,722
Ch-HP	**Deviated side**	0,052	0,828
	Opposite side	0,056	0,815
	Difference	-0,026	0,915
Ch-MSP	**Deviated side**	-0,202	0,392
	Opposite side	**-0,450**	**0,046***
	Difference	**0,454**	**0,044***
En-CP	**Deviated side**	0,264	0,261
	Opposite side	0,185	0,435
	Difference	0,193	0,414
En-HP	**Deviated side**	0,023	0,923
	Opposite side	0,022	0,927
	Difference	0,006	0,980
En-MSP	**Deviated side**	0,063	0,791
	Opposite side	0,081	0,734
	Difference	-0,024	0,921
Ex-CP	**Deviated side**	0,126	0,598

	Opposite side	0,16	0,501
	Difference	-0,074	0,757
Ex-HP	**Deviated side**	-0,371	0,108
	Opposite side	-0,125	0,601
	Difference	-0,291	0,213
Ex-MSP	**Deviated side**	-0,029	0,904
	Opposite side	-0,133	0,578
	Difference	0,077	0,747
Al-CP	**Deviated side**	0,101	0,672
	Opposite side	0,067	0,780
	Difference	0,059	0,805
Al-HP	**Deviated side**	0,120	0,614
	Opposite side	-0,007	0,976
	Difference	0,231	0,327
Al-MSP	**Deviated side**	0,167	0,483
	Opposite side	-0,397	0,083
	Difference	0,437	0,054
Ab-CP	**Deviated side**	-0,053	0,823
	Opposite side	0,056	0,816
	Difference	-0,393	0,086
Ab-HP	**Deviated side**	-0,084	0,724
	Opposite side	-0,086	0,719
	Difference	0,017	0,942
Ab-MSP	**Deviated side**	0,142	0,551
	Opposite side	-0,334	0,151
	Difference	0,370	0,108
NoS-CP	**Deviated side**	-0,072	0,764
	Opposite side	0,049	0,838
	Difference	**-0,717**	**0,000***
NoS-HP	**Deviated side**	-0,205	0,386
	Opposite side	0,010	0,965
	Difference	**-0,544**	**0,013***
NoS-MSP	**Deviated side**	0,194	0,413
	Opposite side	**-0,586**	**0,007***
	Difference	**0,466**	**0,039***
NoI-CP	**Deviated side**	0,069	0,772

	Opposite side	0,123	0,605
	Difference	-0,275	0,240
NoI-HP	**Deviated side**	-0,004	0,986
	Opposite side	-0,039	0,870
	Difference	0,098	0,680
NoI-MSP	**Deviated side**	0,319	0,171
	Opposite side	-0,391	0,088
	Difference	0,440	0,052
NoL-CP	**Deviated side**	-0,019	0,935
	Opposite side	0,082	0,731
	Difference	-0,310	0,184
NoL-HP	**Deviated side**	0,134	0,574
	Opposite side	0,131	0,583
	Difference	-0,020	0,932
NoL-MSP	**Deviated side**	0,086	0,718
	Opposite side	**-0,553**	**0,011***
	Difference	**0,455**	**0,044***

Pearson Correlation Analysis **p<0.05*

According to Table 24, Pog'-CP, Pog'-HP, Pn-CP, Pn-HP, Pn-MSP, Sn-CP, Sn-HP, Sn-MSP, C-CP, C-HP, C-MSP, Ls –CP, Ls –HP, Ls –MSP, Alar base width (total), Nasal protrusion, Nasiolabial angle, Intercommisural width, Interalar width, Internostril width, Alar width, Alar base width, Go'-MSP Nostril Ch-CP length Ch-HP, En-CP, En-HP, En-MSP, Ex-CP, Ex-HP, Ex-MSP, Al-CP, Al-HP, Al-MSP, Ab-CP, Ab-HP, Ab-MSP, NoI-CP, NoI-HP, NoI-MSP, NoL-CP, NoL-HP, NoL-MSP showed no significant correlation to Menton deviation ($p>0.05$).

Pog'-MSP was significantly correlated with Menton deviation ($p:0.000$, $p<0.05$).

Go'-CP ($p:0.001$, $p<0.05$) and Go'-HP difference ($p:0.004$, $p<0.05$) were significantly correlated with Menton deviation ($p<0.05$)

Ch-MSP on opposite side as well as Ch-MSP difference ($p:0.044$, $p<0.05$) between sides showed a significant correlation with Menton deviation.

In nose area, NoS-CP (p:0.000, p<0.05), NoS-HP (p:0.013, p<0.05), NoS-MSP (p:0.039, p<0.05) and NoL-MSP difference between the two sides (p:0.044, p<0.05) were significantly correlated with Menton deviation. NoS-MSP and NoL-MSP on opposite side showed a significant correlation, as well (p<0.05).

7.7 Assessment of postoperative nasal changes

For each group, the preoperative and postoperative nasal measurements were assessed separately and the significance of their change was evaluated (Table 25).

Table 25: Evaluation of the preoperative and postoperative nasal measurements, separately in each group.

	Impaction group (n=10)			**Advancement group (n=10)**		
	Preop	**Postop**	**P**	**Preop**	**Postop**	**p**
	Ort±SS	**Ort±SS**		**Ort±SS**	**Ort±SS**	
Pn-CP	118,35±5,25	120,08±5,22	**0,000***	117,44±4,15	119,24±4,55	**0,000***
Pn-HP	16,52±3,5	15,81±3,65	**0,152**	19,27±2,82	17,76±3,17	**0,017***
Pn-MSP	1,57±1,53	1,89±1,46	**0,252**	1,17±0,51	1,34±0,64	**0,230**
Sn-CP	102,69±4,83	105,06±5,02	**0,000***	101,29±4,13	104,3±5,11	**0,001***
Sn-HP	28,11±3,75	27,73±3,75	**0,359**	30,25±2,53	29,88±1,91	**0,268**
Sn-MSP	1,34±1,36	1,74±1,27	**0,202**	0,87±0,51	1,17±0,58	**0,161**
C-CP	110,88±4,21	113,3±4,55	**0,000***	110,93±4,19	112,54±5,51	**0,023***
C-HP	25,87±3,42	24,15±3,55	**0,000***	28,16±3,1	26,96±3,42	**0,017***
C-MSP	1,42±1,54	1,83±1,52	**0,176**	1,08±0,49	1,33±0,62	**0,111**
Alar base width (total)	29,44±2,83	34,45±2,89	**0,000***	30,44±2,61	33,96±3,27	**0,000***
Nasal protrusion	19,56±1,77	19,26±1,52	**0,384**	19,57±1,71	19,38±1,66	**0,638**
Nasiolabial angle	119,06±11,68	113,72±9,4	**0,002***	110,77±12,96	116,84±11,1	**0,045***
İnteralar width	33,52±2,9	37,72±2,47	**0,000***	35,13±2,69	37,48±3,18	**0,000***
Internostril width	21,98±2,57	24,93±2,12	**0,000***	24,21±1,93	26,26±2,16	**0,000***
Alar width						
Deviated side	16,53±1,98	18,83±2,06	**0,000***	17,29±1,49	18,87±2,01	**0,001***
Opposite side	16,91±2,2	18,76±1,88	**0,001***	17,71±1,73	18,57±1,96	**0,002***

Alar base width						
Deviated side	14,64±2,19	16,87±2,41	**0,000***	15,04±1,43	17,02±1,9	**0,000***
Opposite side	14,76±1,65	17,49±2,04	**0,001***	15,37±1,72	16,9±2,11	**0,001***
Nostril length						
Deviated side	13,61±0,99	12,36±1,37	**0,003***	14,95±1,39	13,94±1,28	**0,000***
Opposite side	13,2±1,19	12,09±1,49	**0,000***	14,5±1,16	13,93±1,61	**0,144**
Al-CP						
Deviated side	97,64±3,42	99,96±3,92	**0,003***	95,81±4,55	98,33±4,32	**0,000***
Opposite side	96,84±4,23	99,33±4,3	**0,000***	96,88±4,08	99,13±3,89	**0,002***
Al -HP						
Deviated side	21,05±3,58	20,19±2,78	**0,221**	22,39±1,8	21,6±1,84	**0,124**
Opposite side	21,24±3,03	19,35±3,02	**0,003***	22,33±2,57	21,76±2,09	**0,243**
Al -MSP						
Deviated side	16,53±1,98	18,83±2,06	**0,000***	17,29±1,49	18,87±2,01	**0,001***
Opposite side	16,91±2,2	18,76±1,88	**0,001***	17,71±1,73	18,57±1,96	**0,002***
Ab-CP						
Deviated side	90,76±3,84	95,14±4,41	**0,000***	89,78±4,67	93,17±5,23	**0,000***
Opposite side	90,89±4,15	94,89±4,62	**0,000***	90,23±4,21	93,41±4,41	**0,000***
Ab-HP						
Deviated side	24,72±3,56	23,59±3,47	**0,057**	25,71±1,85	24,9±2,24	**0,055**
Opposite side	24,74±3,8	22,96±3,64	**0,020***	26,14±1,69	25,41±2,13	**0,065**
Ab -MSP						
Deviated side	14,64±2,19	16,87±2,41	**0,000***	15,04±1,43	17,02±1,9	**0,000***
Opposite side	14,76±1,65	17,49±2,04	**0,001***	15,37±1,72	16,9±2,11	**0,001***
NoS -CP						
Deviated side	109,64±4,06	112±4,81	**0,000***	109,54±4,38	111,4±5	**0,000***
Opposite side	109,69±4,15	111,85±4,64	**0,000***	109,4±4,31	111,27±4,82	**0,001***
NoS -HP						
Deviated side	22,84±4,28	21,9±3,64	**0,151**	25,89±2,94	24,04±3,4	**0,000***
Opposite side	23,02±3,2	21,56±3,15	**0,000***	25,63±2,81	23,02±3,61	**0,070**
NoS-MSP						
Deviated side	4,62±1,6	5,17±2,1	**0,185**	5,36±1,3	5,67±1,85	**0,293**
Opposite side	5,22±2,47	5,59±2,56	**0,241**	5,79±1,62	5,72±1,51	**0,741**
NoI-CP						
Deviated side	97,22±4,6	100,96±4,91	**0,000***	95,49±4,08	98,77±4,9	**0,000***

Opposite side	97,29±4,58	100,91±4,87	**0,000***	95,89±3,87	98,99±4,77	**0,000***
NoI -HP						
Deviated side	25,36±3,16	23,93±3,03	**0,000***	25,62±1,71	24,91±1,89	**0,019***
Opposite side	24,66±3,42	23,71±3,04	**0,004***	25,96±1,8	25,45±1,99	**0,033***
NoI -MSP						
Deviated side	9,03±1,95	9,95±2,64	**0,071**	9,97±0,99	10,8±1,71	**0,083**
Opposite side	9,05±2,26	9,85±1,82	**0,159**	10,33±1,61	10,76±1,68	**0,141**
NoL-CP						
Deviated side	100,71±3,78	104,01±4,62	**0,000***	99,74±4,85	101,92±4,62	**0,002***
Opposite side	100,66±3,95	103,85±4,3	**0,000***	99,64±3,93	102,41±4,66	**0,000***
NoL -HP						
Deviated side	22,79±3,54	21,03±3,66	**0,000***	24,18±1,85	22,59±2,92	**0,009***
Opposite side	22,44±3,64	20,84±3,31	**0,001***	24,29±2,02	23,12±2,5	**0,005***
NoL-MSP						
Deviated side	10,8±1,88	11,9±2,39	**0,108**	11,79±1,36	12,98±1,54	**0,001***
Opposite side	11,15±2,4	13±1,69	**0,015***	12,35±1,66	13,2±1,82	**0,006***

Paired Sample's t Test *$p<0.05$

According to Table 25, in Impaction group no statistically significant changes were found as regard the Pn-HP, Pn-MSP, Sn-HP, Sn-MSP, C-MSP, Nasal protrusion, NoS-MSP, NoI-MSP, Al-HP (deviated side), Ab-HP (deviated side), NoS-HP (deviated side), NoL-MSP (deviated side) ($p>0.05$).

In Advancement group, no significant changes were found as regard the Pn-HP, Pn-MSP, Sn-HP, Sn-MSP, C-MSP, Nasal protrusion, Nostril length (opposite side), NoS-MSP, NoS -HP (opposite side), NoI-MSP, Al-HP, Ab-HP ($p>0.05$).

However, in Impaction group significant changes were found in Pn-CP, Sn-CP, C-CP, C-HP, Alar base width (total), Nasiolabial angle, Interalar width, Internostril width, Alar width and Alar base width in both sides, Nostril length in both sides, Al-CP and Al-MSP in both sides, Al-HP in the opposite side, Ab-CP and Ab-MSP in both sides, Ab-Hp in the opposite side, NoS-CP in both sides, NoS-HP in the opposite side, NoI-CP and NoI-HP in both sides, NoL-CP and NoL-HP in both sides, NoL-MSP in the opposite side ($p<0.05$).

In Advancement group, significant changes were found in Pn-CP, Pn-HP, Sn-CP, C-CP, C-HP, Alar base width (total), Nasiolabial Angle, Interalar width, Internostril width, Alar width and Alar base width in both side, Nostril length in the deviated side, Al-CP and Al-MSP in both sides, Ab-CP and Ab-MSP in both sides, NoS-CP in both sides, NoS-HP in the deviated side, NoI-CP and NoI-HP in both sides, NoL-CP, NoL-MSP and NoL-HP in both sides ($p<0.05$).

Moreover, the nasal changes that occured after the orthognathic surgery were compared between the Impaction and the Advancement group (Table 26). The changes were measured by subtracting the preoperative measurements from the postoperative ones.

Table 26: Comparison of the postoperative nasal changes between the two groups.

	Impaction group (n=10)	**Advancement group (n=10)**	**Total sample (n=20)**	**p**
	Ort±SS	**Ort±SS**	**Ort±SS**	
Pn-CP	1,73±0,75	1,81±0,87	1,77±0,79	**0,843**
Pn-HP	-0,71±1,43	-1,52±1,63	-1,11±1,55	**0,256**
Pn-MSP	0,32±0,84	0,17±0,43	0,25±0,65	**0,620**
Sn-CP	2,37±1,38	3,02±1,85	2,69±1,62	**0,385**
Sn-HP	-0,38±1,24	-0,37±0,99	-0,38±1,09	**0,984**
Sn-MSP	0,4±0,92	0,3±0,62	0,35±0,77	**0,773**
C-CP	2,41±0,88	1,61±1,85	2,01±1,47	**0,233**
C-HP	-1,72±0,8	-1,2±1,3	-1,46±1,08	**0,299**
C-MSP	0,41±0,88	0,25±0,45	0,33±0,69	**0,625**
Alar base width (total)	5±2,1	3,52±1,51	4,26±1,94	**0,086**
Nasal protrusion	-0,3±1,03	-0,19±1,23	-0,24±1,11	**0,832**
Nasiolabial angle	-5,35±4,07	6,08±9,15	0,37±9,05	**0,002***
İnteralar width	4,2±2,12	2,36±0,91	3,28±1,85	**0,022***
Internostril width	2,95±1,47	2,06±0,71	2,5±1,21	**0,108**
Alar width				
Deviated side	2,3±1,15	1,58±0,99	1,94±1,11	**0,152**
Opposite side	1,85±1,13	0,86±0,65	1,35±1,03	**0,027***
Alar base width				

	Deviated side	2,23±1,23	1,98±1,02	2,11±1,11	**0,622**
	Opposite side	2,73±1,67	1,53±1,03	2,13±1,49	**0,069**
Nostril length					
	Deviated side	-1,25±0,97	-1,01±0,44	-1,13±0,74	**0,481**
	Opposite side	-1,11±0,49	-0,57±1,13	-0,84±0,89	**0,182**
Al-CP					
	Deviated side	2,32±1,87	2,52±1,42	2,42±1,62	**0,787**
	Opposite side	2,49±1,4	2,26±1,72	2,37±1,53	**0,745**
Al -HP					
	Deviated side	-0,86±2,06	-0,79±1,48	-0,83±1,74	**0,938**
	Opposite side	-1,89±1,45	-0,57±1,45	-1,23±1,56	**0,057**
Al -MSP					
	Deviated side	2,3±1,15	1,58±0,99	1,94±1,11	**0,152**
	Opposite side	1,85±1,13	0,86±0,65	1,35±1,03	**0,027***
Ab-CP					
	Deviated side	4,38±1,65	3,4±1,32	3,89±1,54	**0,159**
	Opposite side	4±2,04	3,18±1,18	3,59±1,67	**0,286**
Ab-HP					
	Deviated side	-1,12±1,63	-0,81±1,17	-0,97±1,39	**0,629**
	Opposite side	-1,78±1,99	-0,74±1,11	-1,26±1,66	**0,165**
Ab -MSP					
	Deviated side	2,23±1,23	1,98±1,02	2,11±1,11	**0,622**
	Opposite side	2,73±1,67	1,53±1,03	2,13±1,49	**0,069**
NoS -CP					
	Deviated side	2,36±1,16	1,86±1,06	2,11±1,11	**0,324**
	Opposite side	2,16±0,83	1,87±1,13	2,02±0,98	**0,521**
NoS -HP					
	Deviated side	-0,94±1,89	-1,86±1,05	-1,4±1,56	**0,195**
	Opposite side	-1,45±0,68	-2,61±4,02	-2,03±2,86	**0,383**
NoS-MSP					
	Deviated side	0,55±1,21	0,31±0,88	0,43±1,04	**0,622**
	Opposite side	0,38±0,95	-0,08±0,71	0,15±0,85	**0,243**
NoI-CP					
	Deviated side	3,74±1,1	3,28±1,4	3,51±1,24	**0,426**
	Opposite side	3,62±1,06	3,1±1,37	3,36±1,22	**0,358**
NoI -HP					

Deviated side	-1,43±0,84	-0,71±0,79	-1,07±0,88	**0,064**
Opposite side	-0,95±0,77	-0,51±0,64	-0,73±0,73	**0,183**
NoI -MSP				
Deviated side	0,92±1,42	0,83±1,35	0,88±1,35	**0,890**
Opposite side	0,8±1,65	0,43±0,84	0,61±1,29	**0,530**
NoL-CP				
Deviated side	3,3±1,54	2,18±1,59	2,74±1,63	**0,127**
Opposite side	3,19±1,41	2,77±1,3	2,98±1,34	**0,506**
NoL -HP				
Deviated side	-1,76±1,01	-1,6±1,52	-1,68±1,26	**0,773**
Opposite side	-1,6±1,09	-1,18±1	-1,39±1,04	**0,379**
NoL-MSP				
Deviated side	1,1±1,94	1,18±0,81	1,14±1,45	**0,897**
Opposite side	1,85±1,96	0,85±0,74	1,35±1,53	**0,156**

Student t Test **p<0.05*

According to Table 26, no statistically significant difference was found between the groups as regard the postoperative changes in Pn-CP, Pn-HP, Pn-MSP, Sn-CP, Sn-HP, Sn-MSP, C-CP, C-HP, C-MSP, Alar base width (total), Nasal protrusion, Internostril width, Alar base width, Nostril length, Al-CP, Al-HP, Ab-CP, Ab-HP, Ab-MSP, NoS -CP, NoS-HP, NoS-MSP, NoI-CP, NoI-HP, NoI-MSP, NoL-CP, NoL-HP, NoL-MSP ($p>0.05$).

However, a significant difference of the nasal soft tissue changes was found between the groups as regard the Nasiolabial angle (p:0.002; $p<0.05$), the Interalar width (p:0.022; $p<0.05$), the Alar width (Al-MSP) on the opposite side (p:0.027; $p<0.05$).

1. DISCUSSION

8.1 Discussion of Aim

The aim of this study was to investigate pre- and postsurgically the asymmetry of dentofacial and soft tissue structures in skeletal Class III, who underwent double-jaw surgery. Furthermore, contributions from dentoskeletal structures and soft tissues leading to facial asymmetry were examined and nasal asymmetry and changes after orthognathic surgery with maxillary advancement and impaction were evaluated.

In recent years, the combined orthodontic and orthognathic treatment obtained wider acceptance. A growing number of individuals choose to undergo orthognathic surgery in order to correct a severe malocclusion that can not be solved with conventional orthodontic treatment. Important advances in diagnostic tools, treatment planning and surgical techniques have made orthognathic surgery a common and safe procedure for the management of dento-facial deformities (Chew, 2006).

The orthognathic correction of a severe malocclusion aims to improve the welfare of the patients by achieving functional efficiency, structural balance and cosmetic improvement. Associated physical problems, such as temporomandibular joint and masticatory dysfunction, resistance of the upper airway, compromised oral hygiene and speech disorders are also highly improved (Legan, 1992; Reyneke, 2010). However, it has been reported that patients' motives for seeking orthognathic treatment are primarily related to appearance and self image rather than functional issues and, consequently, remarkable satisfaction with the surgical outcome depends on the aesthetical improvement (Liu et al, 2009; Moon and Kim, 2016).

Asymmetry frequently accompanies disturbances in mandibular growth and is perceived as an aesthetic problem if it is severe. Facial asymmetry appears with a frequence of 40-80% in Class III malocclusions, possibly because of excessive mandibular growth in the case of mandibular prognathism (Severt and Proffit, 1997;

Willems et al, 2001; Haraguchi et al, 2002; Yoon et al, 2004; Chew, 2006). As interest in facial esthetic increases, asymmetry poses a great concern to those who want to improve their facial appearance. Precise and accurate diagnosis and surgical treatment to address the underlying cause of the facial asymmetry are important to ensure postsurgical patient satisfaction (Baek et al, 2012).

The frontal morphology of the nose is important for balanced facial esthetic Because of its conspicuous position in the middle of the face, minor asymmetries and irregularities of the nose are easily noticeable. Previous studies reported that nasal morphology is likely to change following the orthognathic surgery, with nose widening and nose deviation being the most commonly observed complications following repositioning of the maxilla (Kramer et al, 2004; Honrado et al, 2006; Chow et al, 2007). Surgeons performing orthognathic procedures must be aware of the potential changes that can occur to the nasal structure so that they may appropriately plan adjunctive procedures and counsel their patients on both the expected aesthetic outcome and the possible need for subsequent surgeries. Since nose appearance plays a significant role in the overall aesthetic balance and symmetry of the face, nose asymmetry and changes after the surgery were also assessed.

Therefore, given the importance of high precision in diagnosis and planning, this study evaluated three-dimensionally the facial asymmetry in skeletal Class III patients who underwent orthognathic surgery. To complement this, the morphological characteristics of skeletal, dental and soft tissue structures were evaluated to determine and quantify possible factors contributing to the appearance of facial asymetry. Soft tissue postoperative changes in the region of nose were also studied.

1. Discussion of Materials and Methods

The sample of this retrospective study consists of CBCT records of 20 skeletal Class III patients (5 males, 15 females, mean age 22,35±5,16 years), who underwent combined orthodontic and surgical treatment at the Department of

Orthodontics, Faculty of Dentistry, Marmara University. All subjects were Caucasian and from the same geographic area (Turkey). They presented moderate mandibular asymmetry, identified as Menton deviation less than 4 mm (Menton deviation 1,76±2,15mm). Individuals with craniofacial syndromes, systemic diseases and anomalies, including cleft lip and palate, or a history of trauma to the jaw were excluded from the sample, since they could present anatomic variations which could affect our results. All subjects presented completed growth and development and were skeletally mature. It is preferable if homogeneity exists among the subjects of the sample, however,we did not divide further this subgroup into males and females due to its small size.

The patients were separated into two groups according to the type of the maxillary surgical movement, 10 of them received pure advancement and 10 received maxillary advancement and impaction. In this retrospective study, an attempt was made to isolate the effect of any additional surgical interventions and muscular tone difference between pre and postoperative CBCT images.Patients that underwent single-jaw surgery or received adjunctive, cosmetic surgical procedures during the orthognathic surgery, including genioplasty and mandibular countering, were exluded. Moreover, all records were taken when the subjects were in maximum intercuspation. Subjects were excluded when lip positions were different between preoperative and postoperative image capture. The difference in the muscular tone of the perioral muscles might have been affective on the original surgically-derived resultant lower face.

A number of surgical adjunctive techniques are available to surgeons to attempt to limit unwanted nasal changes as a result of maxillary surgery. The most commonly used include anterior nasal spine recontouring to reduce nasal tip upturning, VY closure to limit upper lip shortening, and alar base cinch sutures (AC) to limit alar width broadening. The effects of most of these variables and techniques are not certain, with conflicting results among studies (Khamashta-Ledezma and Naini, 2014). In the present study, the nasal region was treated according to the surgeon's estimation. Since this is a retrospective study, not all the subjects were operated by the same surgeon and this can be considered as a limitation of our study.

According to the CBCT images the ANS was reshaped for 12 patients while the suturing and closure technique remained unknown. Khamashta-Ledezma and Naini (2014) studied the effect of suturing technique on the alar widening. Alar and alar base widening did not seem to be minimized by cinch sutures in the alar base cinch sutures group and showed large variations in the cinch-only group. However, in another study modified alar cinch sutures controlled the alar base width more effectively than the conventional one (Liu et al. 2014). Finally, not enough evidence could be found in the literature to support the effect of the ANS recontouring on the nasolabial esthetics (Khamashta-Ledezma and Naini 2014).

To date, postero-anterior cephalogram remains the routine diagnostic approach to evaluate the skeletal asymmetry, while the most commonly-used method to assess soft-tissue asymmetry is based on analysis of en face patient photographs (Edler et al, 2003; Trpkova et al , 2003; Douglas, 2004; Masuoka et al, 2005). The reference points used to set the facial midline, such as the nose, philtrum and chin, may not exactly in the middle of the face, which calls into question the precision of the symmetry-plane determination. The symmetry characteristics of a 2D-projection of a 3D-body greatly depend on the direction of the projection. Hence, the larger the angle formed by the projection direction with the symmetry plane (Trpkova et al , 2003; Hartmann et al, 2007), the greater the asymmetry. Therefore, 2D analyses, whether based on photographs or radiographs, are not particularly suitable for comprehending 3D facial or skull asymmetries .

With the development of different techniques for 3D reproduction of facial topography such as laser scanning, holography and stereophotogrammetry, numerous research groups have attempted to develop suitable analyses for 3D scanning of facial asymmetries. These methods render assessment of the 3D facial surface contact-less and rapid, and have the added advantage of being non-invasive. This permits any number of recordings to be made even during the growth period, or during treatment. Moreover, untreated control groups can also be examined (Hartmann et al, 2007). Although 3D imaging data captured by stereophotogrammetry, laser scanning, electromagnetic or optoelectronic digitizer are valuable for the evaluation of the facial asymmetry, they have limited efficacy in the

assessment of skeletal asymmetry. Differences in the soft tissue thickness in sagittal and transverse directions can distort the clinical perception of skeletal asymmetry (Peck et al, 1991).

In this retrospective study, the skeletal, dental and soft tissue asymmetry was assessed using CBCT images taken with the ILUMA CBCT (Imtec Imaging, Ardmore, OK) scanner. This specific scanner requires a sitting subject which allows the esthetic surgical outcome to be studied in the same head posture with the social interaction. CBCT has been evaluated by several authors and it is considered to be a reliable tool for craniofacial measurements. Regarding the bone measurements, it provides highly accurate data when compared with the gold standard of physical measurements directly on skulls with less than 1% of relative error (Lagravere et al, 2008; Periago et al. 2008; Stratemann et al, 2008). As far as the facial soft tissue is concerned, CBCT was found to be more reliable than lateral cephalograms in presurgical patients (Ludlow et al. 2009) and not different from MRI images (Tai et al. 2011). Furthermore, linear anthropometric measurements on phantoms or cadaver heads using prelabeled or not landmarks have been proved reliable (Moerenhout et al. 2009; Fourie et al. 2011; Kook et al. 2014) with higher error for the tragion-glabella distance only (Fourie et al. 2011). Additionally to its reliability, the CBCT image captures the hard and soft tissue at the same time incorporating them in the same file and coordinate system. This adds to its reliability and cost effectiveness since a second capture with the subsequent superimposition is not necessary. As a very reliable modern tool that makes the third dimension available for the researcher and the clinician, it also boosts the orthodontist's confidence on treatment decisions. However, conservative clinical implementation is strongly recommended as the Cone Beam Computed Tomography is considered a part of the diagnostic armamentarium but not yet a part of the routine diagnostic procedure (Halazonetis 2012).

The cone beam computed tomograms of all patients were taken 1 week before and after 4-6 months postoperatively, to allow the facial soft tissue remodeling and the reduction of the facial swelling to take place. The timing of the postoperative soft tissue analysis is critical because of swelling and soft tissue remodelling and relocations. Moreover, the soft tissue changes are influenced by

many factors, such as underlying hard tissue changes, as well as the soft tissue response to the tonicity of the surrounding muscles and tissue thickness, individual biological differences, and the subject's posture, motion, and facial expression (Soncul and Bamber, 2004). Facial swelling reduces substantially within the subsequent months following surgery.

According to Day and Robert (2006), a nonuniform, asymmetric resolution of facial swelling and adaptation of the soft tissues to the altered skeletal structure occurs principally over the initial 4 months following surgery. However, minor changes continued to occur throughout the study period of 6 months.

Kau et al (2007) reported that the improvements in facial swelling after 1 week, 1 month, and 3 months are 15.43, 63.97, and 77.18% for double-jaw surgery patients. The amount of swelling remaining at 1 month was 24.2% of the initial swelling, which further improved to 14.7% at 3 months. In their study they found that facial morphology recovers to approximately 83% in 3 months. Interestingly, bimaxillary jaw surgery produced a greater amount of swelling but reduced at a faster rate than single-jaw surgery.

Van der Vlis et al. (2014) followed the double-jaw orthognathic surgery cases for one year, and they reported that only the 20% of the initial swelling was present 3 months after the surgery and 6% 6 months after the surgery. Swelling behavior did not vary significantly by gender, but the amount and the reduction rate of swelling is correlated with the preoperative body mass index (BMI). Interestingly, patients with higher BMI had the greatest amount of swelling and the fastest rate of resolution in the initial weeks following the operation (Van der Vlis et al, 2014).

Oh et al (2013) observed considerable soft tissue changes from 2 to 6 months after surgery anc recommended that it is desirable that soft tissue analysis at least 6 months after surgery. These modifications of the soft tissues may be considered complex and may be influenced by many interrelated factors, such as remaining swelling and progressive remodelling of muscles, rather than hard tissue relapse.

While a standardized pharmaceutical protocol of corticosteroid regimen was followed in the aforementioned studies, in the present study neither in pre-operative nor in post-operative stages drug was used. Furthermore, any less traumatic surgical procedure (Spinelli et al. 2014) or special postoperative care were not applied (Moro et al. 2011; Rana et al. 2011; Shetty and Mohan 2013; Gasperini et al. 2014). A possible limitation in our restrospective study may be the fact that there is no evaluation in the long term, in order to assess the stability of the postoperative results.

After all the data were collected, MIMICS 19.0 software was incorporated in order to process the CBCT images and we evaluated the skeletofacial asymmetry by calculation of the displacement of 50 skeletal, dental and soft tissue landmarks in all three planes of space and by assessment of linear and angular measurements of the skeletal, dental and soft tissue structures.

In order to evaluate the degree of asymmetry pre- and post-operatively, it is essential to define a reliable midsagittal plane. The identification of a true midsagittal plane allows correction of head tilt in the image data and facilitates visual and quantitative assessment of symmetry. In addition, the plane can be used in asymmetric deformities to mirror the healthy mandibular side.

A review in literature reveals many attempts to determine the facial symmetry plane in terms of landmarks and describe asymmetry as differences between the paired measurements of the right and left hemifaces, as practiced in anthropometric methods (Farkas and Cheung, 1981; Ferrario et al, 1994; Ras et al, 1995; Damstra et al, 2012). However, there is no consensus to which is the most reliable cephalometric plane to describe craniofacial asymmetry. Most cephalometric 3D analyses rely on midsagittal planes based on midline structures. This has evoked some concerns regarding the validity of these reference planes, since only a limited number of landmarks are used to determine the facial symmetry plane. These methods present low reliability, because inaccuracies while positioning the landmarks may lead to substantial inaccuracies. Moreover, the landmarks may be located in areas affected by asymmetry, and are thus unappropriate for precisely determining the symmetry plane's position (de Momi et al, 2006; Hartmann et al, 2007). It has been suggested

that asymmetry of the internal structures of the skull may exist both in pathological asymmetries and healthy symmetric individuals and midsaggital planes based on cranial landmarks may be not precise in the diagnosis of facial asymmetry (Kwon et al, 2006).

To overcome the possible inaccuracies of cephalometric midsagittal planes, shape analysis by means of morphometric methods such as Procrustes analysis and Euclidean distance matrix analysis has been introduced to evaluate craniofacial asymmetry (Ferrario et al, 1994). Landmark or surface-based Procrustes analysis uses visible facial features as reference to align original and mirrored images (Hajeer et al, 2004). This morphometric approach has been shown to produce very accurate and reliable midsagittal planes that can apply even in severe and congenital asymmetries (Hartman et al, 2007; Damstra et al, 2012). Further advantages are its simplicity and the fact that it can apply to 3D data obtained from laser surface scanners, stereophotogrammetry or CBCT. This method has still limited clinical use and mainly because it requires additional software and training and higher cost compared with the cephalometric analysis.

In our study, surface-based Procrustes analysis was performed and symmetry plane was defined for each patient. The symmetry plane's position was determined by superimposing the original and the mirror image obtained by a reflection along an initially arbitrary plane (Benz et al, 2002). After the fine registration, the symmetry plane was assigned from the correlating points of the original and mirror image (Hartman et al, 2007).

This method was originally developed by Benz et al (2002). The aim of this study was to compute the facial symmetry plane in order to support the surgeon intraoperatively during the repair of a displacement of the globe of the eye in zygomatic fracture cases. The authors pointed out that a symmetry plane is characterized by the agreement between the original face's spatial arrangement and its mirror image. Conversely, a mirror image of the face can be created and the symmetry plane's position can be determined by superimposing the original and its mirror image. The symmetry plane can then be determined by adjusting an arbitrary mirror plane until the original and mirror image are aligned. This study demonstrated

the validity of the constructed symmetry plane both in symmetric and asymmetric cases.

In a subsequent study, Hartman et al (2007) demonstrated the reliability and reproducibility of the landmark-independent method for determination of the facial symmetry plane and degree of asymmetry. They calculated the true symmetry plane and degree of asymmetry from 3D facial data obtained by an optical 3D-sensor in two sets of ten recordings, one set performed consecutively and one performed on different days. The calculation of the mean deviation angle between the symmetry planes served as a measure of the reproducibility of these results. The results showed that the symmetry plane can be computed with high reproducibility and accuracy by the method described by Benz et al (2002) and can be applied to document patient data at different timepoints for later evaluation of therapeutic results.

Cevidanes et al (2011) performed 3D shape analysis in CBCT images to localize and quantify the extent of virtually simulated asymmetry. They tested two mirroring approaches: 1) mirroring on the midsagittal plane determined from landmarks Nasion, Anterior nasal spine, and Basion and 2) mirroring on an arbitrary plane, then registering on the cranial base of the original image. According to this study, mandibular asymmetry can be precisely quantified with both mirroring methods. However, the choice of landmarks used to determine the plane might have a marked impact on the asymmetry quantification. Manual selection of landmarks is time consuming and the result depends on availability and visibility of the anatomic landmarks and on the ability of the user to identify them. In severe asymmetries, as in craniofacial microsomia or cleft patients, entire regions of the anatomy might be missing or severely dislocated. On the other hand, mirroring on an arbitrary plane and cranial base registration has the potential to be used for patients with trauma situations or when key landmarks are unreliable or absent. This method also had acceptable precision and can be used as an alternative assessment method, particularly for patients with marked mandibular asymmetry but relatively symmetric cranial base. This is made possible by subsequent voxel-wise rigid registration of the cranial base. It has been proven that the larger the number of points used for superimposition, the more accurate it becomes.

A well-designed study was conducted by Damstra et al (2012) and compared six different three-dimensional cephalometric midsagittal planes used to describe craniofacial asymmetry and a true symmetry plane derived from partial Ordinary Procrustes Analysis. The sample consisted of 14 dry skulls (9 symmetric and 5 asymmetric) with metallic markers which were imaged with CBCT. Three of the investigated 3D midsagittal planes were passing through three midline structures and three planes were passing through two midline structures being perpendicular to a horizontal plane. The results of the error study validated the morphometric midsagittal plane and confirmed its accuracy and reliability. The midsagittal planes determinated by the midline structures were clinically accurate in the symmetric group, but the mean differences compared to morphometric plane were still more than 1 mm. The 3D cephalometric plane passing from N, S and being perpendicular to the Frankfort horizontal plane resembled the morphometric plane the most in both the symmetric and asymmetric groups with mean differences of less than 1 mm for most variables. However, the standard deviation was often large and clinically significant for these variables. The authors concluded that the midsagittal planes based on midline stuctures may deviate from the true plane of symmetry and may be misleading in the diagnosis of craniofacial asymmetry, whereas morphometric methods present higher accuracy and reliability.

In the present study, after computation of the Midsagittal plane, the Horizontal plane was defined as being perpendicular to the Midsagittal Plane and passing through the right Porion and the right Orbital and the Coronal plane as being perpendicular to the Midsagittal Plane and the Horizontal Plane and passing through the right Porion. These planes were defined by skeletal points that were not affected by the surgical skeletal movement. Furthermore, since the patients, whose images were used in this study, were not growing anymore, the spatial position of these skeletal landmarks could be considered unchanged between the initial and final CBCT acquisition.

A 3-dimensional coordinate system was established and the skeletal, dental and soft tissue measurements consisted of the distances of each point from the reference planes. Each point was characterized by three measurements which were

the distances from the Mid-sagittal Plane (dx), the Horizontal Plane (dy) and the Coronal Plane (dz). For each point, an asymmetry index was calculated pre- and postoperatively. For solitary paramedial landmarks, only the distance to Midsagittal plane was measured and was defined as the asymmetry index. The asymmetry indices of the bilateral landmarks were calculated using the following formula (Katsumata et al, 2005, Maeda et al, 2006):

This formula was designed by Katsumata et al (2005) and has been been used in many reports in the evaluation of craniofacial asymmetry (Maeda et al, 2006; Yanez Vico et al, 2011). In the evaluation of craniofacial morphology, the asymmetry index was often expressed as a percentage to exclude interindividual differences in size. In this study, we did not express the asymmetry index as a percentage because it was impossible to compare the right and left sides for solitary paramedial points (Katsumata et al, 2005).

Identifying the structures implicated in clinically observable apparent facial asymmetry is extremely important for drawing up the treatment plan for surgery. Mandibular deviation may have various causes. In this study, a descriptive analysis of factors contributing to craniofacial asymmetry was performed (Hwang et al, 2006). We considered several variations as possible causes of the facial asymmetry, including Maxillary skeletal and dental height, Mandibular body and ramus length, Gonial angle, Occlusal cant, Frontal and Lateral ramal inclination, and a correlation with the Menton deviation was investigated.

Previous studies reported that nasal morphology is likely to change following the orthognathic surgery, with nose widening and nose deviation being the most commonly observed complications following repositioning of the maxilla (Kramer et al, 2004; Honrado et al, 2006; Chow et al, 2007). Since nose appearance plays a significant role in the overall aesthetic balance and symmetry of the face, nose

asymmetry and changes after the surgery were also assessed. Nostil width and length, Alar base width and Alar width were calculated for both sides, while Nasolabial angle and Nasal protrusion measurements assisted the evaluation of nasal changes after the orthognathic surgery.

2. Discussion of Results

1. Comparison of the skeletal, dental and soft tissue morphological variables between groups and sides

The fact that no statistically significant difference was found among groups as regard the preoperative skeletal morphological variables (Table 12) means that the distribution of patients in the two groups was not biased.

The skeletal, dental and soft tissue variables were evaluated separately in each group, pre- and postperatively. For bilateral measurements, the values of the deviated and the opposite side were compared, in order to evaluate the degree of asymmetry.

Preoperatively, Cor-HP statistically differed ($p:0.025$; $p<0.05$) between the deviated and opposite side in the Impaction group (Table 12). A significant difference of angle of the coronoid process to cranium between the right and left sides has been reported in Class III malocclusions (Yamaoka et al, 2001). Alteration of the temporal muscle due to occlusal disharmony in skeletal Class III asymmetric individuals may cause bone mass changes and, subsequently, Coronoid process asymmetry may co-exist. However, the amplitude of movement of the anterior temporal muscle improves after surgical correction of mandibular prognathism (Ingervall et al.,1979) and adaptation occurs in the phasic timing of jaw-muscle activity after orthognathic surgery (Harper et al.,1997). Postoperatively, no

statistically significant difference was found as regard Cor-HP between the two sides of the Impaction group (p>0.05).

In the Advancement group, Gt-MSP presented a significant discrepancy between the two sides (p:0.013; p<0.05) (Table 12). This suggests that asymmetric appearance of the genial tubercles may be a characteristic in skeletal Class III cases. In this case, CBCT evaluation is required to precisely ecaluate the morphology of the Genial tubercles and thelower boarder of mandible. During 3d diagnosis and virtual surgery achieved with computer-aided surgical simulation genioplasty or recontouring of the genial tubercles may be planned, in order to achieve symmetry in the lower face.

As regard the soft tissue variables, NoI-HP was found to significantly differ among the two sides of the Impaction group (p:0.034; p<0.05) (Table 14). Nostril length was increased in the deviated side, compared to the non-deviated one. In the literature, Nostril asymmetry in skeletal Class III asymmetric cases have not been studied yet. Soft tissue tension caused by the lower jaw asymmetry may be a reasonable cause of the Nostril asymmetry. Moreover, nose deviation in skeletal Class III cases may be the reason of Nostril asymmetry.

Postoperatively, Mandibular Body length was found to differ significantly between sides in the Advancement group (p:0.043, p<0.05) and Cor-CP in the Impaction group (p:0.049, p<0.05). As regard the soft tissues, NoI-HP presented significant asymmetry between the two sides (p:0.036, p<0.05), which may be related to soft tissue tension or nose deviation, as discussed above.

2. Asymmetry indices of the landmarks

The fact that no statistically significant difference was found among groups as regard the preoperative indices of all landmarks means that the distribution of patients in the two groups was not biased.

However, in both groups no significant change was found between the postoperative and postoperative asymmetry indices of most points, indicating that the orthognathic surgery had minor effect in the positional displacement of the points in the three planes of space. This maybe be contributed to parallel anteroposterior or superoinferior movement of the jaws during the orthognathic surgery, which maintained the initial asymmetry.

As regard the skeletal landmarks, in the Impaction group the point Cor showed a statistically significant change (p:0.030; $p<0.05$), as well as the Co lat point (p:0.001; $p<0.05$). In the Advancement group only the Co lat point showed statistically significant change (p:0.017; $p<0.05$). Surprisingly, both Co lat and Cor asymmetry increased after the orthognathic surgery.

Concerning the soft tissue landmarks asymmetry, the Al point present statistically significant change (p: 0.017; $p<0.05$) in the Impaction group and Ch (p:0,038; $p<0.05$) in the Advancement group, with both of them showing higher asymmetry indices postoperatively.

In our sample, orthognathic surgery has been planned using cephalometric prediction and dental model surgery. Facial asymmetry was analyzed using frontal cephalometry and photographs. However, facial asymmetry is a 3-dimensional (3D) deformity, and the effectiveness of the conventional planning approach for asymmetry correction in three dimensions seems to be low. The results of the present study have underscored that traditional orthognathic surgical planning could harbor significant residual asymmetry in patients with facial asymmetry. Over the past decades, the introduction of three-dimensional (3D) measurement technology has significantly improved the surgical planning of facial asymmetry correction as well as the prediction of the treatment outcome.

The results of our study showed that Gt, followed by Go, was the most asymmetric landmark preoperatively, with Asymmetry Indices of 4,55±4,12 mm and 4,24±2,15 mm, respectively. Gonion has been described as the most asymmetric point in previous studies (Katsumata et al, 2005, Maeda et al, 2006, Yanez Vico et al, 2011). In our study we included the point Genial Tubercle, which presented the

highest asymmetry index. In Advancement group, a significant difference of Gt-MSP between the deviated and opposite side has been shown (Table 12). This suggests that, apart from mandibular rotation to the deviated side, mandibular asymmetry might also be due to asymmetric appearance of the genial tubercles. In this case, CBCT evaluation is required to precisely diagnose the asymmetry and plan genioplasty or recontouring of the genial tubercles during the orthognathic surgery.

Postoperatively, Co lat, followed by Go, presented the highest asymmetry index of 5,58±2,57 mm. Asymmetry of Co lat increased statistically significantly after the orthognathic surgery in both groups. The asymmetry of Co lat may be related with the asymmetric movement of condyles of the deviated and opposite side during the postoperative period. The postoperative factors that affect the condylar position include the tension of soft tissue and muscles, remaining growth, and remodeling of the TMJ (Park et al, 2012; Ha et al, 2013; An et al, 2014). An et al (2014) evaluated the effect of postoperative condylar axis changes on mandibular condylar remodeling and found thet condylar inward rotation was closely related to changes of condylar surface. Moreover, it has been suggested that the condyle on the deviated side may be especially vulnerable to resorption due to greater soft tissue tension and structural weakness than the opposite side (Tyan et al, 2017).

In a recent study (Tyan et al, 2017) of the changes of postoperative condylar position in patients with facial asymmetry, it was shown that the condyle on the nonaffected side had a tendency to recover its preoperative position at 3 months after surgery and inclined slightly laterally up to 1 year after the surgery. The condyle on the affected side returned more closely to the glenoid fossa than to its pretreatment position at 3 months after surgery. Thereafter, it showed a more backward and downward position.

Another interesting finding was that the asymmetry of Coronoid point increased significantly after the orthognathic surgery. A significant difference of angle of the coronoid process to cranium between the right and left sides has been reported in Class III malocclusions (Yamaoka et al, 2001). Bone mass changes are possibly a response to the alteration of muscle activity. Occlusal disharmony related to asymmetrical muscular balance of the temporal muscle in true skeletal Class III

malocclusions may be correlated with Coronoid process asymmetry. However, the amplitude of movement of the anterior temporal muscle improves after surgical correction of mandibular prognathism (Ingervall et al.,1979) and adaptation occurs in the phasic timing of jaw-muscle activity after orthognathic surgery (Harper et al.,1997).

Evaluating the dental points, U6 showed the most significant deviation (3,38±1,85 mm) before treatment, which remained high (3,20±1,5 mm) postoperatively. U3 also presented marked asymmetry of 3,28±1,89 mm and 3,21±1,68 mm pre- and postoperatively, respectively. The midpoint of upper incisors (Inc) had a deviation of 1,28±1 presurgically, which decreased to 0.89±0,59 mm postsurgically. These results showed that the deviation of the upper dental midline was improved after the orthognathic surgery, but there was minor improvement in the asymmetry of U6 and U3 asymmetry. This may be contributed to dental alignment in the first phase of orthodontic treatment and asymmetric position of canines and molars in the arch.

As regard the soft tissue landmarks, Go' presented the highest asymmetry (4,99±2,99 mm) preoperatively, which increased significantly (6,01±3,33 mm) postoperatively. This seems a logical result, taking into consideration the high asymmetry of skeletal landmark Gonion. In a previous study of Hwang et al (2012), Go' asymmetry index of 4,63±1,12 mm was found in normal occlusion individuals. In that study, Go' was defined as the most lateral point on the mandibular angle close to bony gonion and landmark-based skeletal reference planes were identified. Although a different definition of Go', different sample and landmark-based midsagittal plane were used in the previous study, the results also showed marked asymmetry of Go'. In the study of Hwang et al (2012), the asymmetry indices showed a tendency to increase according to lower and lateral positioning of the landmarks. Skeletal asymmetry in Gonion could be eliminated if diagnosis through CBCT and 3d planning of the orthognathic surgery had been employed. However, this is a retrospective study of subjects treated in our clinic in the past. Prediction of soft tissue changes after the surgery still remains challenging, since they do not always react in accordance with hard tissues. If apparent asymmetry remains in the

Gonion area postoperatively, adjunctive, cosmetic operation applying outer bone cortex grinding or splitting corticectomy should be performed to address the residual asymmetry.

Significant postoperative changes of asymmetry were found for Al point in the Impaction group and Ch in the Advancement group, both of them presenting a higher asymmetry index after the orthognathic surgery. Alare asymmetry in relation to maxillary rotation during the orthognathic surgery has not been evaluated in literature, but it may offer a logical explanation to our findings.

In literature (Ko et al, 2015; Kang et al, 2016) it has been reported that the amount of the vertical movement of the maxillary canines and molars and that of the mandibular setback were distinct predictors for the change in vertical position of the lip commissure. Taking into the account the low predictability of lip response to orthognathic surgery, asymmetric upper arch, rotation of maxilla or asymmetric setback of mandible during the surgery may affect the commissures and explain our results of deteriorated symmetry after the orthognathic surgery.

Katsumata et al (2005) first introduced the formula to calculate the asymmetry index of points in three planes of space. He investigated the asymmetry of skeletal landmarks in 16 control subjects and 3 subjects with facial asymmetry. They found that for the control group Gonion was the most asymmetric point with an index of 4,6±1,7 mm. This agrees with our results showing an asymmetry index of 4,24±2,15 mm for Go in the total sample. Concerning the asymmetry cases, Menton, Gonion, Condyle top showed marked asymmetry, but the small sample size of asymmetry cases reduces the power of this study and increases the margin of error.

Maeda et al (2006) conducted a study based in the formula that Katsumata et al (2005) introduced, in order to characterize the symmetrical features of patients with facial deformities in comparison with normal subjects and to suggest a classification system for facial asymmetry based on 3D-CT evaluation. In this study, Menton showed marked asymmetry in the prognathic patients, followed by lower molar and incisor. Significant asymmetry was found in the region of area, where Top of condyle, Gonion and Top of coronoid process were assessed. Compared to our

study, Gonion (4,24±2,15 mm), Condyle points (Co med: 3,48±2,25 mm, Co lat: 3,51±1,86 mm, Co top: 3,16±2,22 mm) and Top of coronoid process (2,79±1,6 mm) were also found to be highly asymmetric before the orthognathic surgery.

In the study of Yanez Vico et al (2011) the same formula to calculate the asymmetry of anatomical landmarks was complemented, in order to evaluate asymmetry of a control and an asymmetry group. The subjects of the asymmetric and control groups coincided, both in the distribution of landmarks with the highest asymmetry indices (Gonion and Coronoid) and with the most stable (anterior nasal spine). The Menton point was the third in the asymmetry index for these subjects. These results coincide with ours, since a high asymmetry of Gonion (4,6±1,7 mm) was found in the subjects of this study, although less than Genial Tubercle asymmetry. The top of Coronoid process showed an asymmetry of 2,79±1,6 mm and was the fourth most asymmetric landmark following the Condyle region (Co med, Co lat, Co top).

3. Correlation of skeletal, dental and soft tissue variables with Menton deviation

Menton deviation was significantly correlated with B-MSP, Pog-MSP (p:0.000; $p<0.05$). This is a logical result for the paramedial stuctures, indicating that the mandible was bodily deviated.

As regard the condyle, Co (lat)-MSP difference between the two sides was statistically significantly (p:0.000; $p<0.05$) correlated with Menton deviation . Co (lat)-MSP on the deviated side also showed a significant correlation ($p<0.05$). Tis suggests that condyle displacement in the opposite might contribute to mandibular asymmetry. Our previous results (Table 12) revealed that distance of points Co lat to Mid-sagittal Plane (dx) and Coronal Plane (dz) were increased in the opposite side in comparison with the deviated side, although not statistically significantly, and this may show a lateral and forward displacement of condyle in the opposite side. Moreover, structural asymmetry of the condyles may be a characteristic of individuals with facial asymmetry. In a recent study (Oh et al, 2018) Menton deviation was associated with the condyle asymmetry caused by a smaller condyle on the deviated side, particularly in neck length and neck and head volumes.

In Gonial angle region, Go-CP difference between the deviated and opposite side were statistically significantly correlated with Menton deviation (p:0.000; p<0.05). In the comparison of the structural variables between sides (Table 12), Go-CP was increased in the opposite side, although not significantly. Gonial angle (p:0.036, p<0.05) and Go-HP difference between the two sides (p:0.003, p<0.05) showed also a significant correlation with Menton deviation. No statistically significant differences were found between Gonial angle and Go-HP values among the two sides (p>0.05) (Table 12). These findings suggest that Gonion point asymmetry in Coronal and Horizontal plane followed Menton asymmetry. The fact that Gonion point asymmetry between sides was not significant could be explained by the mild asymmetry of our sample. Gonion point asymmetry between sides did not reach statistical significance, but was correlated with the mild Menton deviation of our sample (Menton deviation 1,76±2,15mm). A more forward, downward and medial position of Gonion point in the non-deviated side was indicated (Table 12). To correct the skeletal Class III malocclusion and produce the downward and forward movement of Go in the deviated side and the lateral movement of Go in the opposite side, a rotational asymmetric setback of the mandible in the transverse plane should be performed during the surgery. Asymmetric setback of the mandible can cause a change in the condylar position and angulation in both the greater setback side and the lesser setback side due to the rotation of the mandible into the greater setback side. After asymmetric setback of the mandible, the condyle maintains anteroposterior, mediolateral, and superior-inferior position in the glenoid fossa, though the condyle and the proximal segment in the greater setback side rotates backward more than those in the lesser setback side (Baek et al 2006).

A significant correlation was found between Menton deviation and Ramus length on the deviated side, as well as the Ramus length (p:0.001, p<0.05) and Lateral Ramal inclination difference between the deviated and the opposite side (p:0.038, p<0.05). Ramus length and lateral inclination discrepancy might be connected with the deviation and rotation of the lower part of the mandible into the deviated side and this is consistent with what has been described as mandibular elongation or horizontal condylar hyperplasia (Jones and Tier, 2012; Walters et al, 2013). In the comparison of the morphological variables between the two sides (Table 12) we also found that Ramus length was increased in the opposite side. The difference between the two sides did not reach statistical significance, and this may be due to the mild asymmetry of the subjects of this study.

Although the Mandibular ramal length on the deviated side, as well as the Ramal length difference between sides were significantly connected to Menton deviation, no such connection was found for Mandibular body length. This may be contributed to compensatory growth of the mandibular body in the deviated side. A negative correlation has been reported between corpus length and ramus height on the same side to compensate for a fundamental asymmetry (Kwon et al, 2006). This means that, during asymmetric setback of the mandible, an uprighting of the ramus inclination of the non-deviated side to the sagittal plane is needed to restore symmetry of the facial contour. If the gonial angle area of the opposite side becomes too prominent after setback of the mandible, gonial angle reduction should be performed.

Cor-CP difference between the deviated and the opposite side was also significantly correlated with Menton deviation (p:0.003; p<0.05). Our previous results showed that Cor

point had a tendency of forward displacement in the opposite side (Table 12). These findings were not statistically significant either because of the small size or the mild asymmetry of the sample of this retrospective study, but they suggest that an asymmetry in Coronoid process co-exist in skeletal Class III patients. As previously discussed, changes in function of temporal muscle in skeletal Class III asymmetric individuals may affect the morphology of Coronoid process.

Gt-MSP difference had a stastically significant correlation with Menton deviation (p:0.000, p<0.05). Gt-CP (p:0.034, p<0.05) and Gt-HP difference between sides (p:0.047, p<0.05), as well as Gt-MSP on the deviated and on the opposite side correlated significanty with Menton deviation (p<0.05). This finding indicates that in clinical practice genial tubercles morphology and asymmetry should also be evaluated preoperatively through CBCT analysis and recontouring of them should be considered in asymmetric cases if alignment of mandible does not restore the asymmetry in the mandibular contour.

Predictive methods of CBCT 3d planning have been described in the literature (Cevidanes et al, 2011, Lin et al, 2016). After mandibular rotation and midline alignment with virtual bilateral sagittal split ramus osteotomy, the non-deviated hemi-mandible can be virtually mirrored along the facial sagittal plane. Superimposition and boolean operation of the mirrored non-deviated hemi-mandible and the initially deviated side could reveal the residual asymmetry between the two sides of the mandible. By applying this method on asymmetric patients with Menton deviation >4mm, the authors concluded that for the symphysis and parasymphysis mental region, the discrepancy in the transversal direction on the deviated side was the major cause of asymmetry. This indicates that in clinical practice, outer bone cortex grinding for considerable transversal discrepancy or splitting corticectomy for minimal transversal discrepancy would be a preferable procedure to inferior mandible border corticectomy. On the contrary, for the mandibular body region, asymmetry was mainly caused by vertical discrepancy rather than transversal discrepancy, thus the suitable approach would be full-thickness inferior mandible border corticectomy followed by outer cortex grinding or splitting corticectomy. In the case of the mandibular angle region, both vertical and transverse discrepancy contributed to the asymmetry. Hence, the combination of the above surgical methods would be necessary to achieve an ideal outcome in the modification of the that region.

Baek et al (2007) studied the factors affecting chin point deviation in skeletal class III malocclusion patients and found as possible causes the greater growth and mesial inclination of the ramus and more maxillary vertical excess in the opposite side. Gonion was located more superiorly and posteriorly in the deviated side than in the opposite side. Menton deviation was also significantly correlated with gonial angle in both sides, differences in the anteroposterior, vertical, and transverse position of the condyle between the two sides and differences in body length. These findings coincide with our results, since a high correlation was found between the Ramal length and lateral inclination difference, the Gonial angle difference, the Condyle and Gonion asymmetry. We did not find any statistical significant correlation of Mandibular Body length and Maxillary Height with Menton deviation, but this may be due to the lower degree of asymmetry of our sample (Menton deviation 1,76±2,15mm), compared with Baek et al study (Menton deviation>4mm).

You et al (2010) examined the asymmetry of morphology and dimensions in condylar, coronoid, angular, body, and chin units of the mandibles in Class III symmetric and asymmetric patients. On the nondeviated side of the asymmetric group,ramus height, condylar and body lengths and ramal volume were significantly greater, and coronoid unit length was significantly shorter compared with the deviated side. No significant discrepancies among the two sides were found in the symmetry group. Menton deviation was significantly correlated with the differences in condylar unit length, body unit length and ramal height. Although the study of You et al (2010) included more severe asymmetric cases our results concide on the correlation of the Ramus length with Menton deviation.

Yanez Vico et al (2011) correlated the structures and craniofacial dimensions that possibly affect the facial asymmetry and asymmetry indices of craniometric landmarks. The asymmetry index of the Menton correlated positively with asymmetry of the frontal ramal inclination and negatively with mandibular body length such that the greater the asymmetry of the menton, the greater the difference between the frontal inclinations of both ramuses (left and right) and the greater the symmetry between left and right mandibular body lengths. The difference between the results of the study of Yanez Vico et al (2011) and the results of the present study may be conditioned by the use of different reference planes in the two studies. Yanez Vico et al (2011) used a landmark-based midsagittal plane: they defined the plane linking the bilateral SLEAM and ELSA as the horizontal reference plane and the sagittal reference plane was defined perpendicularly to the horizontal plane, passing through ELSA and MDFM. However, this midsagittal plane showed clinically relevant (>1.00 mm) difference compared to the true symmetry plane and maybe be misleading in the diagnosis of craniofacial asymmetry (Damstra et al, 2012). Another study (Kim et , 2011) also showed that a midsaggital plane based on cranial landmarks may be not precise and exaggerate the degree of facial asymmetry.

Lee et al (2012) conducted a CBCT study to investigate the differences in mandibular morphology and dimensions between the two sides of the face in two groups: 38 subjects with normal occlusion and 28 skeletal Class III patients with facial asymmetry. Significant differences were found between the deviated and contralateral sides of the asymmetry group in condylar and ramus heights, posterior part of the mandibular body, and mediolateral ramal and anteroposterior condylar inclinations in comparison to those of the normal subjects. The deviated side of the asymmetry group had a significantly larger mediolateral ramal inclination than the nondeviated side. In this study no statistical significant discrepancy of ramus length, lateral ramal inclination and mandibular body length was found among the sides of

the subjects. However, Ramus length on the deviated side, as well as the Ramus length and Lateral Ramal inclination difference between the deviated and the opposite side were correlated with Menton deviation ($p<0.05$). This indicate that the asymmetry of structures may be correlated with the mild Menton deviation that characterize our sample.

Thiesen et al (2017) also analyzed the components related to different degrees of mandibular asymmetry in adults with skeletal Class III using cone-beam computed tomographic (CBCT) images. Mandibular asymmetry was defined and classified according to Gnathion deviation and landmark-based skeletal reference planes were set. For patients with relative asymmetry (less than 2mm) no significant differences were found between sides, except the condylar head which seemed to be located more medially and more posteriorly on the side of mandibular deviation. This is in accordance with our results. For patients with moderate and severe mandibular asymmetry, statistically relevant differences between the contralateral and deviated sides occurred for Go-MSP, Go-Cor, J-MSP, J-Hor, Mandibular Body length and Ramus length. The results of the present study were similar as regard the Go-Cor and Ramus length deviation, but no difference was found for Go-MSP, J-MSP, J-Hor and Mandibular Body length. The unlike severity and definiton of facial asymmetry and the difference in the reference planes may explain the discrepancy between the results of the two studies. Moreover, the lack of asymmetry in Go-MSP, J-MSP, J-Hor and Mandibular Body length may be due to dentoalveolar compensation for the asymmetry of mandible.

U3-CP difference between the deviated and opposite side showed a statistically significant correlation with Menton deviation (p:0.028; $p<0.05$). This suggests that yaw rotation of the maxillary dentition may be connected to mandibular asymmetry. Surprisingly, no correlation was found between mandibular asymmetry and Occlusal cant, U3-HP or U6-HP. This means that the sample of the present study was limited to cases with mild mandibular asymmetry without any maxillary asymmetry and canting of the occlusal plane. In mandibular asymmetry, buccal pressure increases on the deviated side and decreases on the opposite side, causing morphologic alterations of the dentoalveolar segment in three dimensions. Occlusal cant of 9,17±3,39 degrees was found, preoperatively, which did not change significantly (8,74±4,17 degrees) after the surgery. Precise diagnosis should address the dental or skeletal origin of a canting, preoperatively. In case of minor canting, dental correction by intrusion of the maxillary lateral segment in the opposite side can resolve it. However, if the cant is severe, maxillary impaction for superior repositioning of the maxillary lateral segment in the opposite side might be needed.

As regard the soft tissues variables, Pog'-MSP was significantly correlated with Menton deviation (p:0.000; $p<0.05$). The finding that mandibular asymmetry was significantly correlated to the asymmetry in the soft tissue Pogonion in the horizontal aspect indicates that alignment of lower jaw would restore the asymmetry of lower facial part. The hard tissues at menton and in the chin region are covered with a thin layer of soft tissues, which is related to the underlying skeletal structures in a 1:1 ratio (Nur et al, 2016).

In the present study, soft tissue Menton was not included in the assessment of soft tissue asymmetry, because it was out of the field of view of the CBCT in most cases.

Go'-CP (p:0.001; p<0.05) and Go'-HP difference (p:0.004; p<0.05) were significantly correlated with Menton deviation (p<0.05). Soft tissue Gonion followed the asymmetry of the skeletal Gonion. As mentioned above, for areas covered with thin soft tissues the potential for compensation of the underlying skeletal asymmetry decreases. For this reason, asymmetry in skeletal gonial area should be addressed during the surgery, as it may be apparent in the soft tissue contour.

Ch-MSP on opposite side as well as Ch-MSP difference between sides showed a significant correlation with Menton deviation (p:0.044; p<0.05). These results suggest that asymmetry in the outline of lips may co-exist with mandibular asymmetry, which most likely occurs owing to continuity of the orbicularis oris muscle and soft tissue tension.

Hwang et al (2009) evaluated the lip line cant in patients with mandibular asymmetry and they found 2.4^{o} lip cant, which was upward on the chin-deviated side. The lip line cant showed positive correlations with Menton deviation and mandibular anterior occlusal plane cant. Although we did not find find any significant difference in the Ch-HP difference between the deviated and opposite side, Ch-HP value was lower in the deviated side. This suggests a tendency of lip cant. On the other hand, we found a significant correlation between Ch-MSP difference among sides and Menton deviation (p<0.05).

In nose area, NoS-CP (p:0.000, p<0.05) , NoS-HP (p:0.013, p<0.05), NoS-MSP (p:0.039, p<0.05) and NoL-MSP difference between the two sides (p:0.044, p<0.05) were significantly correlated with Menton deviation (p<0.05). NoS-MSP and NoL-MSP on opposite side showed a significant correlation, as well (p<0.05). Previously such correlation has not been reported in literature and it may be related to nose deviation coexisting with mandibular deviation or soft tissue tension connected to the skeletal asymmetry.

Our sample did not contain any subjects with craniofacial anomalies or gross asymmetries. Therefore any asymmetry that was detected could be considered mild. In order to assess the true effects of asymmetry on facial esthetics and possibly the underlying compensation mechanisms, a sample consisting of subjects with more readily noticeable facial asymmetry could be studied in the same manner as the present study.

4. Assessment of the nasal changes

Virtually all LeFort I osteotomies, whether for retropositioning or advancement, result in widening of the alar bases (Schendel and Carlotti, 1991). This is most likely a result of the approach to the maxilla rather than being caused by movement of the bone itself. When the periosteum is elevated off the face of the maxilla, the regional muscles are detached from their insertions, leading to retraction and thus alar widening. The involved muscles include zygomaticus major, levator labiisuperiorus, levator labii superiorus alaeque nasi, and nasalis. A further result of the retraction of these muscles is shortening, flattening, and thinning of the upper lip (O' Ryan and Schendel, 1992). The movement of the

underlying structure of the maxilla will have a greater effect on the lip than on the alar base.

Nasal tip support is provided by the various components of the nasal anatomy and their fibrous connections with one another. The nasal septum, the quality of the lower lateral cartilages, the attachment of the medial crural footplates to the septum, and the junction of the upper and lower lateral cartilages all contribute to tip support. These structures are in direct contact with the maxilla by way of the nasal spine and nasal crest. It follows logically that any movement of the maxilla should have a resultant effect on nasal tip projection and location (Altman and Oeltjen, 2007).

In the evaluation of the nasal changes separately in each group (Table 25), in both groups significant changes were found in Pn-CP, Sn-CP, C-CP, C-HP, Alar base width (total), Nasiolabial Angle, Interalar width, Internostril width, Alar width and Alar base width in both sides, Al-CP and Al-MSP in both sides, Ab-CP and Ab-MSP in both sides, NoS-CP in both sides, NoL-CP and NoL-HP in both sides, NoI-CP and NoI-HP in both sides ($p<0.05$).

In Impaction group, significant changes were found in Nostril length in both sides, Al-HP, Ab-HP, NoS-HP and NoL-MSP in the opposite side ($p<0.05$).

In Advancement group, significant changes were found in Pn-HP, Nostril length and NoS-HP in the deviated side, NoL-MSP in both sides ($p<0.05$).

Soft tissue changes of the nasomaxillary region invariably occur on manipulation of the maxillomandibular area. According to our findings Alar base, Interalar and Internostril width increased significantly for both groups and sides after the orthognathic surgery ($p<0.05$). For Impaction group Nostril length showed a significant decrease for both sides, but in Advancement group, it decreased only in the deviated side ($p<0.05$). Nasiolabial angle decreased significantly in the Impaction group, whereas it increased in the Advancement group.

In the comparison of the nasal changes between the groups a significant difference was found between Nasiolabial angle change ($p:0.002$, $p<0.05$), Interalar width change ($p:0.022$, $p<0.05$) and Alar width of the opposite side ($p:0.027$, $p<0.05$).

The result of these findings are important because patients must be properly informed of these possible changes that can affect the overall aesthetics of the face, keeping in mind that further surgery may need to be performed.

Honrado et al (2006) studied 23 patients that underwent maxillary movement with upward rotation, maxillary movement with downward rotation, or maxillary movement without rotation. The 3d photographs were taken with the 3dMDface System (3dMD, Atlanta, Ga) and preoperative and postoperative measurements were performed for interalar width, internostril width, nasal tip projection, columellar length and nasolabial angle. According to the results of this study, there is a statistically significant increase in postoperative interalar width and Internostril width after maxillary movement, either without rotation or with rotation upward and downward. These changes occur even after the use of an alar cinching suture, which has been thought to control and decrease the amount of alar base flaring that is normally associated with maxillary advancement (Westermark et al, 1991; Mommaerts et al, 1997). However, nasal tip projection,

columellar length did not present a statistically significant change, with the data showing both decreases and increases. Interestingly, impaction of maxilla did have a statistically significant increase in the nasolabial angle. These findings are in accordance with the results of the present study as regard the increase in Interalar and Internostril width in patients that received advancement (2,36±0,91 mm and 2,06±0,71 mm, respectively) or advancement with impaction (4,2±2,12 mm and 2,95±1,47 mm, respectively). However, the results are not similar as regard Impaction group, which presented a decrease of 5,35°±4,07 in Nasiolabial angle in this study. Different methology may be the reason of this discrepancy.

Previous studies that discussed nasal tip projection with respect to orthognathic surgery also showed varied results. Schendel and Williamson (1983) observed an average of 2.4 mm of tip elevation in patients who underwent an average of 6.4 mm of maxillary advancement and impaction. Betts et al (1993) showed a 65% increase in nasal width and a 59% decrease in tip height in 26 patients who underwent advancement. On the other hand, nasal tip projection remained unchanged in the present and other studies (Westermark et al, 1991; Honrado et al 2006).

The fact that there is no change in Nasal tip protrusion after maxillary advancement can be understood in light of the work of Freihofer (1977). He studied 25 patients without cleft and 25 with cleft lip or palate who underwent Le Fort I maxillary advancement and observed that the nasal base was advanced by a ratio of 4:7 with the maxilla, while the nasal tip was advanced by a ratio of 1:3 with the maxilla. Clinically, this results in a nose that becomes flatter as the nasal base is advanced twice the amount of the tip. Anatomically, anterior-posterior compression of the cartilaginous nasal skeleton occurs, resulting in a reduction in Nasal tip protrusion and a compensatory increase in nasal width.

Chung et al (2008) performed direct anthropometric measurements to detect the postsurgical changes in the nasal morphology in patients that underwent maxillary advancement with impaction. Additional ANS contouring in patients with a larger amount of maxillary impaction and advancement to reduce the anterior movement of the supportive bone at the nasal base area. A modified cinch suture was placed directly beneath the alar base area passing through the fibro-adipose tissue of the alar base and sutured as a double loop using slowly absorbable 2-0 vicryl. Even though modified cinch sutures had been carefully performed, the Interalar width increased by a mean of 2.2±0.93 mm and the alar base width by 1.24±0.93 mm. The widening of the alar base width was similar between the narrow-nose and broad-nose groups regardless of gender. The Nostril length increased significantly and the Nasal projection decreased after surgery. In the current study, Nostril length and Nasal projection showed a statistically insignificant tendency towards decrease after the surgery.

Park et al (2011) evaluated, by the CBCT superimposition method, nasal morphologic changes in skeletal class III deformities treated by Le Fort I advancement with impaction and mandibular setback. The upward and forward movement of maxilla appeared to cause anterosuperior shift of the nasal tip and widening of the alar base (2.45±1.52 mm) and nostrils. The nasolabial angle had increased an average of 10.34±7.36°, which is inconsistent our results where a decrease of 5,35±4,07° was found in the Impaction group. In the subjects of the Park et al (2011) study alar cinch suture and V-Y

soft-tissue closure were performed, which may explain the discrepancy with our study 's findings. In the evaluation of the protrusion of the nasal tip, the average decrease was 1.08±0.83 mm (P < 0.05), which indicates a more significant decrease than we found (-0,3±1,03 mm).

In an interesting study of Kim et al (2013a), the patterns of soft tissue changes between bimaxillary, including posterior impaction of the maxilla with a Le Fort I osteotomy, and mandibular setback surgeries were compared. As in the present study, the alar base showed significant lateral movement in the double-jaw surgery patients. Single-jaw surgery patients showed slight narrowing of the alar base area, but this amount was clinically insignificant. There was no significant difference in changes to the nasal tips between the two surgery groups. Forward and upward movement occurred in both groups

Khamashta-Ledezma and Naini (2014) also found a significant increase in Interalar (2.62mm; SD:1.4 mm) and Alar base width (3.09 mm; SD: 3.5 mm) with maxillary advancement procedures. These results are comparable with the findings of the present study, where increase of the Interalar and Alar base width were 3,28±1,85 mm and 4,26±1,94 mm for the total sample. The subjects that received alar base cinch closure experienced slightly less widening of this, the P value was only 0.042, and the difference between the means was clinically insignificant (0.08 mm). The authors concluded that, whereby if cinch sutures limit alar base widening, they do so to a clinically insignificant degree. The Nasolabial angle increased by a mean of 1.88^{o}, and cinch sutures seemed to increase this further. The increase in the Nasolabial angle was moderately correlated to the maxillary advancement at A-point (r 5 0.45; P<0.01). However, in this study subjects were not divided according to the type of surgery (maxillary advancement with or without impaction).

Dantas et al (2015) conducted a clinical prospective study of 20 patients who underwent maxillary advancement surgery. This study showed an upward rotation of the nasal tip in 80% of cases, downward rotation in 10%, and no rotation ofthe nasal tip in 10% of patients. The measurement of postoperative Interalar width increased in 95% of cases. Again the sample was not subgrouped according to the surgical movement of maxilla.

van Loon et al. (2015) used CBCT images to measure the maxillary translation and 3dMD images to measure the nasal volume, upper lip volume and the inter-alar width changes in patients who underwent a Le Fort I osteotomy, with or without a bilateral sagittal split osteotomy. According to the results, anterior translation of the maxilla did not significantly influence nose volume. In accordance with the results of the current study, a positive correlation between cranial translation of the maxilla and an increase in the Interalar width was found. Interestingly, rotations of the maxilla did not show any correlated nose changes.

In summary, the changes in nasal morphology after orthognathic surgery are difficult, if not impossible, to predict. The difficulty of predicting nasal changes after

LeFort I osteotomies is complicated by the myriad of preoperative differences between patients and the confounding attributes that affect nasal morphology. Skin thickness and elasticity, nasal tip support structures, and subtle differences in facial muscle structure all contribute to blunt or enhance the predicted effects (Gassmann et al, 1989). Widening of the Interalar and Alar base width are the most consistent changes seen in the literature, followed by increased tip projection after maxillary advancement. The changes might be advantageous for patients with a narrow nose, but they can have a negative effect on the overall esthetics of the face in those with a wide nasal width.Even these changes, however, cannot be predicted quantitatively and consistently show no correlation to the degree of maxillary displacement.

2. CONCLUSIONS

For skeletal Class III patients with facial asymmetry, it is important to identify the structures involved in the facial appearance of asymmetry in order to plan the surgery. To reduce random error due to landmark identification, a repeatable landmark-independent method for facial symmetry plane determination has been developed. Preoperatively, Coronoid, Genial tubercle, Gonion and soft tissue Gonion presented significant asymmetry. The system developed in the present study contributes data which is helpful in making the diagnosis for the orthognathic surgery of patients with facial deformities.

Traditional orthognathic surgical planning could harbor significant residual asymmetry in patients with facial asymmetry. In the present study, residual asymmetry was found, postsurgically, in the Coronoid and Condylar process, Gonion, Mandibular body length and soft tissue Gonial area. To improve the surgical planning of facial asymmetry correction, 3d diagnosis and virtual surgery achieved with computer-aided surgical simulation are indicated since they deliver better and more predictable outcomes in the treatment of Class III asymmetric cases.

In the investigation of factors contributing to mandibular deviation, Condyle and Coronoid asymmetry, asymmetry in Gonial area, Ramus length and Lateral ramal inclination discrepancy were significantly correlated with Menton deviation. In soft tissue evaluation, Pogonion, Cheilion and Gonion region asymmetry presented a strong connection to Menton deviation. These factors should be considered in the treatment planning of Class III skeletal asymmetric cases.

Finally, Alar base, Interalar and Internostril width tend to increase after orthognathic surgery. Nasiolabial angle has a tendency to decrease after maxillary impaction, whereas it increases in maxillary advancement. Based on these results, individual nasal characteristics and morphology should be taken into account during the planning for surgical treatment. In addition, the high susceptibility of nasal widening and the possible need for secondary rhinoplasty for esthetic improvement should be part of the informed consent for the patients.

3. REFERENCES

Abdullah RTH, Kuijpers MAR, Berge SJ, Katsaros C. Steiner cephalometric analysis: predicted and actual treatment outcome compared. Orthod Craniofac Res, 2006; 77-83

Ackerman JL, Proffit WR, Sarver DM. The emerging soft tissue paradigm in orthodontic diagnosis and treatment planning. Clin Orthod Res. 1999; 2(2), 49-52.

Ahlqvist J, Eliasson S, Welander U. The cephalometric projection. Part II. Principles of image distortion in cephalography. Dentomaxillofac Radiol 1983;12:101-108.

An SB, Park SB, Kim IY, Son WS. Effect of post– orthognathic surgery condylar axis changes on condylar morphology as determined by 3-dimensional surface reconstruction. Angle Orthod. 2014;84:316-21.

Altman JI, Oeltjen JC. Nasal deformities associated with orthognathic surgery: analysis, prevention, and correction. J Craniofac Surg. 2007;18(4):734-79.3

Angle E. Classification of malocclusion. Dent. Cosmos. 1899; 41:248.

Arnett G, Bergman R. Facial keys to orthodontic diagnosis and treatment planning. Part I. Am J Orthod Dentofac Orthop. 1993;103:299-312.

Baccetti T, Franchi L, McNamara JA, Jr. Cephalometric variables predicting the long-term success or failure of combined rapid maxillary expansion and facial mask therapy. Am J Orthod Dentofacial Orthop. 2004; 126(1), 16-22.

Baccetti T, Reyes BC, McNamara JA, Jr. Gender differences in Class III malocclusion. Angle Orthod.2005;75(4):510-520.

Baek SH, Kim TK, Kim MJ. Is there any difference in the condylar position and angulation after asymmetric mandibular setback? Oral Surg Oral Med Oral Pathol Oral Radiol Endod 2006;101:155-163.

Baek SH, Cho IS, Chang YI, Kim MJ. Skeletodental factors affecting chin point deviation in female patients with class III malocclusion and facial asymmetry: a

three-dimensional analysis using computed tomography. Oral Surg Oral Med Oral Pathol Oral Radiol Endod. 2007;104(5):628-639.

Baek C, Paeng JY, Lee JS, Hong J. Morphologic evaluation and classification of facial asymmetry using 3-dimensional computed tomography. J Oral Maxillofac Surg. 2012;70(5):1161-1169.

Bagheri SH, Bell B, Khan HA. Current Therapy In Oral and Maxillofacial Surgery. 1st Edition. St. Louis: Saunders, 2012.

Baik HS. Limitations in Orthopedic and Camouflage Treatment for Class III Malocclusion. Semin Orthod. 2007;13:158-174.

Baik HS, Kim SY. Facial soft-tissue changes in skeletal Class III orthognathic surgery patients analyzed with 3-dimensional laser scanning. Am J Orthod Dentofacial Orthop. 2010;138(2), 167-178.

Belden, C. J. The skull base and calvaria. Adult and pediatric. Neuroimaging Clin N Am.1998;8(1):1-20.

Benz M, Laboureux X, Maier T, Nkenke E, Seeger S, Neukam FW, Häusler G. The symmetry of faces. In: Greiner G, Niemann H, Ertl T, Girod B, Seidel HP eds. Vision, Modeling, and Visualization. Amsterdam: IOS Press, 2002:332-339.

Bergersen EO. Enlargement and distortion in cephalometric radiography: compensation tables for linear measurements. Angle Orthod 1980;50:230-244.

Betts NJ, Vig KW, Vig P, Spalding P, Fonseca RJ. Changes in the nasal and labial soft tissues after surgical repositioning of the maxilla. Int J Adult Orthodon Orthognath Surg. 1993;8:7-23.

Bishara S, Fahl J, Peterson L. Longitudinal chages in the ANB angle Wits appraisal: Clinical implications. Am J Orthod. 1983;84:133-139.

Brunelle JA, Bhat M, Lipton JA. Prevalence and distribution of selected occlusal characteristics in the US population, 1988-1991. J Dent Res. 1996; 75 Spec No, 706-713.

Burgersdijk R, Truin GJ, Frankenmolen F, Kalsbeek H, van't Hof M, Mulder J. Malocclusion and orthodontic treatment need of 15-74-year-old Dutch adults. Community Dent Oral Epidemiol. 1991;19(2):64-67.

Burke PH. Growth of the soft tissues of middle third of the face between 9 and 16 years. Eur J Orthod. 1979;1:1-13.

Burstone CJ: Diagnosis and treatment planning of patients with asymmetries. Semin Orthod. 1998;4:153.

Byrd KE. Masticatory movements and EMG activity following electrolytic lesions of the trigeminal motor nucleus in growing guinea pigs. Am J Orthod. 1982;81: 292-298.

Carlo WA. Fetal alcohol syndrome. In: Kliegman RM, Behrman RE, Jenson HB, Stanton BF, eds. Nelson Textbook of Pediatrics. 18th ed. Philadelphia, Pa: Saunders Elsevier. 2007.

Cevidanes LH, Alhadidi A, Paniagua B, Styner M, Ludlow J, Mol A, Turvey T, Proffit WR, Rossouw PE. Three-dimensional quantification of mandibular asymmetry through cone-beam computerized tomography. Oral Surg Oral Med Oral Pathol Oral Radiol Endod. 2011;111(6):757-770.

Chan GK. Class 3 malocclusion in Chinese (Cantonese): etiology and treatment. Am J Orthod. 1974; 65(2), 152-157.

Chan HJ, Woods M, Stella D. Three-dimensional computed craniofacial tomography (3D-CT): potential uses and limitations. Australian orthodontic journal. 2007;23(1):55.

Chang HP, Liu PH, Chang HF, et al. Thin-plate spline (TPS) graphical analysis of the mandible on cephalometric radiographs. Dentomaxillofac Radiol. 2002;31:137-141.

Chang HP, Tseng YC, Chou TM. An enlarged sella turcica on cephalometric radiograph. Dentomaxillofac Radiol. 2005a; 34:308-312.

Chang HP, Chuang MC, Yang YH, et al. Maxillofacial growth in children with unilateral cleft lip and palate following secondary alveolar bone grafting: an interim evaluation. Plast Reconstr Surg. 2005b;115:687-695.

Chebib FS, Chamma AM. Indices of craniofacial asymmetry. Angle Orthod. 1981;51:214-226.

Cheong YW, Lo LJ. Facial Asymmetry: Etiology, Evaluation, and Management. Chang Gung Med J. 2011;34:341-351.

Chew MT. Spectrum and management of dentofacial deformities in a multiethnic Asian population. Angle Orthod. 2006;76:806-809.

Chung C, Lee Y, Park KH, Park SH, Park YC, Kim KH. Nasal changes after surgical correction of skeletal Class III malocclusion in Koreans. Angle Orthod. 2008;78(3):427-432.

Chia MSY, Naini FB, Gill D. The Aetiology, Diagnosis and Management of Mandibular asymmetry. Ortho Update 2008; 1: 44-52.

Choi JW, Lee JY, Oh TS, Kwon SM, Yang SJ, Koh KS. Frontal soft tissue analysis using a 3 dimensional camera following two-jaw rotational orthognathic surgery in skeletal class III patients. J Craniomaxillofac Surg. 2014;42:200-206.

Chow LK, Singh B, Chiu WK, Samman N. Prevalence of postoperative complications after orthognathic surgery: a 15-year review. J Oral Maxillofac Surg. 2007;65:984-992.

Ciuffolo F, Manzoli L, D'Attilio M, Tecco S, Muratore F, Festa F, Romano F. Prevalence and distribution by gender of occlusal characteristics in a sample of Italian secondary school students: a cross-sectional study. Eur J Orthod. 2005;27(6):601-606.

Claman L, Patton D, Rashid R. Standardized portrait photography for dental patients. Am J Orthod Dentofacial Orthop 1990; 98:197-205.

Cohen MM Jr. Perspectives of craniofacial asymmetry. Part III. Common and/or well known causes of asymmetry. Int J Oral Maxillofac Surg. 1995;24:127-133.

Colbert S, Seah TE, Ilankovan V, Bellis H. Simultaneous orthognathic surgery and rhinoplasty. Br J Oral Maxillofac Surg. 2011;49:43.

Dahan J. Die Diagnose der Gesichts- und Schädelasymmetrien. Ein kephalometrisches Problem. Fortschr Kieferorthop. 1968;29: 289-333.

Damstra J, Fourie Z, De Wit MF, Ren Y. A three-dimensional comparison of a morphometric midsagittal plane to cephalometric midsagittal planes for craniofacial asymmetry. Clin Oral Investig. 2012;16:285-294.

Dantas WR, Silveira MM, Vasconcelos BC, Porto GG. Evaluation of the nasal shape after orthognathic surgery. Braz J Otorhinolaryngol. 2015;81(1):19-23.

Darras BT, Jones HR, Ryan MM, De Vivo DC. Neuromuscular disorders of infancy, childhood, and adolescence : a clinician's approach. 2nd edition. London: Elsevier, 2015.

Day CJ, Robert T. Three-dimensional assessment of the facial soft tissue changes that occur postoperatively in orthognathic patients. World J Orthod. 2006; 7(1), 15-26.

De Menezes M, Sforza C. What's new in Dentistry Three-dimensional face morphometry. Dental Press Journal of Orthodontics. 2010; 15 (1), 13-15.

Diewert VM. A morphometric analysis of craniofacial growth and changes in spatial relations during secondary palatal development in human embryos and fetuses. Am J Anat. 1983;167:495-522.

Douglas T. Image processing for craniofacial landmark identification and measurement: a review of photogrammetry and cephalometry. Comput Med Imaging Graph. 2004;28:401-409.

Downs WG. Studies in the causes of dental anomalies. J Dent Res. 1928;8:367-79.

Am J Orthod Dentofacial Orthop. 2004 Apr;125(4):435-443.

Edler R, Wertheim D, Greenhill D. Clinical and computerized assessment of mandibular asymmetry. Eur J Orthod 2001;23: 485-494.

Edler R. Wertheim D, Greenhill D. Mandibular outline assessment in three groups of orthodontic patients. Eur J Orthod 2002;24:605-614.

Edler R, Wertheim D, Greenhill D. Comparison of radiographic and photographic measurement of mandibular asymmetry. Am J Orthod Dentofacial Orthop 2003;123:167-174.

Edler R, Wertheim D, Greenhill D. Outcome measurement in the correction of mandibular asymmetry. Am J Orthod Dentofacial Orthop. 2004;125(4):435-443.

El-Gheriani AA, Maher BS, El-Gheriani AS, et al. Segregation analysis of mandibular prognathism in Libya. J Dent Res. 2003;82:523-527.

El H, Palomo JM. Measuring the airway in 3 dimensions: a reliability and accuracy study. Am J Orthod Dentofacial Orthop. 2010; 137(4 Suppl), S50 e51-59; discussion S50-2.

Elisabetta B, Alessandro Z, Francesca B, Giampietro F. Cephalometric Diagnosis with Cbct: Algorithm of Correlation between Sagittal and Vertical Dimensions. J Med Diagn Meth. 2013; 2:135.

Ellis E, 3rd, McNamara JA, Jr. Components of adult Class III malocclusion. J Oral Maxillofac Surg. 1984;42(5), 295-305.

El-Mangoury NH, Mostafa YA, Epidemiologic panorama of dental occlusion. Angle Orthod.1990;60(3):207-214.

Emrich RE, Brodie AG, Blayney JR, Prevalence of Class 1, Class 2, and Class 3 malocclusions (Angle) in an urban population. An epidemiological study. J Dent Res.1965; 44(5): 947-953.

Evans CA, Scarfe WC, Ahmad M, Cevidanes LH, Ludlow JB, Palomo JM, Simmons KE, White SC. Clinical recommendations regarding use of cone beam computed tomography in orthodontics. Position statement by the American Academy of Oral and Maxillofacial Radiology. Oral Surg Oral Med Oral Pathol Oral Radiol. 2013;116(2):238-257.

Farkas LG, Cheung G. Facial asymmetry in healthy North American Caucasians. An anthropometrical study. Angle Orthod. 1981;51:70-77.

Farronato G, Perillo L, Bellincioni F, Briguglio F, Farronato D, Dominici AD. Direct 3D Cephalometric analysis performed on CBCT. J Inform Tech Software Engr.2012;2:107.

Fattahi T. Aesthetic surgery to augment orthognathic surgery. Oral Maxillofac Surg Clin North Am. 2007;19(3):435-447.

Ferrario VF, Sforza C, Miani A, Tartaglia G. Craniofacial morphometry by photographic evaluations. Am J Orthod Dentofacial Orthop. 1993;103(4):327-337.

Ferrario VF, Sforza C, Poggio CE, Tartaglia G. Distance from symmetry: a three-dimensional evaluation of facial asymmetry. J Oral Maxillofac Surg. 1994; 52(11), 1126-1132.

Ferrario VF, Sforza C, Miani A, Serrao G. A three dimensional evaluation of human facial asymmetry. J Anat. 1995;186:103-110.

Ferrario VF, Sforza C, Schmitz JH, Santoro F. Three-dimensional facial morphometric assessment of soft tissue changes after orthognathic surgery. Oral Surg Oral Med Oral Pathol Oral Radiol Endod. 1999;88(5),549-556.

Ferrario VF, Sforza C, Ciusa V, Dellavia C, Tartaglia GM. The effect of sex and age on facial asymmetry in healthy subjects: a cross-sectional study from adolescence to mid-adulthood. J Oral Maxillofac Surg. 2001;59(4):382-388.

Fosberg CT, Burstone CJ, Hanley KJ. Diagnosis and treatment planning of skeletal asymmetry with the submental vertical radiograph. American Journal Orthodontics. 1984;85: 224-237.

Foster TD, Day AJ. A survey of malocclusion and the need for orthodontic treatment in a Shropshire school population. Br J Orthod. 1974; 1(3), 73-78.

Fourie Z, Damstra J, Gerrits PO, Ren Y. Accuracy and repeatability of anthropometric facial measurements using cone beam computed tomography. Cleft Palate Craniofac J. 2011a; 48(5), 623-630.

Fourie Z, Damstra J, Gerrits PO, Ren Y. Evaluation of anthropometric accuracy and reliability using different three-dimensional scanning systems. Forensic Sci Int. 2011b; 207(1-3), 127-134.

Freihofer HP Jr. Changes in nasal profile after maxillary advancement in cleft and non-cleft patients. J Maxillofac Surg. 1977;5:20-27.

Gardner DE, Luschei ES, Joondeph DR. Alterations in the facial skeleton of the guinea pig following a lesion of the trigeminal motor nucleus. Am J Orthod. 1980;78: 66-80.

Gasperini G, Rodrigues de Siqueira IC, Rezende Costa L. Does low-level laser therapy decrease swelling and pain resulting from orthognathic surgery? Int J Oral Maxillofac Surg. 2014; 43(7), 868-873.

Gassmann CJ, Nishioka GJ, Van Sickels JE, Thrash WJ.. A lateral cephalometric analysis of nasal morphology following Le Fort I osteotomy applying photometric analysis techniques. J Oral Maxillofac Surg. 1989;47:926-930.

Gelgor IE, Karaman AI, Ercan E. Prevalence of malocclusion among adolescents in central anatolia. Eur J Dent. 2007; 1(3), 125-131.

Gold JK. A new approach to the treatment of mandibular prognathism. Am J Orthod. 1949;35:893-912.

Gorlin RJ, Cohen MM, Levin LS. Syndromes of the head and neck (3rd edition). New York: Oxford University Press, 1990.

Graber TM, Rakosi TH, Petrovic AG. Dentofacial orthodontics with functional appliance. 2nd ed. St. Louis: Mosby. 1997.

Grauer D, Cevidanes LS, Styner MA, Heulfe I, Harmon ET, Zhu H, Proffit WR. Accuracy and landmark error calculation using cone-beam computed tomographygenerated cephalograms. The Angle orthodontist. 2010;80(2):286-294.

Grummons DC, Kappeyne van de Coppello MA. A frontal asymmetry analysis. J Clin Orthod. 1987;21:448-465.

Guyer EC, Ellis EE, 3rd, McNamara JA, Jr., Behrents RG. Components of class III malocclusion in juveniles and adolescents. Angle Orthod. 1986; 56(1), 7-30.

Ha MH, Kim YI, Park SB, Kim SS, Son WS. Cone-beam computed tomographic evaluation of the condylar remodeling occurring after mandibular set-back by bilateral sagittal split ramus osteotomy and rigid fixation. Korean J Orthod. 2013;43:263-270.

Hagg U, Tse A, Bendeus M, Rabie AB. Long-term follow-up of early treatment with reverse headgear. Eur J Orthod. 2003; 25(1), 95-102.

Hajeer MY, Ayoub AF, Millett DT. Three-dimensional assessment of facial soft-tissue asymmetry before and after orthognathic surgery. Br J Oral Maxillofac Surg. 2004;42(5),396-404.

Halazonetis DJ. Cone-beam computed tomography is not the imaging technique of choice for comprehensive orthodontic assessment. Am J Orthod Dentofacial Orthop. 2012; 141(4), 403, 405, 407 passim.

Haraguchi S, Takada K, Yasuda Y. Facial asymmetry in subjects with skeletal Class III deformity. Angle Orthod. 2002 ;72(1):28-35.

Haraguchi S, Iguchi Y, Takada K. Asymmetry of the face in orthodontic patients. Angle Orthod. 2008;78(3):421-426.

Hardy DK, Cubas YP, Orellana MF. Prevalence of angle class III malocclusion: A systematic review and meta-analysis. Open Journal of Epidemiology.2012;2: 75-82.

Harper RP, de Bruin H, Burcea I. Muscle activity during mandibular movements in normal and mandibular retrognathic subjects. J Oral Maxillofac Surg. 1997;55(3):225-233.

Hartman J, Meyer-Marcotty P, Hausler G, Stellzig-Eisenhauer A. Reliability of a method for computing facial symmetry plane and degree of asymmetry based on 3D-data. J Orofac Orthop. 2007;68:477-490.

Harvold EP. Neuromuscular and morphological adaptation in experimentally induced oral respiration. In McNamara JA (eds): Naso-respiratory function and craniofacial growth. Monograph 9, Craniofacial Growth Series, Center for Human Growth and Development, Ann Arbor, 1979, University of Michigan.

Hayashi K, Muguruma T, Hamaya M, Mizoguchi I. Morphologic characteristics of the dentition and palate in cases of skeletal asymmetry. Angle Orthod. 2004;74(1):26-30.

Haynes S. The prevalence of malocclusion in English children aged 11-12 years. Rep Congr Eur Orthod Soc. 1970, 89-98.

Hegtvedt AK. Diagnosis and management of facial asymmetry. In: Peterson LJ, Indressano AT, Marciani RD, Roser SM, eds. Oral and Maxillofacial Surgery. Vol 3. Philadelphia: Lippincott, 1993:1400-1414.

Hofmann E, Schmid M, Steinhäuser-Andresen S, Hirschfelder U. Three-dimensional CT evaluation of oculoauriculovertebral spectrum patients use of Katsumata's asymmetry index. J Orofac Orthop. 2016;77(3):176-184.

Honrado CP, Lee S, Bloomquist DS, Larrabee WF, Jr. Quantitative assessment of nasal changes after maxillomandibular surgery using a 3-dimensional digital imaging system. Arch Facial Plast Surg. 2006; 8(1), 26-35.

Horner K, Islam M, Flygare L, Tsiklakis K, Whaites E. Basic principles for use of dental cone beam computed tomography: consensus guidelines of the European Academy of Dental and Maxillofacial Radiology. Dentomaxillofac Radiol. 2009;38(4):187-195.

Horsey DG. Post-surgical Stability for Class III Patients with Asymmetry: A Comparison of Mandibular Setback, Maxillary Advancement, and Bimaxillary Surgeries [dissertation]. Chapel Hill: University of North Carolina, 2007.

Huang CS, Liu XQ, Chen YR. Facial asymmetry index in normal young adults. Orthod Craniofac Res. 2013;16(2):97-104.

Hwang SJ, Haers PE, Seifert B, Sailer HF. Non-surgical risk factors for condylar resorption after orthognathic surgery. J Cranio-Maxillo-Facial Surg 2004;32:103-111.

Hwang HS, Hwang CH, Lee KH, Kang BC. Maxillofacial 3-dimensional image analysis for the diagnosis of facial asymmetry. Am J Orthod Dentofacial Orthop. 2006;130(6):779-785.

Hwang HS , Min YS, Lee SC, Sun MK, Lim HS. Change of lip-line cant after 1-jaw orthognathic surgery in patients with mandibular asymmetry. Am J Orthod Dentofacial Orthop. 2009;136(4):564-569.

Hwang HS, Yuan D, Jeong KH, Uhm GS, Cho JH, Yoon SJ. Three-dimensional soft tissue analysis for the evaluation of facial asymmetry in normal occlusion individuals. Korean Journal of Orthodontics. 2012;42(2):56-63.

Ingervall B, Ridell A, Thilander B. Changes in activity of the temporal, masseter and lip muscles after surgical correction of mandibular prognathism. International Journal of Oral Surgery. 1979;8:290-300.

Ishizaki K, Suzuki K, Mito T, Tanaka EM, Sato S. Morphologic, functional, and occlusal characterization of mandibular lateral displacement malocclusion. Am J Orthod Dentofacial Orthop. 2010;137(4):454.e1-9.

Iwaki H. Hereditary influence of malocclusion. Am J Orthod Oral Surg. 1938;24:328-336.

Jacobson A, Evans WG, Preston CB, Sadowsky PL. Mandibular prognathism. Am J Orthod. 1974;66(2): 140-171.

Jones RH, Tier GA. Correction of facial asymmetry as a result of unilateral condylar hyperplasia. J Oral Maxillofac Surg. 2012;70:1413.

Jung YJ, Kim MJ, Baek SH. Hard and soft tissue changes after correction of mandibular prognathism and facial asymmetry by mandibular setback surgery: three-dimensional analysis using computerized tomography. Oral Surg Oral Med Oral Pathol Oral Radiol Endod. 2009;107763.e8–71.e8

Kang SH, Kim MK, An SI, Lee JY. The effect of orthognathic surgery on the lip lines while smiling in skeletal class III patients with facial asymmetry. Maxillofacial Plastic and Reconstructive Surgery. 2016;38(1):18.

Kanno Z, Kim Y, Soma K. Early correction of a developing skeletal Class III malocclusion. Angle Orthod. 2007;77(3):549-556.

Karatas OH, Toy E. Three-dimensional imaging techniques: A literature review. Eur J Dent. 2014;8(1),132-140.

Katsumata A, Fujishita M, Maeda M, Ariji Y, Ariji E, Langlais RP. 3D-CT evaluation of facial asymmetry. Oral Surg Oral Med Oral Pathol Oral Radiol Endod. 2005;99(2):212-20.

Kau CH, Richmond S, Palomo JM, Hans MG. Three-dimensional cone beam computerized tomography in orthodontics. J Orthod. 2005; 32(4), 282-293.

Kau CH, Richmond S, Savio C, Mallorie C. Measuring adult facial morphology in three dimensions. Angle Orthod. 2006;76:773-778.

Kau CH, Cronin AJ, Richmond S. A three-dimensional evaluation of postoperative swelling following orthognathic surgery at 6 months. Plast Reconstr Surg. 2007; 119(7), 2192-2199.

Kau CH, Richmond S. Three-dimensional imaging for orthodontics and maxillofacial surgery. Chichester, West Sussex, U.K. ; Ames, Iowa: Wiley-Blackwell. 2010.

Keeler CE. Heredity in dentistry. Dent Cosmos. 1935;77: 1147-1163.

Khamashta-Ledezma L, Naini FB. Systematic review of changes in maxillary incisor exposure and upper lip position with Le Fort I type osteotomies with or without cinch sutures and/or VY closures. Int J Oral Maxillofac Surg. 2014;43(1):46-61.

Kim TY, Baik JS, Park JY, Chae HS, Huh KH, Choi SC. Determination of midsagittal plane for evaluation of facial asymmetry using three-dimensional computed tomography. Imaging Sci Dent. 2011; 41:79-84.

Kim BR, Oh KM, Cevidanes LH, Park JE, Sim HS, Seo SK, Reyes M, Kim YJ, Park YH. Analysis of 3D soft tissue changes after 1- and 2-jaw orthognathic surgery in mandibular prognathism patients. J Oral Maxillofac Surg. 2013a;71(1),151-161.

Kim EJ, Ki EJ, Cheon HM, Choi EJ, Kwon KH. 3-Dimensional analysis for class III malocclusion patients with facial asymmetry. J Korean Assoc Oral Maxillofac Surg. 2013b;39(4):168-174.

Kim SJ, Baik HS, Hwang CJ, Yu HS. Diagnosis and evaluation of skeletal Class III patients with facial asymmetry for orthognathic surgery using three-dimensional computed tomography. Semin Orthod. 2015;21:274-282.

Ko JM, Choi JY, Baek SH. Evaluation of Lip Cant Change by 2-Jaw Surgery in Class III Asymmetry Cases Using Three-Dimensional Facial Scan in Conjunction With Computed Tomographic Images. J Craniofac Surg. 2015;26(4):e283-288.

Koff E, Borod JC, White B. Asymmetries for hemiface size and mobility. Neuropsychologia. 1981;19:825-830.

Koff E, Borod J, Strauss E. Development of hemiface size asymmetry. Cortex. 1985;21:153-156.

Koh EH, Lee KH, Hwang HS. Effects of vertical head rotation on the posteroanterior cephalometric measurements. Korean J Orthod. 2003;33:73-84.

Kook MS, Jung S, Park HJ, Oh HK, Ryu SY, Cho JH, Lee JS, Yoon SJ, Kim MS, Shin HK. A comparison study of different facial soft tissue analysis methods. J Craniomaxillofac Surg. 2014; 42(5), 648-656.

Kramer FJ, Baethge C, Swennen G, Teltzrow T, Schulze A, Berten J, et al. Intra- and perioperative complications of the LeFort I osteotomy: a prospective evaluation of 1000 patients. J Craniofac Surg. 2004;15:971-977.

Kraus BS, Wise WJ, Frie RA. Heredity and the craniofacial complex. Am J Orthod. 1959;45:172-217.

Kreiborg S. (1981). Crouzon Syndrome. A clinical and roentgencephalometric study. Scand J Plast Reconstr Surg Suppl, 18:1-198.

Kumar SA, Shetty KS, Prakash AT. Pseudo-Class III: Diagnosis and Simplistic Treatment. J Ind Orthod Soc. 2011;45(4):198-201.

Kusayama M, Motohashi N, Kuroda T. Relationship between transverse dental anomalies and skeletal asymmetry. Am J Orthod Dentofacial Orthop, 2003;123(3):329-337.

Kwon TG, Park HS, Ryoo HM, Lee SH. A comparison of craniofacial morphology in patients with and without facial asymmetry--a three-dimensional analysis with computed tomography. Int J Oral Maxillofac Surg. 2006;35(1):43-48.

Kwong JC, Palomo JM, Landers MA, Figueroa A, Hans MG. Image quality produced by different cone-beam computed tomography settings. Am J Orthod Dentofacial Orthop, 2008;133(2):317-327.

Lagravere MO, Carey J, Toogood RW, Major PW. Three-dimensional accuracy of measurements made with software on cone-beam computed tomography images. Am J Orthod Dentofacial Orthop. 2008; 134(1), 112-116.

Legan HL. Orthodontic considerations of orthognathic surgery. L.J. Peterson (Ed.), Principles of oral and maxillofacial surgery, 3. Philadelphia, Pa, USA: Lippincott. 1992.

Lane C, Harrell W. Completing the 3-dimensional picture. Am J Orthod Dentofacial Orthop. 2008;133(4),612-620.

Lee MS1, Chung DH, Lee JW, Cha KS. Assessing soft-tissue characteristics of facial asymmetry with photographs. Am J Orthod Dentofacial Orthop. 2010;138(1):23-31.

Lee JW, Park KH, Kim SH, Park YG, Kim SJ. Correlation between skeletal changes by maxillary protraction and upper airway dimensions. Angle Orthod. 2011; 81(3), 426-432.

Lee H, Bayome M, Kim SH, Kim KB, Behrents RG, Kook YA. Mandibular dimensions of subjects with asymmetric skeletal class III malocclusion and normal occlusion compared with cone-beam computed tomography. Am J Orthod Dentofacial Orthop. 2012;142(2):179-185.

Lee ST, Mori Y, Minami K, An CH, Park JW, Kwon TG. Does skeletal surgery for asymmetric mandibular prognathism influence the soft tissue contour and thickness? J Oral Maxillofac Surg. 2013;71(9):1577-1587.

Lew KK, Tay DK. Submentovertex cephalometric norms in male Chinese subjects. American Journal of Orthodontics and Dentofacial Orthopedics. 1993; 103: 247-252.

Lin H, Zhu P, Lin Q, Huang X, Xu Y, Yang X. Comprehensive Analysis of Mandibular Residual Asymmetry after Bilateral Sagittal Split Ramus Osteotomy Correction of Menton Point Deviation. PLoS One. 2016;29:11(8):e0161601.

Litton SF, Ackerman LV, Isaacson RJ, Shapiro B. A genetic study of Class III malocclusion. Am J Orthod. 1970;58:565-577.

Liu Z, McGrath C, Hägg U. The impact of malocclusion/orthodontic treatment need on the quality of life. A systematic review. Angle Orthod. 2009;79(3):585-591.

Ludlow JB, Ivanovic M. Comparative dosimetry of dental CBCT devices and 64-slice CT for oral and maxillofacial radiology. Oral Surg Oral Med Oral Pathol Oral Radiol Endod 2008;106:106-14.

Ludlow JB, Gubler M, Cevidanes L, Mol A. Precision of cephalometric landmark identification: cone-beam computed tomography vs conventional cephalometric views. Am J Orthod Dentofacial Orthop. 2009; 136(3), 312 e311-310; discussion 312-313.

Lundström A. Tooth Size and Occlusion in Twins. Stockholm: A.B. Fahlcrantz Boktryckeri, 1948.

Lundström A. Some asymmetries of the dental arches, jaws, and skull, and their etiological significance. Am J Orthod. 1961;47(2):81-106.

Maeda M, Katsumata A, Ariji Y, Muramatsu A, Yoshida K, Goto S, Kurita K, Ariji E. 3D-CT evaluation of facial asymmetry in patients with maxillofacial deformities. Oral Surg Oral Med Oral Pathol Oral Radiol Endod.2006;102(3):382-390.

Mah JK, Danforth RA, Bumann A, Hatcher D. Radiation absorbed in maxillofacial imaging with a new dental computed tomography device. Oral Surg Oral Med Oral Pathol Oral Radiol Endod. 2003;96(4),508-513.

Major PW, Glover K. Treatment of anterior cross-bites in the early mixed dentition. J Can Dent Assoc. 1992;58(7):574-579.

Masuoka N, Momoi Y, Ariji Y, Nawa H, Muramatsu A, Goto S, Ariji E. Can cephalometric indices and subjective evaluation be consistent for facial asymmetry? Angle Orthod. 2005;75(4):651-655.

McCance AM, Moss JP, Wright WR, Linney AD, James DR. A three-dimensional soft tissue analysis of 16 skeletal Class III patients following bimaxillary surgery. Br J Oral Maxillofac Surg. 1992;30:221-232.

McNamara JA Jr. A method of cephalometric evaluation. Am J Orthod. 1984;86:449-469.

McNamara JA Jr. An orthopedic approach to the treatment of Class III malocclusion in young patients. J Clin Orthod. 1987;21:598-608.

Melsen, B. Time of closure of the spheno-occipital synchondrosis determined on dry skulls. A radiographic craniometric study. Acta Odontol Scand. 1969;27(1):73-90.

Meneghini F. Clinical Facial Analysis. Verlag Berlin Heidelberg: Springer. 2005.

Miller L, Morris DO, Berry E. Visualizing three-dimensional facial soft tissue changes following orthognathic surgery. Eur J Orthod. 2007;29(1):14-20. Epub 2006 Sep 6.

Mohamed WV, Perenack JD. Aesthetic adjuncts with orthognathic surgery. Oral Maxillofac Surg Clin North Am. 2014; 26(4), 573-585.

De Momi E, Chapuis J, Pappas I, Ferrigno G, Hallerman W, Schramm A, Caversaccio M. Automatic extraction of the mid-facial plane for craniomaxillofacial surgery planning. Int J Oral Maxillofac Surg. 2006;35:636-642.

Mommaerts MY, Abeloos JV, De Clercq CA, Neyt LF. The effect of the subspinal Le Fort I–type osteotomy on interalar rim width. Int J Adult Orthodon Orthognath Surg. 1997;12:95-100.

Monteleone L, Duvigneaud JD. Prognathism. J Oral Surg. 1963;21:190-195.

Moon W, Kim J. Psychological considerations in orthognathic surgery and orthodontics. Semin Orthod. 2016;22(1):12-7.

de Moraes ME, Hollender LG, Chen CS, Moraes LC, Balducci I. Evaluating craniofacial asymmetry with digital cephalometric images and cone-beam computed tomography. Am J Orthod Dentofacial Orthop. 2011;139(6):e523-531.

Moss JP, McCance AM, Fright WR, Linney AD, James DR. A three-dimensional soft tissue analysis of fifteen patients with Class II, Division 1 malocclusions after bimaxillary surgery. Am J Orthod Dentofacial Orthop. 1994;105(5):430-437.

Motta AT, de Assis Ribeiro Carvalho F, Cevidanes LH, de Oliveira Almeida MA. Assessment of mandibular advancement surgery with 3D CBCT models superimposition. Dental Press J Orthod. 2010;15:45e1–45e12.

Mulick JF. An investigation of craniofacial asymmetry using the serial twin-study method. American Journal of Orthodontics 1965; 51(2): 112-129.

Nanda RS. Biomechanics and Esthetic Strategies in Clinical Orthodontics. St Louis, Mo: Elsevier. 2005.

Ngan P, Hu AM, Fields HW Jr. Treatment of Class III problems begins with differential diagnosis of anterior crossbites. Pediatr Dent. 1997;19(6):386-395.

Nur RB, Çakan DG, Arun T. Evaluation of facial hard and soft tissue asymmetry using cone-beam computed tomography. Am J Orthod Dentofacial Orthop. 2016;149:225-237.

Obwegeser HL, Makek MS. Hemimandibular hypertrophy, hemimandibular elongation.Journal of Maxillofacial Surgery 1986; 14: 183-208.

Oh KM, Seo SK, Park JE, Sim HS, Cevidanes LH, Kim YJ, Park YH. Post-operative soft tissue changes in patients with mandibular prognathism after bimaxillary surgery. J Craniomaxillofac Surg. 2013;41(3):204-211.

Oh MH, Kang SJ, Cho JH. Comparison of the three-dimensional structures of mandibular condyles between adults with and without facial asymmetry: A retrospective study. Korean J Orthod. 2018;48(2):73-80.

O'Ryan F, Schendel SA Jr. Nasolabial Esthetics and Maxillary Surgery. In: Bell WH, ed. Modern Practice in Orthognathic and Reconstructive Surgery. St. Louis: W.B. Saunders, 1992.

Oxford Dictionary. Oxford dictionaries. Oxford University Press. April 2010.

Ozsoy U, Demirel BM, Yildirim FB, Tosun O, Sarikcioglu L. Method selection in craniofacial measurements: advantages and disadvantages of 3D digitization method. J Craniomaxillofac Surg. 2009;37(5):285-290.

Padwa BL, Kaiser MO, Kaban LB: Occlusal cant in the frontal plane as a reflection of facial asymmetry. J Oral Maxillofac Surg 1997;55:811-816.

Park SB, Yoon JK, Kim YI, Hwang DS, Cho BH, Son WS. The evaluation of the nasal morphologic changes after bimaxillary surgery in skeletal class III maloccusion by using the superimposition of cone-beam computed tomography (CBCT) volumes. J Craniomaxillofac Surg. 2011;40(4),e87-92.

Park SB, Yang YM, Kim YI, Cho BH, Jung YH, Hwang DS. Effect of bimaxillary surgery on adaptive condylar head remodeling: metric analysis and image interpretation using cone-beam computed tomography volume superimposition. J Oral Maxillofac Surg. 2012;70:1951–1959.

Pascoe JJ, Hayward JR, Costich ER. Mandibular prognathism: its etiology and a classification. J Oral Surg. 1960; 18:21-24.

Pearson K, Woo TL. Further investigation of the morphometric characters of the individual bones of the human skull. Biometrika. 1935; 2: 423-465.

Peck H, Peck S. A concept of facial esthetics. Angle Orthod. 1970;40:284-318.

Peck BS, Peck L, Kataja M. Skeletal asymmetry in aesthetically pleasing faces. Angle Orthodontist. 1991;61: 43-48.

Periago DR, Scarfe WC, Moshiri M, Scheetz JP, Silveira AM, Farman AG. Linear accuracy and reliability of cone beam CT derived 3-dimensional images constructed using an orthodontic volumetric rendering program. Angle Orthod. 2008; 78(3), 387-395.

Pirttiniemi PM. Associations of mandibular and facial asymmetries-a review. Am J Orthod Dentofacial Orthop 1994;106: 191-200.

Posnick JR. Principles and Practice of Orthognathic Surgery. St. Louis: Saunders. 2013.

Pirttiniemi P, Miettinen J, Kantomaa T. Combined effects of errors in frontal-view asymmetry diagnosis. Eur J Orthod. 1996;18: 629-636.

Proffit WR, Fields HW, Jr., Moray LJ. Prevalence of malocclusion and orthodontic treatment need in the United States: estimates from the NHANES III survey. Int J Adult Orthodon Orthognath Surg. 1998; 13(2), 97-106.

Proffit WR. The soft tissue paradigm in orthodontic diagnosis and treatment planning: a new view for a new century. J Esthet Dent. 2000; 12(1), 46-49.

Proffit W, White R, Sarver D. Contemporary Treatment of Dentofacial Deformity. St. Louis: Mosby. 2003.

Proffit WR, Fields HW, Sarver DM. Contemporary orthodontics. St. Louis, Mo.: Mosby Elsevier. 2007.

Rabie AB , Gu Y. Diagnostic criteria for pseudo-Class III malocclusion. Am J Orthod Dentofacial Orthop. 2000;117(1):1-9.

Rabie AB, Wong RW, Min GU. Treatment in Borderline Class III Malocclusion: Orthodontic Camouflage (Extraction) Versus Orthognathic Surgery. Open Dent J. 2008;2:38-248.

Ramieri GA, Spada MC, Nasi A, Tavolaccini A, Vezzetti E Tornincasa S, Bianchi SD, Verzé L. Reconstruction of facial morphology from laser scanned data. Part I: reliability of the technique. Dentomaxillofac Radiol. 2006;35(3):158-164.

Rana M, Gellrich NC, Joos U, Piffko J, Kater W. 3D evaluation of postoperative swelling using two different cooling methods following orthognathic surgery: a randomised observer blind prospective pilot study. Int J Oral Maxillofac Surg. 2011; 40(7), 690-696.

Ras F, Habets L, van Ginkel FC, Prahl-Andersen B. Method for quantifying facial asymmetry in three dimensions using stereophotogrammetry. Angle Orthod. 1995;65:233-239.

Reyneke JP, Tsakiris P, Kienle F. A simple classification for surgical planning of maxillomandibular asymmetry. Br J Oral Maxillofac Surg. 1997;35:349-351.

Reyneke JP. Essentials of orthognathic surgery. Hanover Park, IL: Quintessence Pub. 2010.

Ricketts RM. Cephalometric Analysis and Synthesis. Angle Orthod. 1961;31(3):141-156.

Ricketts RM. Respectives in the clinical application of cephalometrics. Angle Orthod. 1981; 14:554-571.

Ritucci R, Burstone CJ. Use of the submental vertical radiograph in the assessment of asymmetry [thesis]. Farmington: University of Connecticut; 1981.

Rodriguez-Cardenas YA, Arriola-Guillen LE, FloresMir C. Björk-Jarabak cephalometric analysis on CBCT synthesized cephalograms with different dentofacial sagittal skeletal patterns. Dental Press J Orthod. 2014;19(6):46-53.

Rosen HM. Lip-nasal aesthetics following LeFort I osteotomy. Plast Reconstr Surg. 1988;81:171-179.

Rossi M, Ribeiro E, Smith R. Craniofacial asymmetry in development: an anatomical study. Angle Orthod. 2003;73(4):381-385.

Ryu HS, An KY, Kang KH. Cone-beam computed tomography based evaluation of rotational patterns of dentofacial structures in skeletal Class III deformity with mandibular asymmetry. Korean Journal of Orthodontics. 2015;45(4):153-163.

Salonen L,. Mohlin B, Gotzlinger B, Hellden L. Need and demand for orthodontic treatment in an adult Swedish population. Eur J Orthod. 1992;14:359-368.

Samman N , Tong AC, Cheung DL, Tideman H. Analysis of 300 dentofacial deformities in Hong Kong. Int J Adult Orthodon Orthognath Surg. 1992;7(3):181-185.

Sanborn R. Differences Between the Facial Skeletal Patterns Of Class III Malocclusion and Normal Occlusion. The Angle Orthodontist. 1955; 25(4), 208-222.

Sanders DA, Chandhoke TK, Uribe FA, Rigali PH, Nanda R. Quantification of skeletal asymmetries in normal adolescents: cone-beam computed tomography analysis. Prog Orthod. 2014;15(1):26.

Sarver DM, Rousso DR. Plastic surgery combined with orthodontic and orthognathic procedures. Am J Orthod Dentofacial Orthop. 2004; 126(3), 305-307.

Sayin MO, Turkkahraman H. Malocclusion and crowding in an orthodontically referred Turkish population. Angle Orthod. 2004; 74(5), 635-639.

Schendel SA, Williamson LW. Muscle reorientation following superior repositioning of the maxilla. J Oral Maxillofac Surg. 1983;41:235-240.

Schendel SA, Carlotti AE Jr. Nasal considerations in orthognathic surgery. Am J Orthod Dentofacial Orthop. 1991;100: 197-208.

Schmid W, Mongini F, Felisio A. A computer based assessment of structural and displacement asymmetries of the mandible. Am J Orthod Dentofacial Orthop 1991;100: 19-34.

Schoenwetter RF. A possible relationship between certain malocclusions and difficult or instrument deliveries. Angle Orthod. 1974;44:336-340.

Schulze C. On prognathism in twins. Stoma. 1965;18: 250-266.

Schulze C, Wiese W. On the heredity of prognathism. Fortschr Kieferorthop. 1965;26:213-229.

Severt TR, Proffit WR. The prevalence of facial asymmetry in the dentofacial deformities population at the University of North Carolina. Int J Adult Orthodon Orthognath Surg. 1997;12(3):171-176.

Sforza C, Dellavia C, Colombo A, Serrao G, Ferrario VF. Nasal dimensions in normal subjects: conventional anthropometry versus computerized anthropometry. Am J Med Genet A. 2004;130A(3), 228-233.

Sforza C, Peretta R, Grandi G, Ferronato G, Ferrario VF. Three-dimensional facial morphometry in skeletal Class III patients. A non-invasive study of soft-tissue changes before and after orthognathic surgery. Br J Oral Maxillofac Surg. 2007;45(2),138-144.

Shah SM, Joshi MR. An assessment of asymmetry in the normal craniofacial complex. Angle Orthod. 1978;48:141-148.

Shetty V, Mohan A. A prospective, randomized, double-blind, placebo-controlled clinical trial comparing the efficacy of systemic enzyme therapy for edema control in orthognathic surgery using ultrasound scan to measure facial swelling. J Oral Maxillofac Surg. 2013; 71(7): 1261-1267.

Silva RG, Kang DS. Prevalence of malocclusion among Latino adolescents. Am J Orthod Dentofacial Orthop. 2001; 119(3):313-315.

Sinclair PM, Proffit WR. Class III Problems: Mandibular Excess - Maxillary Deficiency. In: Surgical Orthodontic Treatment, Proffit WR, White RP. St Louis USA: Mosby. 1991.

Soh J, Sandham A, Chan YH. Occlusal status in Asian male adults: prevalence and ethnic variation. Angle Orthod. 2005;75(5):814-820.

Soncul M, Bamber MA. Evaluation of facial soft tissue changes with optical surface scan after surgical correction of Class III deformities. J Oral Maxillofac Surg. 2004;62(11), 1331-1340.

Spinelli G, Lazzeri D, Conti M, Agostini T, Mannelli G. Comparison of piezosurgery and traditional saw in bimaxillary orthognathic surgery. J Craniomaxillofac Surg. 2014; 42(7), 1211-1220.

Steiner SS. Cephalometrics in clinical paractice. Angle Orthod. 1959;29:8-29.

Stiles KA, Luke JE. The inheritance of malocclusion due to mandibular proganthism. J Hered. 1953;44:241-245.

Stratemann SA, Huang JC, Maki K, Miller AJ, Hatcher DC. Comparison of cone beam computed tomography imaging with physical measures. Dentomaxillofac Radiol. 2008; 37(2), 80-93.

Susami R, Kushida S, Onishi K, et al. Clinical information of mandibular prognathism cases. J Jpn Orthod Soc. 1968; 27:118-124.

Suzuki S. Studies on the so-called reverse occlusion. J Nihon Univ Sch Dent. 1961;3:51-58.

Swennen GRJ, Schutyser F, Hausamen J-E. Three-dimensional cephalometry : a color atlas and manual. New York, NY: Springer. 2005.

Swennen GR, Schutyser F. Three-dimensional cephalometry: spiral multi-slice vs cone-beam computed tomography. Am J Orthod Dentofacial Orthop. 2006;130(3),410-416.

Tai K, Park JH, Hayashi K, Yanagi Y, Asaumi JI, Iida S, Shin JW. Preliminary study evaluating the accuracy of MRI images on CBCT images in the field of orthodontics. J Clin Pediatr Dent. 2011; 36(2), 211-218.

Tai B, Goonewardene MS, Murray K, Koong B, Islam SM. The reliability of using postero-anterior cephalometry and cone-beam CT to determine transverse dimensions in clinical practice. Aust Orthod J. 2014;30(2):132-142.

Tang EL. Occlusal features of Chinese adults in Hong Kong. Aust Orthod J.1994;13:159-163.

Thiesen G, Gribel BF, Kim KB, Freitas MPM. Maxillofacial Features Related to Mandibular Asymmetries in Skeletal Class III Patients. J Oral Maxillofac Surg.2017;75(5):1015-1025.

Tod, MA, Taverne AA. Prevalence of malocclusion traits in an Australian adult population.Aust Orthod J.1997q;5:16-22.

Trauner R, Obwegeser H. The surgical correction of mandibular prognathism and retrognathia with consideration of genioplasty. I. Surgical procedures to coreect

mandibular prognathism and reshaping of the chin. Oral Surg Oral Med Oral Patholo 1957;10:677-689.

Trpkova B, Prasad NG, Lam EW, Raboud D, Glover KE, Major PW. Assessment of facial asymmetries from posteroanterior cephalograms: validity of reference lines. Am J Orthod Dentofacial Orthop. 2003;123(5):512-520.

Tyan S, Kim HH, Park KH, Kim SJ, Kim KA, Ahn HW. Sequential changes of postoperative condylar position in patients with facial asymmetry. Angle Orthod. 2017;87(2):260-268.

Ubaya T, Sherriff A, Ayoub A, Khambay B. Soft tissue morphology of the naso-maxillary complex following surgical correction of maxillary hypoplasia. Int J Oral Maxillofac Surg. 2012; 41(6), 727-732.

Uslu O, Akcam MO, Evirgen S, Cebeci I. Prevalence of dental anomalies in various malocclusions. Am J Orthod Dentofacial Orthop. 2009; 135(3): 328-335.

van der Vlis M, Dentino KM, Vervloet B, Padwa BL. Postoperative swelling after orthognathic surgery: a prospective volumetric analysis. J Oral Maxillofac Surg. 2014; 72(11), 2241-2247.

Van Elslande DC, Russett SJ, Major PW, Flores-Mir C. Mandibular asymmetry diagnosis with panoramic imaging. Am J Orthod Dentofacial Orthop. 2008;134(2):183-192.

Van Keulen C, Martens G, Dermaut L. Unilateral posterior crossbite and chin deviation: is there a correlation? Eur J Orthod. 2004;26(3):283-288.

van Loon B, van Heerbeek N, Bierenbroodspot F, Verhamme L, Xi T, de Koning MJ, Ingels KJ, Berge SJ, Maal TJ. Three-dimensional changes in nose and upper lip volume after orthognathic surgery. Int J Oral Maxillofac Surg. 215; 44: 83-89.

Verdenik M, Ihan Hren N. Differences in three-dimensional soft tissue changes after upper, lower, or both jaw orthognathic surgery in skeletal class III patients. Int J Oral Maxillofac Surg. 2014;43(11),1345-1351.

Vig PS, Hewitt AB. Asymmetry of the human facial skeleton. Angle Orthod. 1975;45:125-129.

Waite PD, Matukas VJ, Sarver DM. Silmutaneous rhinoplasty procedures in orthognathic surgery. Int J Oral Maxillofac Surg. 1988;17:298-302.

Walters M, Claes P, Kakulas E, Clement JG. Robust and regional 3D facial asymmetry assessment in hemimandibular hyperplasia and hemimandibular elongation anomalies. Int J Oral Maxillofac Surg. 2013;42:36.

Washburn SL. The effect of facial paralysis on the growth of the skull of the rat and rabbit. The Anatomical Record. 1946; 94(2):163-168.

Wells AP, Sarver DM, Proffit WR. Long-term efficacy of reverse pull headgear therapy. Angle Orthod. 2006;76(6):915-922.

Westermark AH, Bystedt H, Von Konow L, Sallstrom KO. Nasolabial morphology after Le Fort I osteotomies: effect of alar base suture. Int J Oral Maxillofac Surg. 1991;20:25-30.

White JE, Ayoub AF, Hosey MT, Bock M, Bowman A, Bowman J, Siebert JP, Ray A. Three-dimensional facial characteristics of Caucasian infants without cleft and correlation with body measurements. Cleft Palate Craniofac J. 2004;41(6),593-602.

White SC, Pharoah MJ. Oral radiology principles and interpretation. St. Louis: Mosby Elsevier, 2009:236-237.

Willems G, De Bruyne I, Verdonck A, Fieuws S, Carels C. Prevalence of dentofacial characteristics in a belgian orthodontic population. Clin Oral Investig. 2001;5:220-226.

Williams S, Andersen CE. The morphology of the potential Class III skeletal pattern in the growing child. Am J Orthod. 1986; 89(4), 302-311.

Wolff G, Wienker TF, Sander H. On the genetics of mandibular prognathism: analysis of large European noble families. J Med Genet. 1993;30:112-116.

Yamaoka M, Okafuji N, Furusawa K, Hasumi-Nakayama Y, Hayama H, Yamada AS, Kurihara S. Alteration of the angle of the coronoid process in prognathism. J Oral Rehabil. 2001;28(5):479-484.

Yáñez-Vico RM, Iglesias-Linares A, Torres-Lagares D, Gutiérrez-Pérez JL, Solano-Reina E. Three-dimensional evaluation of craniofacial asymmetry: an analysis using computed tomography. Clin Oral Investig. 2011;15(5):729-736.

Yoon KS, Jung YS, Kang GC, Park HS. Facial asymmetry with mandibular prognathism: a new trial of classification and interpretation. J Korean Assoc Oral Maxillofac Surg. 2004;30:108-120.

You KH, Lee KJ, Lee SH, Baik HS. Three-dimensional computed tomography analysis of mandibular morphology in patients with facial asymmetry and mandibular prognathism. Am J Orthod Dentofacial Orthop. 2010;138(5):540.e1-8.

Zellner EG, Reid RR, Steinbacher DM. The Pierre Robin Mandible is Hypoplastic and Morphologically Abnormal. J Craniofac Surg. 2017 Nov;28(8):1946-1949.

1. CURRICULUM VITAE

I was born in Athens, Greece in June 1990. I studied at the Dental School of Aristotle University of Thessaloniki from September 2008, until September 2013. Since September of 2015, I have been enrolled in the MSc in Orthodontics program at the Department of Orthodontics, Faculty of Dentistry, Marmara University, Istanbul, Turkey.

PERSONAL INFORMATION

Name	STAVROULA	**Surname**	SARAFOPOULOU
Birth of Place	ATHENS	**Birth Date**	07/06/90
Citizen	GREEK		
E-mail	ssarafop@gmail.com	**Phone**	05531486421

EDUCATION LEVEL

	The Institute Graduated From	**Graduation Year**
Doctorate		
Master		
Licence	Dental School, Aristotle University of Thessaloniki	2013
High school	Mandoulides College, Thessaloniki, Greece	2008

WORK EXPERIENCE

JOB	INSTITUTE	**DURATION (year)**
GENERAL DENTIST	PRIVATE DENTAL PRACTICE	2013-2015

LANGUAGE SKILLS

FOREIGN LANGUAGE	**COMPREHENSION ***	**SPEAKING ***	**WRITING***
ENGLISH	Excellent	Excellent	Excellent
GERMAN	Excellent	Excellent	Excellent
TURKISH	Well	Intermediate	Invalid

***** Evaluate as Excellent , Well , Intermediate , Invalid

FOREIGN LANGUAGE COMPETENCY (ENGLISH)								
KPDS	ÜDS	IELTS	TOEFL IBT	TOEFL PBT	TOEFL CBT	FCE	CAE	CPE
			94/120			B		Pass

it is to be written all the successfull examinations

KPDS: Kamu Personeli Yabancı Dil Sınavı; ÜDS:Interuniversity Board Foreign Language Examination ; IELTS: International English Language Testing System; TOEFL IBT: Test of English as a Foreign Language-Internet-Based Test TOEFL PBT: Test of English as a Foreign Language-Paper-Based Test; TOEFL CBT: Test of English as a Foreign Language-Computer-Based Test; FCE: First Certificate in English; CAE: Certificate in Advanced English; CPE: Certificate of Proficiency in English.

FOREIGN LANGUAGE COMPETENCY (GERMAN)	
Zertifikat Deutsch B1, Goethe Institut	203,5/225
Mittelstufe B2, Goethe Institut	82,50/100

	Quantitative	Equally Weighted	Verbal
Academic staff and graduate education entrance examination (ALES)			
OTHER SCORE **GRE**	159		149

COMPUTER KNOWLEDGE

PROGRAM	ABILITY TO USE
MICROSOFT OFFICE ECDL	Excellent

*****Evaluate as Excellent , Well , Intermediate, Invalid

International and national editions/proclamations/ certificate /prizes/ other

2002 Six-year scholarship from "Mandoulides College", that is given to the first student passing grade scholarship examinations.

2008 Honorary Scholarship by the Greek State Scholarship Foundation for the excellent entry grades at the School of Dental Medicine, Aristotle University of Thessaloniki, Greece.

2013 Graduation praise from "Society of Graduate Students of Dental School of the Aristotle University", that is given to the three first graduate students

1. Financial award-Foundation of professor Xanania Azaria, that is provided to the two first graduate students of Dental School of the Aristotle University for excellent grading and completing the dental studies without any time extension

T.C.
MARMARA ÜNİVERSİTESİ
Diş Hekimliği Fakültesi
Klinik Araştırmalar Etik Kurulu

Projenin Adı: Three dimensional evaluation of skeletofacial asymmetry in skeletal Class III patients treated with double-jaw orthognathic surgery
Proje yürütücüsü: Yrd.Doç.Dr. Kadir Beycan
Projedeki Araştırıcılar:Dt. Stavroula Sarafopoulou
Onay tarihi ve sayısı:25.04.2017, 2017-92

Sayın Yrd.Doç.Dr. Kadir Beycan

2017-95 Protokol nolu "Three dimensional evaluation of skeletofacial asymmetry in skeletal Class III patients treated with double-jaw orthognathic surgery " isimli anket çalışmanız Marmara Üniversitesi Klinik araştırmalar Etik kurulu tarafından incelenmiş ve etik yönden uygunluğuna karar verilmiştir.

M.Ü.Diş Hekimliği Fakültesi
Klinik Araştırmalar Etik Kurulu Başkanı
Prof.Dr.Nimet Gençoğlu

Adı Soyadı	İmza
Prof. Dr. Nimet Gençoğlu	
Prof. Dr. Ilknur Tanboğa	
Prof. Dr. Ali Recai Menteş	
Prof. Dr. Yaşar Özkan	
Prof. Dr. Ahu Acar	
Prof. Dr. Zühre Hale Cimilli	
Doç. Dr. Buket Evren	
Prof. Dr. Şebnem Erçalık Yalçınkaya	
Prof. Dr. Filiz Onat	
Dr. Zerrin Kurşun	
Doç. Dr. Tolga Güven	
Doç. Dr. Afife Binnaz Hazar Yoruç	
Avukat Burçak Çopuroğlu	
Gürol Pekel (sivil üye)	

Marmara Üniversitesi
Nişantaşı Kampüsü Diş
Hekimliği Fakültesi 34365
Nişantaşı/Şişli/İSTANBUL

0 (212) 246 52 47 (Faks)
0 (212) 231 91 20

dishekimligi@marmara.edu.tr
http://dental.marmara.edu.tr

Ayrıntılı bilgi için: İ.SOYADI Unvanı

ARAŞTIRMACI ÖZGEÇMİŞ

Adı-Soyadı	: Stavroula Sarafopoulou , Master of Science, Student.
Doğum Tarihi-Yeri	: 07/06/1990 (Athens, Greece)
Medeni Hali	: Bekar
Öğrenim	: Dental School of the Aristotle University, Thessaloniki, Greece
Yabancı Dili	: İngilizce, Almanca, Türkçe, Yunanca
Bilimsel Kuruluşlara Üyelikler	:Türk Ortodonti Derneği, Orthodontic Society of Northern Greece